

**IDH mutations as immune target and their effect on dendritic cell
differentiation and metabolism**



Dissertation
zur Erlangung des Doktorgrades
der Biomedizinischen Wissenschaften
(Dr. rer. physiol.)

der
Fakultät für Medizin
der Universität Regensburg

vorgelegt von
Kathrin Hammon
aus
Freiburg im Breisgau

im Jahr
2018

**IDH mutations as immune target and their effect on dendritic cell
differentiation and metabolism**



Dissertation
zur Erlangung des Doktorgrades
der Biomedizinischen Wissenschaften
(Dr. rer. physiol.)

der
Fakultät für Medizin
der Universität Regensburg

vorgelegt von
Kathrin Hammon
aus
Freiburg im Breisgau

im Jahr
2018

Dekan: Prof. Dr. Dr. Torsten E. Reichert

Betreuer: Prof. Dr. Wolfgang Herr

Tag der mündlichen Prüfung: Noch nicht bekannt

SELBSTÄNDIGKEITSERKLÄRUNG

“Ich, Hammon. Kathrin geboren am 12.04.1989 in Freiburg im Breisgau, erkläre hiermit, dass ich die vorliegende Arbeit ohne unzulässige Hilfe Dritter und ohne Benutzung anderer als der angegebenen Hilfsmittel angefertigt habe.

Die aus anderen Quellen direkt oder indirekt übernommenen Daten und Konzepte sind unter Angabe der Quelle gekennzeichnet. Insbesondere habe ich nicht die entgeltliche Hilfe von Vermittlungs- bzw. Beratungsdiensten (Promotionsberater oder andere Personen) in Anspruch genommen.

Die Arbeit wurde bisher weder im In- noch im Ausland in gleicher oder ähnlicher Form einer anderen Prüfungsbehörde vorgelegt.

Ort, Datum

eigenhändige Unterschrift des Promovenden

Die vorliegende Arbeit entstand im Zeitraum von September 2014 bis September 2018 an der Klinik und Poliklinik für Innere Medizin III des Universitätsklinikums Regensburg.

The present work was carried out from September 2014 to September 2018 at the Department of Internal Medicine III at the University Hospital Regensburg.

“Science never solves a problem without creating ten more.”

George Bernard Shaw

Table of content

SELBSTÄNDIGKEITSERKLÄRUNG
List of Figures	VI
List of Tables.....	VIII
List of Abbreviations.....	IX
1 Introduction	1
1.1 <i>Acute Myeloid Leukemia</i>	1
1.1.1 Mutations in AML	1
1.1.1.1 IDH mutation	2
1.1.1.1.1 Prognosis in AML patients with IDH mutation.....	3
1.1.1.2 Production of 2-hydroxyglutarate	3
1.1.1.3 Effects of 2-hydroxyglutarate	4
1.2 <i>Epigenetic</i>	5
1.2.1 DNA Methylation	5
1.3 <i>Immunological background</i>	5
1.3.1 T cells	5
1.3.2 Antigen presenting cells	6
1.3.2.1 Dendritic cells	7
1.3.2.2 HLA class II molecules.....	7
1.4 <i>Cellular therapy as cancer treatment</i>	8
1.4.1 Target antigen for cellular therapy	9
1.5 <i>Metabolites interfere with immune cells</i>	10
1.5.1 Glucose metabolism	10
1.5.2 Citric acid cycle	10
1.5.3 Oxidative phosphorylation.....	11
1.5.4 Metabolism of dendritic cells	12
1.5.5 Oxidative stress.....	13
1.5.5.1 Production of reactive oxygen species.....	13
1.5.5.1.1 Role of ROS in DCs	13
1.6 <i>Project aims</i>	14
2 Material and Methods	15
2.1 <i>Material</i>	15
2.1.1 Equipment and consumables	15
2.1.2 Chemicals	16
2.1.3 Fluorescence probes and antibodies	17
2.1.4 Cell culture material	18
2.1.5 Kits	19
2.1.6 Software.....	20
2.2 <i>Methods</i>	21
2.2.1 IDH2 _{Mut} specific stimulation of T cells	21
2.2.1.1 <i>In silico</i> Peptide prediction	21
2.2.1.1.1 SYFPEITHI	21
2.2.1.1.2 BIMAS	21

2.2.1.1.3	NetMHCPan	21
2.2.1.1.4	IDH2 R140Q specific Peptides	21
2.2.1.2	Preparation of IDH mRNA	22
2.2.1.2.1	Digestion	22
2.2.1.2.2	Agarose gel	22
2.2.1.2.3	PCR Purification with High pure PCR product purification kit	23
2.2.1.2.4	Dephosphorylation of phosphates on the ends of the linearized vector	23
2.2.1.2.5	Ligation of insert in the vector	23
2.2.1.2.6	Transformation of Plasmid DNA	24
2.2.1.2.7	Plasmid isolation out of bacteria	24
2.2.1.2.8	Concentration measurement with nano drop	25
2.2.1.2.9	Sequencing of inserts	25
2.2.1.2.10	Mutagenese Quickchange	25
2.2.1.2.11	Linearization of vector	27
2.2.1.2.12	Phenol-Chlorophorm extraction	27
2.2.1.2.13	In-vitro transcription and purification of mRNA	28
2.2.1.2.14	RNA gel	28
2.2.1.3	General cell culture	29
2.2.1.3.1	Counting of cells	29
2.2.1.3.2	Thawing of cells	29
2.2.1.3.3	Freezing of cells	29
2.2.1.4	Isolate Peripheral blood mononuclear cell from blood samples of healthy donors	29
2.2.1.4.1	Pancoll separation	30
2.2.1.4.2	Isolation of CD8 positive cells from PBMCs by Magnetic-activated cell separation (MACS)	30
2.2.1.4.3	Isolation of CD4 and CD8 positive cells from PBMCs	31
2.2.1.4.4	Isolation of CD45RA positive cells from PBMCs	31
2.2.1.4.5	Fluorescent associated cell sorting	31
2.2.1.5	Generating of mature FAST-DC for T cell stimulation	32
2.2.1.5.1	Transfection of in vitro transcribed mRNA and T cell stimulation with DCs expressing IDH2 R140Q	32
2.2.1.6	T cell stimulation with Peptide loaded APCs	33
2.2.1.7	Measurement of IFN γ secretion by ELISpot	33
2.2.2	Analyzing effect of D-2-HG on monocyte maturation and differentiation to DCs	34
2.2.2.1	Isolation of monocytes by elutriation	34
2.2.2.2	Generation of monocyte-derived DCs	34
2.2.2.3	Electron microscopic analyses of DCs treated with D-2-HG	35
2.2.2.4	Phagocytosis Assay	35
2.2.2.5	Allogeneic mixed lymphocyte reaction	36
2.2.2.6	Enzyme-linked immunosorbent assay (ELISA)	36
2.2.2.7	Measurement of cAMP level by ELISA	37
2.2.2.8	Flow cytometric analyses	37
2.2.2.8.1	Staining of surface molecules	37
2.2.2.8.2	Intracellular staining	37
2.2.2.8.3	Measurement of cytosolic ROS with 2',7'-Dichlorofluorescin diacetate	38
2.2.2.8.4	Cystine staining	38
2.2.2.8.5	Measurement of mitochondrial ROS with MitoSox red	38
2.2.2.8.6	Staining of mitochondria with Mitotracker Green	39
2.2.2.9	Determining mitochondrial respiration by high-resolution respirometry	39
2.2.2.9.1	Oxygen measurement in whole cells	39
2.2.2.9.2	Oxygen measurement in permeabilized cells	40
2.2.2.10	Analyze of pH value and oxygen concentration of DCs	41
2.2.2.11	Lactate and glucose determination	42
2.2.2.12	Methylation analysis	42
2.2.2.12.1	Culture and treatment of DCs for methylation analysis	42

2.2.2.12.2	Isolation of DNA with DNeasy Blood and tissue	42
2.2.2.13	Protein isolation	43
2.2.2.14	Fractionized protein isolation	43
2.2.2.15	Protein determination by Lowry	44
2.2.2.16	Analyzing protein of interest by western blot	44
2.2.2.16.1	SDS gel electrophoresis.....	44
2.2.2.16.2	Western blot	45
2.2.2.16.3	Protein transfer on membrane	45
2.2.2.16.4	Detection of protein of interest.....	46
2.2.2.16.5	Elimination of antibodies bound on membrane.....	46
3	Results.....	47
3.1	<i>Generation of IDH 2 R140Q specific T cell.....</i>	47
3.1.1	HLA binding prediction by <i>in silico</i> programs.....	47
3.1.2	T cell stimulation with peptide loaded antigen presenting cells	48
3.1.2.1	T cell stimulation with peptide loaded PBMC	48
3.1.2.2	T cell stimulation with peptide loaded DCs.....	49
3.1.2.2.1	Stimulation with peptide pools in 96-well format	50
3.1.2.3	Summary of stimulation with peptide loaded antigen presenting cells.....	51
3.1.3	T cell stimulation with electroporated DC.....	52
3.1.4	Stimulation of T cells with Influenza peptide.....	53
3.2	<i>Effect of D-2-HG on metabolism and differentiation of monocyte-derived dendritic cells.....</i>	55
3.2.1	Uptake of D-2-HG in monocytes.....	55
3.2.2	Changes of DC morphology upon D-2-HG treatment.....	56
3.2.2.1.1	Dendritic cell structures analyzed by electron microscopy	57
3.2.2.1.2	Vesicle structure of D-2-HG treated DCs analyzed by electron microscopy	58
3.2.2.2	Expression analyze of late endosome marker Rab9 by western blot	60
3.2.2.3	Expression analyze of the autophagy marker LC-3B by western blot.....	61
3.2.2.4	HLA-class II expression of bafilomycin A1 treated DCs	63
3.2.3	Effect of D-2-HG differentiation and maturation of DCs.....	63
3.2.3.1	CD14 and CD1a expression of D-2-HG treated DCs	63
3.2.3.2	DC-SIGN expression on D-2-HG treated DCs	64
3.2.3.3	HLA class I molecules of D-2-HG of DCs	65
3.2.3.3.1	Surface expression of HLA class II molecules.....	66
3.2.3.3.2	Intracellular staining of HLA class II molecules	67
3.2.3.3.3	Western blot analyses of HLA class II molecules	68
3.2.3.4	Expression of co-stimulatory molecules CD80/CD86.....	69
3.2.4	Effects of D-2-HG on DC function	69
3.2.4.1	Effect of D-2-HG on cytokine production in DCs.....	69
3.2.4.2	Effect of D-2-HG on T cell stimulatory capacity of DCs	70
3.2.4.2.1	IFN γ secretion and proliferation of bulk and naïve enriched T cells.....	70
3.2.4.2.2	Impact of D-2-HG on differentiation of regulatory T cells	71
3.2.4.3	Expression of inhibitory molecules on D-2-HG treated DCs	72
3.2.4.4	Effect of D-2-HG on phagocytosis activity of immature DCs.....	73
3.2.5	Effect of D-2-HG on G protein receptor signaling	74
3.2.6	Impact of D-2-HG on DC metabolism	76
3.2.6.1	Lactate production and glucose consumption of D-2-HG treated DCs	76
3.2.6.2	Effect of D-2-HG on mTOR phosphorylation in DCs	77
3.2.6.3	Effect of D-2-HG on respiration of DCs.....	78
3.2.6.4	Determination of mitochondrial content in DCs.....	81
3.2.6.5	Measurement of ATP content of DCs.....	82
3.2.6.5.1	Effect of mutant IDH1/2 protein expression on respiration of DCs	83
3.2.6.6	Effect of D-2-HG on mitochondrial structure of DCs	85
3.2.7	Effect of D-2-HG on reactive oxygen species of DCs.....	85
3.2.7.1	Establishment of measurement of cytosolic ROS by DCFDA	86

3.2.7.2	Short-term effects of D-2-HG on cytosolic ROS in DCs.....	87
3.2.7.3	Short-term effect of D-2-HG on mitochondrial ROS of DCs.....	88
3.2.7.4	Long-term effect of D-2-HG ROS levels and cystine uptake in DCs.....	88
3.2.8	Effect of oxidants and antioxidants on DCs.....	89
3.2.8.1	Analyses of peroxide treatment on HLA-DP, -DR and CD1a expression on DCs.....	89
3.2.8.2	Antioxidant treatment to rescue D-2-HG treated DCs.....	90
3.2.8.2.1	HLA class II expression on trolox and vitamin C treated DCs.....	90
3.2.8.2.2	DC-SIGN and CD1a expression of trolox and vitamin C treated DCs.....	91
3.2.8.2.3	IL-12 secretion of trolox and vitamin C treated DCs.....	92
3.2.8.2.4	Reactive oxygen species of Vitamin C treated DCs.....	93
3.2.9	Rescue experiments with modulator of metabolism.....	94
3.2.9.1	Respiration of metformin and pioglitazone treated DCs.....	94
3.2.9.2	HLA class II expression of metformin and pioglitazone treated DCs.....	95
3.2.9.3	DC-SIGN expression after pioglitazone treated DCs.....	96
3.2.9.4	IL-12 secretion of metformin and pioglitazone treated DCs.....	97
3.2.9.5	ROS levels in metformin and pioglitazone treated DCs.....	98
3.2.10	Methylation analysis of DC differentiation.....	99
3.2.11	Primary AML blast from IDH mutated leukemias.....	102
3.2.11.1	RNA _{seq} data of primary AML IDH _{MUT} blasts from the cancer genome atlas.....	102
3.2.11.2	HLA class II protein expression of primary AML IDH _{MUT} blasts.....	103
3.2.11.3	HLA expression on AML blasts analyzed by western blot.....	103
4	Discussion.....	105
4.1	<i>Generation of IDH2 R40Q specific T cells.....</i>	<i>105</i>
4.1.1	T cell stimulation with peptide and protein of mutant IDH2 R140Q.....	105
4.1.2	Peptide prediction with <i>in silico</i> algorithms.....	105
4.1.3	Influenza peptide is similar to mutant IDH2 R140Q derived peptide IQN9.....	106
4.2	<i>Effects of D-2-HG on differentiation and metabolism of monocytes derived dendritic cells.....</i>	<i>107</i>
4.2.1	Uptake of D-2-HG.....	107
4.2.2	D-2-HG inhibits DC differentiation.....	107
4.2.2.1	T cell stimulation activation in an allogeneic MLR.....	108
4.2.3	Multi-laminar vesicles in DCs.....	108
4.2.4	Impact of D-2-HG on autophagy.....	108
4.2.4.1	Intracellular signaling of D-2-HG.....	109
4.2.5	Effect of D-2-HG on metabolism.....	111
4.2.5.1	Effect of D-2-HG on glycolytic activity.....	111
4.2.5.2	Effect of D-2-HG on respiration.....	112
4.2.6	IDH mutant cells and D-2-HG addition interfere with ROS level.....	112
4.2.6.1	Rescue of D-2-HG effects with trolox treatment.....	113
4.2.6.2	Rescue of D-2-HG effects on metabolism with metformin.....	113
4.2.6.3	Rescue of D-2-HG effects on metabolism with pioglitazone.....	114
4.2.7	Effect of D-2-HG on DNA methylation and vitamin C treatment.....	114
4.2.8	Expression of mutant IDH protein versus exogenous D-2-HG.....	115
3.2.12	Conclusion.....	116
5	Summary.....	118
5.1	<i>Generation of IDH2 R140Q specific T cells.....</i>	<i>118</i>
5.2	<i>Effect of D-2-HG on metabolism and differentiation of monocyte-derived dendritic cells....</i>	<i>118</i>
6	Zusammenfassung.....	121
6.1	<i>Generierung von IDH2 R140Q spezifischer T Zellen.....</i>	<i>121</i>
6.2	<i>Effekt von D-2-HG auf den Metabolismus und die Differenzierung von DZs.....</i>	<i>121</i>

References	124
Danksagung.....	
Lebenslauf.....	

List of Figures

Figure 1.1: Production and effects of 2-HG on α -ketoglutarate dependent dioxygenases.....	4
Figure 1.2: Compartments containing HLA molecules.....	8
Figure 1.3: Complexes of electron transport chain in the inner mitochondrial membrane	12
Figure 2.1: Map of pGEM4Z-65A vector containing the region of IDH2 R140Q.....	27
Figure 2.2: Phase separation after pancoll density separation.....	30
Figure 3.1: CD8 T cells stimulation with autologous IDH2 R140Q specific peptide loaded PBMCs.....	48
Figure 3.2: CD8 T cells stimulation with autologous IDH2 R140Q specific peptide loaded DCs	49
Figure 3.3: CD8 T cells stimulation with autologous IDH2 R140Q specific peptide pool loaded DCs	51
Figure 3.4: Transfection efficiency 4 and 24h after electroporation..	52
Figure 3.5: CD4 T cells stimulation with autologous IDH2 R140Q protein expressing DCs.....	53
Figure 3.6: CD8 T cells stimulation with autologous IDH2 R140Q or influenza peptide loaded DCs.....	54
Figure 3.7: 2-HG concentration in cell pellets of monocytes (MO).....	55
Figure 3.8: Viability (A), cell yield (B) and mean diameter (C)of D-2-HG treated DCs on day 7.....	56
Figure 3.9: Bright field pictures of DCs (A) and DCs treated 7 days with D-2-HG (B).....	56
Figure 3.10: Electron microscope images of day 8 DCs treated with D-2-HG	57
Figure 3.11: EM images of day 8 mature DCs treated and activated with LPS	58
Figure 3.12: EM image of control (A) and D-2-HG treated DCs (B)	59
Figure 3.13: EM images of d8 DCs treated with D-2-HG	60
Figure 3.14: Rab9 expression analysis in DC treated with D-2-HG by western blot.....	61
Figure 3.15: LC-3B expression analysis in DC treated with D-2-HG by western blot	62
Figure 3.16: LC-3B expression analysis in DC treated with D-2-HG by western blot	62
Figure 3.17: HLA-DP (A) and HLA-DR (B) expression of bafilomycin treated DCs.....	63
Figure 3.18: CD14 (A) and CD1a (B) expression of D-2-HG treated DCs	64
Figure 3.19: Surface expression of DC-SIGN after 7d incubation with D-2-HG	65
Figure 3.20: Impact of D-2-HG on surface expression of HLA-class I molecules after 7 days of culture	65
Figure 3.21: Analyses of HLA-DR expression of D-2-HG treated DCs (titration).....	66
Figure 3.22: HLA-DQ (A), -DP (B) and -DR expression of D-2-HG treated DCs.....	67
Figure 3.23: Intracellular staining of HLA class II molecules in D-2-HG treated DCs.....	68
Figure 3.24: HLA class II expression analysis in DC treated with D-2-HG by western blot.....	68
Figure 3.25: Expression of CD80 (A) and CD86 (B) in D-2-HG treated immature and mature DCs.....	69
Figure 3.26: IL-12, IL-10, TNF and IL-6 secretion of mature DCs treated with D-2-HG	70
Figure 3.27: IFN γ secretion of bulk CD4 and CD4/CD45RA enriched T cells	71
Figure 3.28: CD4/CD25 (A) and CD4/CD25/FoxP3 (B) positive T cells.....	72
Figure 3.29: Expression of inhibitory molecules on D-2-HG treated DCs.	73
Figure 3.30: Phagocytose positive cells of D-2-HG treated DCs on day 7	74
Figure 3.31: Western blot Analysis of PKC protein in cytosol and membrane fractions of DCs	75
Figure 3.32: cAMP levels of D-2-HG treated DCs	76
Figure 3.33: Lactate production (A) and glucose consumption (B) of D-2-HG treated DCs.....	77
Figure 3.34: Online measurement of pH value during 7 days of culture	77

Figure 3.35: mTOR phosphorylation (Ser2448) of monocytes	78
Figure 3.36: Oxygen concentration over time in DC cultures treated with D-2-HG.....	79
Figure 3.37: Oxygen consumption of D-2-HG treated DCs after 16 hours, 4 and 7 days.....	80
Figure 3.38: OXPHOS the presence and absence of D-2-HG in DCs (A) and T cells (B).	81
Figure 3.39: Mitochondrial mass (A) and maximum capacity of electron transport chain (B).....	82
Figure 3.40: ATP content (A) and oxygen consumed to produce ATP (B)	83
Figure 3.41: Oxygen consumption of DCs electroporated with IDH.....	84
Figure 3.42: Oxygen consumption of DCs derived from monocytes electroporated with IDH	84
Figure 3.43: EM images of d8 DCs treated with D-2-HG (Donor1).....	85
Figure 3.44: Oxygen consumption after inhibition of electron transport chain with rotenone.....	86
Figure 3.45: DCFDA staining of monocytes after addition of H ₂ O ₂	87
Figure 3.46: Short-term effects of D-2-HG on ROS levels in monocytes.....	87
Figure 3.47: Short-term effect of D-2-HG on mitochondrial ROS in monocytes	88
Figure 3.48: DCFDA, MitoSox and cystine staining of 7 days cultured DCs.....	89
Figure 3.49: HLA class II expression of peroxide treated DCs.....	90
Figure 3.50: HLA class II expression after trolox treatment DCs.....	91
Figure 3.51: CD1a (A) and DC-SIGN (B) expression after trolox and vitamin C treatment	92
Figure 3.52: IL-12 secretion after trolox treatment.	93
Figure 3.53: Mitochondrial (A) and cytosolic (B) ROS levels of vitamin C treated DCs.....	93
Figure 3.54: Basal respiration of DCs treated with metformin	95
Figure 3.55: HLA-DP (A) and HLA-DR (B) expression on metformin treated.....	96
Figure 3.58: CD1a (A) and DC-SIGN (B) expression on metformin and pioglitazone treated DCs	97
Figure 3.56: IL-12 secretion of DCs treated with metformin and pioglitazone	98
Figure 3.57: Mitochondrial (A) and cytosolic (B) ROS levels in metformin and pioglitazone treated DCs.....	99
Figure 3.59: Methylation analysis of DC differentiation.	101
Figure 3.60: RNAseq Data of the Cancer Genome Atlas.....	102
Figure 3.61: HLA-DP (A), -DQ (B) and -DR (C) expression of AML blasts.....	103
Figure 3.62: HLA class II expression of IDH mutant and wild type blasts analyzed by western blot	104

List of Tables

Table 2.1: List of equipment	15
Table 2.2: List of plastic consumables	15
Table 2.3: Equipment and consumables used for respiration analysis	15
Table 2.4: List of chemicals	16
Table 2.5: Reagents used for flow cytometry analyses	16
Table 2.6: Material and reagents used for SDS gels and western blotting	17
Table 2.7: Components of agarose gel to analyze RNA	17
Table 2.8: List of antibodies used for flow cytometry analyses	17
Table 2.9: List of fluorescence probes used in flow cytometry	18
Table 2.10: List of antibodies used for western blot analyses	18
Table 2.11: Cell culture media and supplementaries	18
Table 2.12: List of cytokine used in cell culture	18
Table 2.13: Other substances	19
Table 2.14: Material for magnetic-activated cell separation	19
Table 2.15: Material and reagents used for ELISpot	19
Table 2.16: Enzymes	19
Table 2.17: List of kits	19
Table 2.19: Peptide sequences of IDH2 and IDH2 R140Q specific peptides	22
Table 2.20: Dephosphorylation reaction	23
Table 2.21: Reagents for ligation	23
Table 2.22: Components of lysogeny broth (LB) media	24
Table 2.23: Values for DNA/RNA purity	25
Table 2.24: Sequencing primer	25
Table 2.25: Reagents used for quickchange mutagenese	26
Table 2.26: Cycler protocol for quickchange mutagenesis	26
Table 2.27: Components for linearization of plasmid	27
Table 2.28: Substances used to modulate oxygen consumption	40
Table 2.29: Components of MIRO5 used for permeabilized cells in oxygraph	40
Table 2.30: Substrates used to measure activity of different complexes of electron transport chain	41
Table 2.31: Genomic position of analyzed CpG residues	43
Table 3.1: Result scores of in silico HLA binding prediction	47
Table 3.2: Peptides used for peptide pool stimulation in 96-well format	50
Table 3.3: Summary of results of stimulation with peptide loaded antigen presenting cells	52

List of Abbreviations

°C	Degree celcius
AC	Adenylyl cyclase
AEC	3-Amino-9-Ethyl-carbazole
AKT	Protein kinase B
AML	Acute myeloid leukemia
APC	Antigen presenting cell
ATP	Adenosintriphosphate
BafA1	Bafilomycin A1
bp	Base pairs
BSA	Bovine serum albumin
BTLA	B and T lymphocyte attenuator
LAG-3	Lymphocyte activation gene-3
cAMP	Cyclic adenine monophosphate
CFSE	Carboxyfluorescein succinimidyl ester
CIITA	Class II major histocompatibility complex transactivator
CIP	Alkaline phosphatase from calf intestinal
CLIP	Class II-associated invariant chain peptide
CREB	CAMP response element-binding protein
CT	Cancer testis
D-2-HG	D-2-hydroxyglutarate
DC	Dendritic cell
DCFDA	2',7'-Dichlorofluorescein diacetate
DC-SIGN	Dendritic Cell-Specific Intercellular adhesion molecule-3-Grabbing Non-integrin
DEPC	Diethylpyrocarbonat
DMSO	Dimethylsulfoxid
DNMT	DNA methyltransferases
DNMT3A	DNA methyltransferase 3A
dNTP	Desoxyribonukleosidtriphosphate
EDTA	Ethylene-Diamine-Tetra-Acetic acid

EGTA	Glycol-bis(2-aminoethylether)-N,N,N',N'-tetraacetic acid
ELISA	Enzyme-linked immunosorbent assay
ELISpot	Enzyme-Linked ImmunoSpot
EM	Electron microscopy
ER	Endoplasmatic reticulum
ETC	Electron transport chain
FACS	Fluorescence assisting cell sorting
FCCP	Carbonyl cyanide-p-trifluoromethoxyphenylhydrazone
FCS	Fetal calf sera
FLT3	Fms-like tyrosine kinase 3
FoxP3	Forkhead box P3
GFP	Green fluorescence protein
GM-CSF	Granulocyte Macrophage Colony- Stimulating Factor
GPCR	G protein coupled receptor
h	Hour
HEPES	Hydroxyethyl piperazineethanesulfonic acid
Hif 1a	Hypoxia inducible factor 1a
HIS	Histidin
HK2	Hexokinase 2
HLA	Human leucocyte antigen
HS	Human sera
HSC	Hematopoietic stem cell
ICAM	Intercellular adhesion molecule
iDC	Immature DC
IDH	Isocitrate dehydrogenase
IFN γ	Interferon γ
IKK ϵ	Inhibitor of nuclear factor- κ B kinase subunit- ϵ
IL	Interleucin
ILT-2	Immunoglobulin-like transcript 2
ILT-3	Immunoglobulin-like transcript 3
IQN9/10	9/10 mer peptide of mutant IDH

KDM	Lysine demethylases
LB	Lysogeny broth
LC-3B	Microtubule-associated proteins 1A/1B light chain 3B
LHGDH	L-hydroxyglutarate dehydrogenase
li	invariant chain
LPS	Lipopolysaccharide
MACS	Magnetic-activated cell separation
MAGE	Melanoma-associated antigen
MALDI-TOF	Matrix Assisted Laser Desorption Ionization - Time of flight
MAPK	Mitogen-activated protein kinase
MDDCs	Monocyte-derived dendritic cell
min	Minute
mL	Milliliter
MLR	Mixed lymphocyte reaction
MNC	Mononucleated cells
MOPS	3-(N-morpholino)propanesulfonic acid)
MS	Mass spectrometry
mTOR	Mammalian Target of Rapamycin
Mut	Mutant
MVB	Multivesicular bodies
NF- κ B	Transcription factor nuclear factor-kappaB
NPM1	Nucleophosmin 1
OCR	Oxygen consumption rate
OCT1	Organic anion transporter 1
OD	Optical density
PBMC	Peripheral blood mononucleated cells
PBS	Phosphate buffered saline
PCR	Polymerase chain reaction
PDL-1	Programmed cell death ligand 1
PGC1 α	PPAR γ co-activator 1 α
PGE2	Prostaglandin 2

PhD	Prolyl hydroxylase
PKC	Protein kinase C
PolyA	Poly adenin
PPAR γ	Peroxisome proliferator-activated receptor- γ
Rab9	Ras-related protein 9
ROS	Reactive oxygen species
RPKM	Reads per kilobase million
RPKM	Reads per kilobase million
rpm	Rounds per minute
s	Second
SDS	Sodium dodecyl sulfate
SLC13A3	Solute carrier family 13 member 3
SLC22A6	Solute carrier family 22 member 6
SOD	Superoxide dismutase
TAE	TRIS-Acetate-EDTA
TBK1	TANK-binding kinase 1
TCA	Tricarboxylic acid
TCGA	The cancer genome atlas
TCR	T cell receptor
TET2	Tet methylcytosine dioxygenase 2
TIM-3	T cell immunoglobulin-3
TLR	Toll-like receptor
TMPD	Tetramethylphenylendiamin
TNF	Tumor necrosis factor
T _{reg}	Regulatory T cells
TSA	Tumor-specific antigens
V	Volt
DCFDA	2',7'-Dichlorofluorescein diacetate
MOPS	3-(N-morpholino)propanesulfonic acid)
AEC	3-Amino-9-Ethyl-carbazole
IQN9/10	9/10 mer peptide of mutant IDH

AML	Acute myeloid leukemia
ATP	Adenosintriphosphate
AC	Adenylyl cyclase
APC	Antigen presenting cell
BTLA	B and T lymphocyte attenuator
BafA1	Bafilomycin A1
bp	Base pairs
BSA	Bovine serum albumin
CREB	CAMP response element-binding protein
FCCP	Carbonyl cyanide-p-trifluoromethoxyphenylhydrazine
CFSE	Carboxyfluorescein succinimidyl ester
CIITA	Class II major histocompatibility complex transactivator
CLIP	Class II-associated invariant chain peptide
cAMP	Cyclic adenine monophosphate
D-2-HG	D-2-hydroxyglutarate
°C	Degree celcius
DC	Dendritic cell
DC-SIGN	Dendritic Cell-Specific Intercellular adhesion molecule-3-Grabbing Non-integrin
dNTP	Desoxyribonukleosidtriphosphate
DEPC	Diethylpyrocarbonat
DMSO	Dimethylsulfoxid
DNMT3A	DNA methyltransferase 3A
EM	Electron microscopy
ETC	Electron transport chain
ER	Endoplasmatic reticulum
ELISA	Enzyme-linked immunosorbent assay
ELISpot	Enzyme-Linked ImmunoSpot
EDTA	Ethylene-Diamine-Tetra-Acetic acid
FCS	Fetal clalf sera
FACS	Fluorescence assisting cell sorting

FLT3	Fms-like tyrosine kinase 3
FoxP3	Forkhead box P3
GPCR	G protein coupled receptor
EGTA	Glycol-bis(2-aminoethylether)-N,N,N',N'-tetraacetic acid
GM-CSF	Granulocyte Macrophage Colony- Stimulating Factor
GFP	Green fluorescence protein
HSC	Hematopoietic stem cell
HK2	Hexokinase 2
HIS	Histidin
h	Hour
HLA	Human leucocyte antigen
HS	Human sera
HEPES	Hydroxyethyl piperazineethanesulfonic acid
Hif 1a	Hypoxia inducible factor 1a
iDC	Immature DC
ILT-2	Immunoglobulin-like transcript 2
ILT-3	Immunoglobulin-like transcript 3
IKK ϵ	Inhibitor of nuclear factor- κ B kinase subunit- ϵ
IFN γ	Interferon γ
IL	Interleucin
IDH	Isocitrate dehydrogenase
LHGDH	L-hydroxyglutarate dehydrogenase
LPS	Lipopolysaccaride
LAG-3	Lymphocyte activation gene-3
KDM	Lysine demethylases
LB	Lysogeny broth
MACS	Magnetic-activated cell separation
mTOR	Mammalian Target of Rapamycin
MALDI-TOF	Matrix Assisted Laser Desorption Ionization - Time of flight
LC3B	Microtubule-associated proteins 1A/1B light chain 3B
mL	Milliliter

min	Minute
MAPK	Mitogen-activated protein kinase
MLR	Mixed lymphocyte reaction
MDDCs	Monocyte-derived dendritic cell
MNC	Mononucleated cells
MVB	Multivesicular bodies
Mut	Mutant
NPM1	Nucleophosmin 1
OD	Optical density
OCT1	Organic anion transporter 1
OCR	Oxygen consumption rate
PBMC	Peripheral blood mononucleated cells
PPAR γ	Peroxisome proliferator-activated receptor- γ
PBS	Phosphate buffered saline
PolyA	Poly adenin
PCR	Polymerase chain reaction
PGC1 α	PPAR γ co-activator 1 α
PDL-1	Programmed cell death ligand 1
PhD	Prolyl hydroxylase
PGE2	Prostaglandin 2
AKT	Protein kinase B
PKC	Protein kinase C
Rab9	Ras-related protein 9
RPKM	Reads per kilobase million
RPKM	Reads per kilobase million
ROS	Reactive oxygen species
RBC	Red blood cells
T _{reg}	Regulatory T cells
rpm	Rounds per minute
s	Second
SDS	Sodium dodecyl sulfate

SLC13A3	Solute carrier family 13 member 3
SLC22A6	Solute carrier family 22 member 6
TIM-3	T cell immunoglobulin-3
TBK1	TANK-binding kinase 1
TET2	Tet methylcytosine dioxygenase 2
TMPD	Tetramethylphenylendiamin
TCGA	The cancer genome atlas
TLR	Toll-like receptor
NF- κ B	Transcription factor nuclear factor-kappaB
TCA	Tricarboxylic acid
TNF	Tumor necrosis factor
V	Volt

1 Introduction

1.1 Acute Myeloid Leukemia

All blood cells originate from hematopoietic stem cells (HSCs) in the bone marrow. HSC can differentiate to multipotent stem cells and further to lymphoid or myeloid progenitor cells. Myeloid progenitor cells give rise to red blood cells, platelets, eosinophils, basophils, neutrophils and monocytes which further differentiate to macrophages or DCs. Lymphoid progenitor cells can differentiate to natural killer cells, B cells and T cells ¹.

In patients with acute myeloid leukemia (AML) a cancer of myeloid blood cells this differentiation is altered. This leads to a high number of progenitor cells without any function and a reduced number of erythrocytes, thrombocytes and leucocytes. It is the most common type of acute leukemia in adults. As its incidence is rising with age as well as life expectancy, the number of AML patients will also increase ². In older patients, prognosis is poor due to high relapse rates after induction chemotherapy. But the prognosis also depends on recurrent molecular and cytogenetic abnormalities and the mutational load of the patients. Today about 35-40% of patients under 60 years go to remission after chemotherapy and stem cell transplantation ³. Also, mutation specific and immunomodulatory treatments are under investigation in ongoing clinical studies like fms-like tyrosine kinase 3 (FLT3) and isocitrate dehydrogenase (IDH) 1 and 2 inhibitors ^{4,5}

1.1.1 Mutations in AML

There are multiple recurrent genetic mutations known in AML, but as with most cancer types the disease-causing mutations differ between subtypes of AML. The mutations known in AML can be classified in 9 categories, transcription factor fusions, the nucleophosmin 1 (NPM1) genes, tumor suppressor genes, DNA methylation-related genes, myeloid transcription factor genes, cohesion complex genes, and spliceosome complex genes ⁶⁻⁸. There are also mutations interfering with more than one cellular process. Some mutation lead to a gain of function like in the case of the IDH, others are driver mutation. IDH mutations are no driver mutations, the mutation alone is not able to start leukemia development ⁹. The mutational landscape of AML patients is dynamic due to coexisting competing clones, there is disease evolution. Based on the genetic abnormalities patients can be classified in risk categories (favorable, intermediate and adverse). For example are mutations in the NPM1 gene are favorable, FLT-3 gene abnormalities are highly diverse and are found in all

categories and DNA methyltransferase 3A (DNMT3A) and IDH mutations are not yet classified⁸.

FLT3 is involved in proliferation, differentiation and survival of early hematopoietic progenitor cells. An internal tandem repeat mutation (repetition of one or more base pairs inside the gene) in the FLT3 gene is present in 20% of all AML patients¹⁰. In patients younger than 65 years with normal karyotype the prognosis of patients with a FLT3 mutation is poor in other patient groups the prognosis is still unclear¹¹⁻¹⁴.

NPM1 is mutated in 30% of AML patients. NPM1 is a protein moving proteins from cytosol to nucleus and back to prevent accumulation of proteins in nucleolus. NPM1 is involved in other cellular processes such as the regulation of centrosome function and biosynthesis of ribosomes and p53 tumor suppressor pathways¹⁵. 40% of patients with NPM1 mutation also have a FLT3-internal tandem duplication (ITD) mutation and in 25% additional to NPM1 IDH is mutated. If NPM1 is mutated without an FLT3 mutation, younger adults had a higher relapse free and overall survival^{14,16}.

Mutations in DNMT3A lead to an altered epigenetic landscape. DNMT3A is responsible for de novo methylation of DNA after replication. Methylations of promotor regions are associated with gene silencing. Mutation in DNMT3A may lead to a lack of silencing of self-renewal genes during differentiation of hematopoietic stem cells. DNMT3A mutations are present in 20% of AML patients; the mutation is conserved during blast evolution. In clinical studies patients with a DNMT3A mutation had a shorter event free and overall survival than patients expressing wild type DNMT3A^{14,17,18}. Another mutation interfering with the epigenetic landscape is the IDH mutation.

1.1.1.1 IDH mutation

There are three isoforms of the metabolic enzyme IDH. IDH1 is present in cytoplasm, while IDH2 and IDH3 are mainly present in mitochondria. IDH converts isocitrate to α -ketoglutarate. Alternatively α -ketoglutarate can also be generated from glutamine taken up from the extracellular space (glutaminolysis)¹⁹.

If IDH is mutated it gains the ability to convert α -ketoglutarate to the onco-metabolite D-2-hydroxyglutarate (D-2-HG)^{20,21}. The mutation of the IDH2 gene, has a frequency of about 10% in AML patients. The most frequent mutation of IDH2 is the substitution of arginine with glutamine at position 140 (R140Q); there is another mutation at position 172 where an arginine is substituted by lysine (R172K). IDH1 mutations are less frequent in AML

patients (6%)²². There are six mutations known IDH1 -R132H, -R132C, -R132S, -R132L, -R132G and -R132P. The most common are the IDH1-R132C and -R132H mutations (together about 50% of IDH1 mutation)²³.

1.1.1.1.1 Prognosis in AML patients with IDH mutation

As IDH mutations promotes tumorigenesis, but could not cause leukemia by its own it is difficult to estimate its impact on prognosis of AML patients⁹. In the case of gliomas its more straightforward several studies have shown that glioma patients with an IDH1 mutation showed a higher overall survival²⁴⁻²⁶. In AML, the prognosis of patients with IDH mutations is not yet clarified. Wang et al analyzed 2-HG serum level in AML patients. They found that high 2-HG (produced by mutant IDH1/2) levels were associated with lower overall survival and event-free survival in cytogenetically normal AML patients²⁷. Other studies showed similar results in IDH1 mutated AML patients, they had a reduced event-free survival but comparable overall survival^{28,29}. Another study with 826 patients (165 mutated; 59 IDH1-R132, 83 IDH2-R140, and 23 IDH2-R172) found no difference in the cohorts IDH wild type and mutated³⁰. To conclude the prognosis of AML patients with IDH mutation depends on mutation site. In general, prognosis also depend on patient age and treatment regime and cannot be generalized.

1.1.1.1.2 Production of 2-hydroxyglutarate

As mentioned above mutations in the IDH gene leads to the production of D-2-HG. D-2-HG can be measured in sera of AML patients (up to 600 μM)²⁸ but also in much higher concentrations in tissues of glioma patients. Here concentrations up to 35 mM were measured³¹. In AML patients D-2-HG level in sera differ depending on the IDH mutation. In a study were 2-HG level of AML patients with IDH1 R132H mutations were compared with IDH2 R140Q and R172K revealed a comparable level of 2-HG in IDH1 R132H and IDH2 R140Q mutated patients but a higher level in patients with IDH2 R172K mutation³². In another study IDH1 R132H mutated patients had the highest 2-HG level in the sera³³. But there are tumor entities with high 2-HG level without an IDH mutation. In breast cancer cells expressing the transcription factor MYC 2-HG level were also elevated, due to production of 2-HG from glutamine-derived ketoglutarate (glutaminolysis) supported by MYC signaling³⁴.

In addition to the D enantiomere also L-2-HG can be produced. L-2-HG is produced in healthy cells under hypoxic conditions. Malate dehydrogenase 1 and 2 and lactate dehydrogenase A produce L-2-HG out of α -ketoglutarate derived from glutamine³⁵. L-2-HG

is also known to accumulate in renal cell carcinoma; here a mutation in the gene of L-hydroxyglutarate dehydrogenase (LHGDH), an enzyme responsible for the breakdown of L-2-HG, is mutated³⁶.

D-2-HG can be degraded and converted back to α -ketoglutarate; this is catalyzed by D-2-HG dehydrogenase. In this reaction the co-factor FAD is reduced to FADH₂. Ketoglutarate can enter the citric acid cycle and fuel energy production³⁷.

1.1.1.1.3 Effects of 2-hydroxyglutarate

There are several effects and enzyme targets of 2-HG already known. For 2-HG production NADPH is needed and NADP⁺ produced, this alters the NADPH/NADP⁺ ratio and possibly has an influence on the redox balance³⁸⁻⁴⁰.

As shown in Figure 1.1 D-2-HG and L-2-HG inhibit α -ketoglutarate dependent dioxygenases like lysine demethylases (KDM) and Tet methylcytosine dioxygenase 2 (TET2). These enzymes change chromatin accessibility and thereby regulate also gene transcription. The alteration of the epigenetic landscape can lead to a block in differentiation and thereby to tumorigenesis^{41,42}.

2-HG also interferes with Prolyl hydroxylase 2, which destabilize HIF-1 α ^{43,44}. This induces for example the expression of glucose transporters and thereby alters the glucose metabolism of the cell. Collagen maturation is also inhibited by D-2-HG^{39,45}.

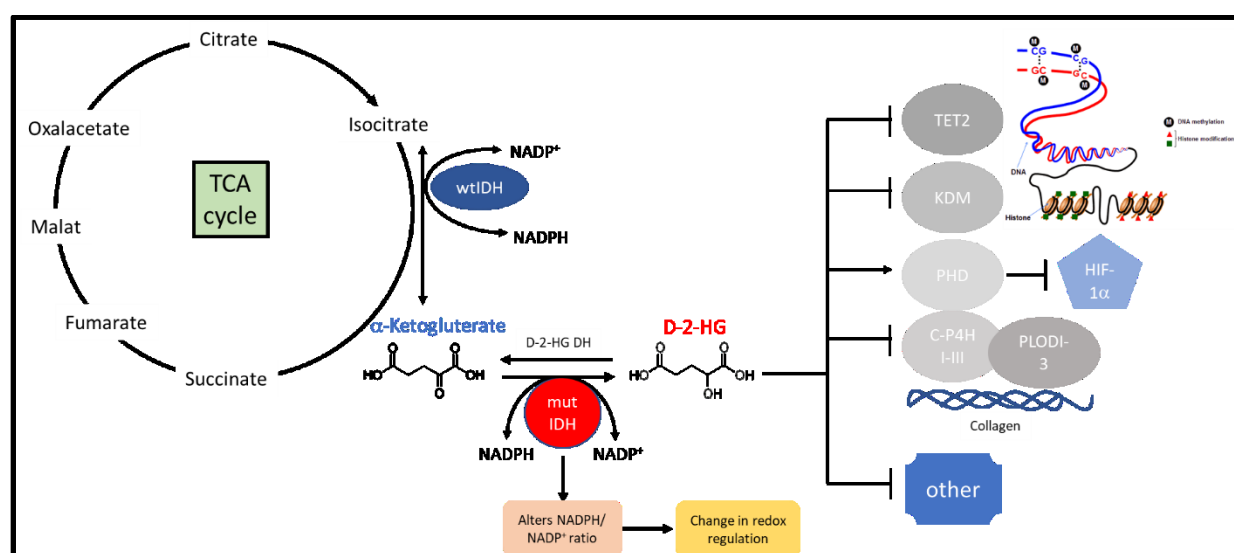


Figure 1.1: Production and effects of 2-HG on α -ketoglutarate dependent dioxygenases

Isocitrate dehydrogenase 2 converts isocitrate to α -Ketoglutarate in citric acid cycle. It acts as a homodimer. If there is a mutation in the enzyme it gains a new function and is able to produce D-2-HG from α -Ketoglutarate and act as a heterodimer with one wild type and one mutated unit. This reaction consumes NADPH and thereby changes the ratio of NADPH/NADP⁺ and redox regulation. D-2-HG itself inhibits α -Ketoglutarate dependent dioxygenases due to the structural similarity to α -

Ketoglutarate. Dioxygenases like TET2 and KDM are involved in DNA and histone methylation. If these enzymes are inhibited changes in the epigenetic landscape may cause a block in differentiation. Prolyl hydroxylase 2(PhD) is also inhibited by D-2-HG, this leads to a stabilization of HiF-1 α . C-H4P and PLODI-3 is also inhibited by 2-HG, this interferes with collagen maturation. KDM, lysine demethylase; TET2, Tet methylcytosine dioxygenase 2; PhD, Prolyl hydroxylase; C-H4P, collagen heavy chain precursor 4. (Adopted from ⁴⁵)

1.2 Epigenetic

Epigenetic factors change gene expression but not by changing the gene sequence; they cause a phenotypic alteration without changing the genotype. The epigenetic landscape can be altered by environmental chemicals, pharmaceuticals/drugs, aging/reactive oxygen species and the diet ^{46,47}. Epigenetics mainly focus on histone and DNA modification. Triggered by an epigenetic factor, histones can for example acetylated which alters how tight DNA is wrapped around histones and finally gene accessibility. The same is true for DNA methylations; here one or more methyl groups are added to DNA base ^{46,48}.

1.2.1 DNA Methylation

In general DNA methylation occurs in cytosine and guanine rich areas, so called “CpG islands”. Methylation can be added or removed to C-5 position of the cytosine ring to modulate gene expression. Sites can be de novo methylated or re-established after replication. De novo methylations are performed by DNA methyltransferases (DNMTs), as mentioned above mutation in these genes are present in leukemia patients.

DNA methylation in most cases is associated with gene silencing ⁴⁹. During differentiation cells need to change the portfolio of expressed genes, so the methyl groups must be removed. This is done by demethylases, for example in dendritic cells (DCs) the dominant demethylase is TET2. TET2 is responsible for the demethylation of gene regions important for differentiation of monocytes to DCs ⁵⁰.

1.3 Immunological background

1.3.1 T cells

There are two main classes of T cells defined by expression of either the costimulatory molecule CD4 (T helper cell) or CD8 (cytotoxic T cells). Depending on the cytokines in the environment CD4 T cells can differentiate into regulatory T cells (T_{reg}, regulation of immune responses) T_H1 cells (protection against intracellular microbes), T_H2 cells (protection against parasites) and T_H17 cells (control of infections) ¹.

CD8 T cell receptors (TCR) recognize peptides of a length of 8-10 amino acids bound to HLA (human leukocyte antigen) class I molecules, while CD4 T cells recognize 14-20

amino acid peptides bound to HLA class II molecules. In general HLA class I peptides are derived from proteins in the cytosol like viral or mutated proteins. HLA class I molecules are expressed on all nucleated cells, while under non-inflammatory conditions class II molecules are only expressed on immune cells and present peptides from phagocytosed extracellular proteins. In some cases also HLA class I molecules can present exogenous proteins, this is known as cross-presentation ¹.

Dendritic cells (DCs) are the only antigen presenting cells (APCs) able to prime and activate naïve T cells ¹. For T cell priming adhesion molecules of DCs (ICAM-1, ICAM-2 and CD58) bind to adhesion molecules on T cells (LFA-1 and CD2). This is important for T cells to scan HLA molecules loaded with antigens presented on HLA molecules of DCs. If naïve T cells recognize their HLA-peptide ligand with the TCR, the affinity of the adhesion molecules increases; this is needed for proliferation and differentiation into effector T cells ¹.

Binding of the TCR, the CD4/CD8 co-receptor and the CD3 molecule (T cell site) to peptide bound HLA molecule (DC site) is only one of at least three signals T cells need to get activated and become a full functional T effector cell. Survival of T cells is induced by binding of the costimulatory molecule CD28 to CD80 or CD86 expressed on APCs (second signal). Finally, the secretion of pro-inflammatory cytokines like interleukine-6 (IL-6), IL-12, IL-4 and IL-23 leads to T cell differentiation and activation ¹. CD28-dependent co-stimulation also leads to IL-2 production and IL-2 receptor α chain (also known as CD25) synthesis. Before stimulation only the β and γ chains of the IL-2 receptor are expressed, and the α chain increases the affinity of the receptor to IL-2. This leads to a higher proliferation rate ¹. After the activation of T cells, they can execute their function as an effector cell and kill pathogens or activate other immune cells. If the activation was strong enough memory cells are generated for a faster response in case of a second infection ¹.

1.3.2 Antigen presenting cells

Professional APCs are DCs, macrophages and B cells. B cells take up antigens by antigen specific receptors, while DCs and macrophages perform micropinocytosis (non-selective uptake of solute molecules, nutrients and antigens) or phagocytosis (uptake solid matter or pathogens). As mentioned above these antigens are then presented on HLA molecules.

1.3.2.1 Dendritic cells

Immature DCs are characterized by high phagocytic activity. After phagocytosis and/or contact with bacterial components, such as lipopolysaccharide (LPS), DCs get activated. LPS

is a bacterial molecule present in the membrane of gram-negative bacteria. LPS activates toll-like receptor 4 (TLR4). There are 10 TLRs known in human. Binding of LPS to TLR4 sequentially leads to the activation of Mitogen-activated protein kinase (MAPK) and transcription factor nuclear factor-kappaB (NF- κ B). This finally leads to activation of DCs and the production and secretion of pro-inflammatory cytokines like IL-12, IL-6 and TNF⁵¹. After activation DCs leave the peripheral tissue and migrate through the lymph system to secondary lymphoid organs. This is possible due to a reorganization of adhesion molecules and the cytoskeleton. During maturation, DCs upregulate the expression of costimulatory molecules and surface marker like CD80/CD86, DC-SIGN and HLA class I and II molecules.

1.3.2.2 HLA class II molecules

The main regulator of HLA class II gene expression is the class II major histocompatibility complex transactivator (CIITA), which is constitutively expressed in professional APCs (DCs, B cells) and can be induced in non-professional APCs for example by interferon γ (IFN γ). DCs and B cells upregulate HLA class II expression during differentiation^{52,53}.

After translation HLA class II molecules enter the endoplasmatic reticulum (ER) and associate with the invariant chain (Ii). Through golgi apparatus traffic machinery HLA class II molecules get delivered to the cell membrane. From there HLA class II molecules reach the multivesicular antigen-processing compartments, in these compartments the Ii is cleaved and only the class II-associated invariant chain peptide (CLIP) remains bound in the peptide groove of the HLA class II molecule⁵⁴.

HLA-DM also present in the antigen-processing compartment, enables the binding of peptide antigens and is regulated by HLA-DO⁵⁵. Antigens enter the antigen-processing compartment through clathrin-mediated endocytosis, macropinocytosis autophagy and phagocytosis. The antigens get proteolytic cleaved in vesicles (endosomes, macropinosomes, autophagosomes and phagolysosomes). These vesicles then fuse to the antigen-processing compartment⁵⁴. It was also shown that HLA molecules bound to Ii reach the antigen-processing compartment without being on the cell membrane before⁵⁶.

If peptides are bound on HLA class II molecule the compartment does a tubulation which allow peptide bound HLA molecule to traffic to and to get released on the cell membrane^{57,58}.

Walseng et al. estimated that about 80% of peptide bound HLA class II molecules are on the cell membrane and 20% intracellular. HLA class II molecules get recycled after

peptide binding and internalization, but this is only possible in mature DCs. After one peptide is released from the HLA class II molecule it can be loaded with another peptide and transported again to the cell membrane⁵⁶.

Electron microscopic analysis revealed different compartments containing HLA class II molecules, there are simplified summarized from literature in Figure 1.2. How these compartments are formed and how they are related is not fully understood.

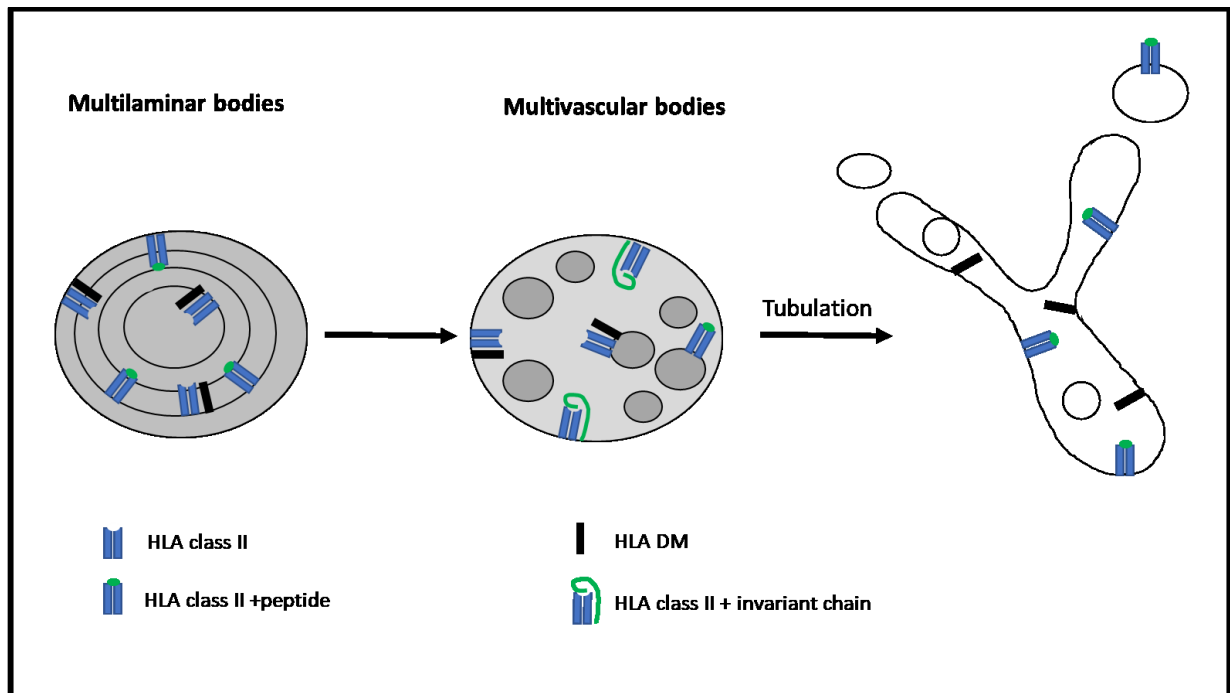


Figure 1.2: Compartments containing HLA molecules. There are different compartments in the cell where HLA class II are present in antigen presenting cells. HLA-DR gold staining revealed the presence of HLA-DR in multilaminar bodies and multivesicular bodies (MVB). MVB undergo tubulation under their maturation. In the tubular structure small vesicles containing peptide loaded HLA-DR get separated and transported to the cell surface (Adopted from⁵⁷⁻⁶⁰).

1.4 Cellular therapy as cancer treatment

In the last decades cellular therapy is evolved a promising strategy to cure cancer. For cellular therapy modified autologous or allogenic cells are transferred to patients for anti-tumor response. Somehow also allogenic stem cell transplantation is a cellular therapy in which the immune cells of the donor eliminate remaining tumor cells after chemotherapy (so called Graft-versus-leukemia effect). To optimize anti-tumor activity, immune cells can be genetically modified before the transfer into patients. T cells are one of the most promising cell types for immune therapy.

It is known that T cells can infiltrate tumor tissue. Clinical studies showed a positive correlation between infiltrated T cells and patients overall survival⁶¹. In another studies in hepatocellular carcinoma and breast cancer, it was found that it was critical which subset was

present, activated CD8 T cells were favorable, while high numbers of regulatory T cells (T_{regs}) were not^{62,63}.

One advantage of using T cells for cellular therapy is that they circulate in blood and lymph nodes scanning for abnormalities and inflammation. As they circulate in the whole body, they can find tumor cells in the whole body. Tumor specific T cells get stimulated by tumor proteins, to proliferate and survive as long as the tumor cells are present. T cells are also able to generate cellular memory by differentiation into memory T cells; they persist and can protect patients from relapse.

1.4.1 Target antigen for cellular therapy

The most important point in the treatment of cancer with cellular therapy is the right cellular target to specifically kill tumor cells without harming healthy cells. There are different types of antigens used as cellular target.

Tumor-associated antigens are over expressed in tumors but also expressed on healthy body cells. But therapies based on tumor-associated antigens showed low efficacy, due to the clearance of TCRs against self-antigens in T cell development⁶⁴. One example are the cancer testis antigens found in melanoma patients, melanoma-associated antigen (MAGE)-1 was the first protein discovered in patients, later also related proteins were found. These proteins are only expressed in tumor cells and healthy testis, MAGE pattern antigens are therefore known as cancer testis (CT) antigens⁶⁵.

Another more promising approach is the use of the tumor-specific antigens (TSA), these antigens are based on somatic missense mutations which are responsible for tumor onset or progression and therefore not expressed in healthy non-tumor cells. T cells stimulated with such antigens would specifically eliminate tumor cells without harmful side effects. In the first part of my PhD project we stimulated T cells with peptides specific for the IDH2 R140Q mutation, where, as mentioned above, the arginine residue present in the wild type enzyme at position 140 is exchanged by a glutamine. Viral proteins in tumors caused by virus injections also give rise to TSAs⁶⁶.

But cellular therapy only targeting one antigen drives the tumor towards a clonal evolution and antigen loss to escape the immune systems. Other strategies are the down regulation of HLA molecule expression. This lowers the level of presented putative tumor specific antigens on tumor cells. Another way is to upregulate inhibitory molecules like PD-

L1, which inhibit T cell function. Tumor cells can also secrete anti-inflammatory cytokines like IL-10 to recruit T_{regs} and inhibit maturation of DCs^{67,68}.

1.5 Metabolites interfere with immune cells

As mentioned above (1.1.1.3) D-2-HG accumulates in cells with IDH mutations. There are also mutations known in succinate dehydrogenase and fumarate hydratase, which lead to an accumulation of succinate and fumarate. All three mutations support the transformation of cells into tumor cells. The metabolites lead to DNA and histone hypermethylation, metabolic changes and changes in post-translational modifications⁶⁹. Accumulation of metabolites in the tumor environment possibly inhibit immune response and lead to an immune escape^{44,69}. One example is lactate, a metabolite produced by anaerobic metabolism of tumor cells, which inhibits T cell and DC function^{70,71}. There is one recently published report showing the effect of D-2-HG on T cells. They show that D-2-HG leads to hypoxia inducible factor 1 α (Hif 1 α) destabilization and thus to an increase in oxidative phosphorylation activity. They also saw a higher frequency of regulatory T cells and a reduced polarization towards Th17 cells⁷². This is in line with results obtained from Xu et al. where there so a reduced Th17 polarization⁷³.

1.5.1 Glucose metabolism

Glucose is transported through the cell membrane by glucose transporters such as Glut1. In the cytosol glucose gets metabolized to pyruvate in glycolysis. In this process 2 ATP molecules and 2 NADH+ 2 H⁺ are produced (Glucose + 2 P_i + 2 ADP + 2 NAD⁺ into 2 Pyruvate + 2 ATP+ 2 NADH+2 H⁺ + 2 H₂O). Under anaerobic conditions pyruvate is converted to lactate. This is done to recycle NAD⁺ as an electron acceptor for glycolysis⁷⁴.

1.5.2 Citric acid cycle

If oxygen is available pyruvate is metabolized further in the mitochondria to acetyl-coA (oxidative decarboxylation) which fuels the tricarboxylic acid (TCA) cycle. TCA cycle is a cycle of 8 enzymes where the released energy and electrons are stored in GTP, NADH and FADH. TCA cycle intermediates serves as a source of precursors for amino acid and lipid synthesis. The high energetic molecules NADH and FADH enter the electron transport chain in the inner mitochondrial membrane⁷⁴.

1.5.3 Oxidative phosphorylation

Oxidative phosphorylation takes place in the mitochondria, more precise in the inner mitochondrial membrane. The inner membrane is folded into numerous cristae, to increases

their surface and provide more space for complexes of the respiration chain. Between the inner and outer mitochondrial membrane, in the intermembrane space, the proton gradient is built through oxidative phosphorylation ⁷⁴.

From the mitochondrial matrix protons and electrons of $\text{NADH} + \text{H}^+$ enter complex I (NADH dehydrogenase) of the respiration chain. FADH_2 is already produced by complex II (succinate dehydrogenase) as an enzyme of the TCA cycle and fuels its proton and electron directly in complex II. Protons are transported through mitochondria matrix into the intermembrane space. Electrons are transported further to complex III (ubiquinol–cytochrome c oxidoreductase) through ubiquinone (Q) which can move in the mitochondria matrix along the inner membrane. Complex III and IV (cytochrome c oxidase) also transport protons into the intermembrane space. The proton gradient is used to activate ATP synthase and induce the movement of the upper part of the ATP synthase (proton motoric force). This is needed for ATP production from inorganic phosphate and ADP ⁷⁴.

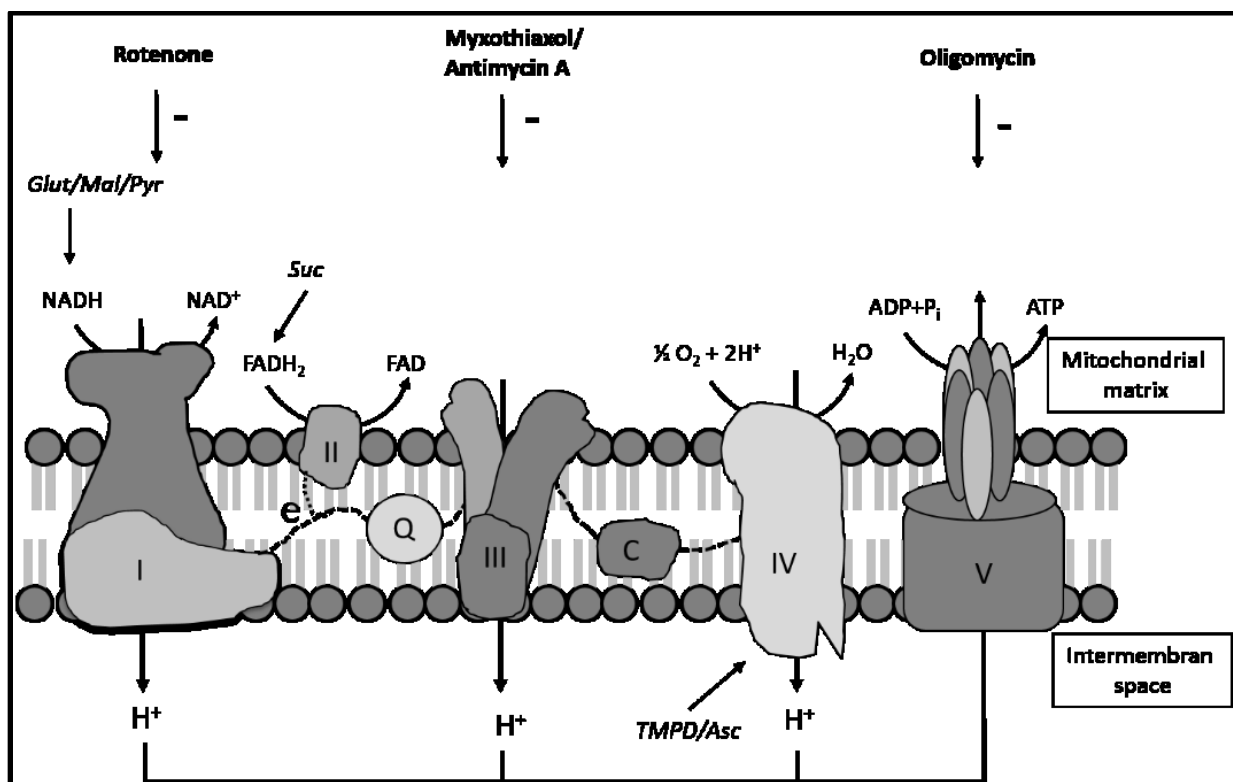


Figure 1.3: Complexes of electron transport chain in the inner mitochondrial membrane

Electrons from NADH/FADH are transported through the complexes of electron transport chain (ETC) to complex IV where water is produced. Protons from NADH/FADH were transported into intermembrane space of mitochondria to establish proton gradient. Proton gradient is used to produce ATP from inorganic phosphate. Respiration activity can be modulated by the addition of different inhibitors. Rotenone inhibits complex I, myxothiazol or antimycin A inhibit complex II and complex V is inhibited by oligomycin. Glutamate, malate and pyruvate are substrates for complex I, while succinate enters oxidative phosphorylation from complex II. (Adopted from ⁷⁵)

1.5.4 Metabolism of dendritic cells

During DC differentiation from monocytes metabolism is mainly based on oxidative phosphorylation in the mitochondria. Monocyte culture with granulocyte– macrophage colony-stimulating factor (GM-CSF) and interleukin-4 (IL-4) leads to an increased expression of peroxisome proliferator-activated receptor- γ (PPAR γ)^{76,77}. PPAR γ a transcription factor regulating lipid metabolism, and controls PPAR γ co-activator 1 α (PGC1 α). Both, upregulation of PPAR γ and PGC1 α leads to an increase in mitochondrial biogenesis⁷⁸. *In vitro* DC development out of monocytes also depend on fatty acid synthesis⁷⁹. Fatty acid oxidation is also the main metabolic process in immature DCs⁸⁰.

Activation of DCs by TLR agonists leads to a rapid increase of glucose uptake and lactate production⁷⁹. These metabolic changes are caused by downstream pathway of TLRs that involves protein kinase B (AKT), TANK-binding kinase 1 (TBK1), inhibitor of nuclear factor- κ B kinase subunit- ϵ (IKK ϵ) and hexokinase 2 (HK2).

In the activated stage DCs remain glycolytic under the control of mammalian Target of Rapamycin (mTOR) and HIF1 α ⁸⁰. Glycolysis is important for activation as inhibition of glycolysis with 2-deoxyglucose (an inhibitor of hexokinase) also inhibits DC activation⁸¹.

1.5.5 Oxidative stress

Oxidative stress rises if there is an imbalance of free radicals produced and the buffering capacity of the antioxidant defense system. Oxidative stress can lead to modifications on proteins, lipids and DNA⁸².

1.5.5.1 Production of reactive oxygen species

During electron transport through the inner membrane of the mitochondria in oxidative phosphorylation reactive oxygen species (ROS) may be formed. Electrons which prematurely exit the chain may reduce oxygen to form superoxide (O₂^{-•}). Each complex in the electron transport chain can form superoxides, while complex I and III are the main producer in the mitochondria. It is estimated that about 0.2-2.0% of the oxygen consumed is transformed to ROS⁷⁵.

Another source of ROS is the NADPH oxidase. NADPH oxidase catalyzes the production of superoxide from oxygen and NADPH. Also, other ROS like peroxide can be produced by dismutation of superoxide. NADPH oxidase is present in professional phagocytes neutrophils, eosinophils, monocytes and macrophages in stages of their

development. NADPH oxidase produces agents, which get released (oxidative burst) to kill pathogens in contact with the phagocyte. Neutrophils, monocytes and macrophages then take up the pathogens⁸¹.

1.5.5.2 Role of ROS in DCs

There are different studies done on the role of ROS in the differentiation and activation of DCs. Harari and Liao et al. showed an inhibitory effect of antioxidant addition (during DC differentiation) on HLA class II expression⁸³. ROS were also reported to be important for DC activation as LPS increase ROS level in DCs⁸⁴ and addition of ROS led to the activation of DCs⁸⁵. Del Prete et al. also suggest that ROS play a crucial role in DC differentiation and addition of catalase (neutralize peroxide) inhibit DC function⁸⁶. In contrast to this, Malinarich et al. showed that induced tolerogenic DCs (induced by dexamethasone and vitamin D3) showed higher ROS production due to a higher mitochondrial activity⁸⁷.

1.6 Project aims

In AML there are high relapse rates especially in elderly. The aim of my first PhD project was the generation of leukemia specific T cells. As a target the mutant IDH2 R140Q was chosen because is not expressed in healthy cells and therefore a tumor specific tumor antigen.

For the generation of IDH2 specific T cells, T cells were stimulated with a IDH2 R140Q specific antigen bound to an HLA molecule on APCs. The specific antigen was provided by expression, processing and presentation of the mutated protein (IDH2 R140Q) in DCs or by exogenous loading of mutation specific peptides. The reactivity of these T cells was assayed by interferon γ ELISpots. T cells specificity against the mutated protein or peptide was evaluated with corresponding wild type peptide loaded and IDH2 wild type expressing DCs. If IDH2 R140Q specific T cells were generated, in long perspective, they should be used for cell therapy to eliminate blasts in patients with minimal rest disease.

The “oncometabolite” D-2-HG produced by IDH has several known targets in the cell which promotes tumorigenesis but could not cause leukemia by its own. The aim of my second project was to find out how D-2-HG interferes with the differentiation from monocytes to DCs. This was analyzed by flow cytometric analysis of dendritic cell specific surface marker expression (HLA class I and II, costimulatory molecules, differentiation marker). Further characterization was done by cytokine ELISAs and functional tests like phagocytosis assay

and mixed lymphocyte reaction in an allogeneic setting. The influence of D-2-HG on the metabolism of DCs was analyzed by glucose, oxygen and lactate concentration analysis and reactive oxygen species measurements.

Based on the results we tried to rescue the effects caused by D-2-HG with anti-metabolic and anti-oxidative drugs.

2 Material and Methods

2.1 Material

2.1.1 Equipment and consumables

Table 1: List of equipment

Advice	Company
Steri-cycle CO ₂ incubator	Fischer Scientific
Reaction tube centrifuge	Eppendorf
Centrifuge 16R, 40R	Fischer Scientific
Lamina flow	Fischer Scientific
Scale	Kern
Inverted microscope	Zeiss
Flow cytometer, BDCalibur	Becton Dickinson
Cell sorter, BD Aria III	Becton Dickinson
CASY Cell Counter and Analyzer System Model TT	Roche Innovatis AG
pH-Meter	Hanna Instruments
Well wash 4 MK 2	Thermo Electron Corporation
NanoDrop ND1000	PeqLab
CTL Elispot reader	ImmunoSpot
Pipet boy	Integra
Centrifuge Avanti J-20XP; Rotor JE 5.0	Beckmann Coulter
Elutriator Avanti J-20XP	Beckmann Coulter
Flow chamber (elutration)	Beckmann Coulter
Shaker	Heidolph
Electrophorese system	BioRad
Blotting device	Blue power plus
Photometer	Eppendorf
Western blot imager, Fusion Pulse	Vilber
Bioluminescence reader	Berthold
Typhoon Gel and Blot Imaging Systems	GE healthcare
Gene pulser, electroporator	Biorad
PCR cycler	Eppendorf

Table 2: List of plastic consumables

Component	Company
Plates for ELISA	Costar
Sterile Filter	Millipore
Pipettes (2, 5, 10, 25, 50 ml)	Greiner
Cell culture flasks (T25, T75, T175)	Greiner
Cell culture plates	Greiner
14mL, 50mL tubes	Greiner
Polyprene tubes	Becton Dickinson
0.5, 1.5, 2.0 mL tubes (safe look, RNase free)	Eppendorf
Kuvette (electroporation)	Biorad
Kuvette plastic (OD measurement)	Roche

Table 3: Equipment and consumables used for respiration analysis

Equipment	Company
------------------	----------------

Gastight 1700 Syringes (10,25,50µl)	Hamilton
Hot-Air Disinfectable Gassed Incubator BBD	Termo Fisher
OxoDish®, HydroDish®	PreSens
Oxygraph-2k	Oroborus Instruments
SDR SensorDish® Reader	PreSens

2.2.1 Chemicals

Table 4: List of chemicals

Component	Company
L-2-HG, D-2-HG	Sigma Aldrich
Trolox	Sigma Aldrich
Tempol	Santa cruz
Ethanol (96%)	Roth
Milk powder	Sucofin
Isopropanol	Roth/Braun
Chloroform	Sigma Aldrich
Phenol/chloroform	Roth
BSA	Sigma Aldrich
Vitamin C	Sigma Aldrich
Metformin	Sigma Aldrich
Pioglitazone	Sigma Aldrich
Peroxide	Sigma Aldrich
Methanol	Merck
DMSO	Roth
Malate	Sigma Aldrich
Digitonin	Sigma Aldrich
ADP	Sigma Aldrich
MgCl ₂	Roth
Pyruvate	Sigma Aldrich
Glutamate	Sigma Aldrich
Succinate	Sigma Aldrich
FCCP	Sigma Aldrich
Rotenone	Sigma Aldrich
Myxothiazol	Sigma Aldrich
TMPD	Sigma Aldrich
Sodium azide	Sigma Aldrich
EGTA	Roth
MgCl ₂ 6 H ₂ O	Roth
Lactobionic acid	Sigma Aldrich
Taurine	Sigma Aldrich
KH ₂ PO ₄	Sigma Aldrich
HEPES	Sigma Aldrich
D-Sucrose	Sigma Aldrich
BSA, essentially fatty acid free	Sigma Aldrich
RIPA Buffer	Sigma Aldrich
Protease inhibitor	Roche
Dimethylformamid	Sigma Aldrich

Table 5: Reagents used for flow cytometry analyses

Reagent	Company
FACS clean	BD Biosciences, Franklin Lakes, NJ, USA

FACS flow	BD Biosciences, Franklin Lakes, NJ, USA
FACS rinse	BD Biosciences, Franklin Lakes, NJ, USA

Table 6: Material and reagents used for SDS gels and western blotting

Reagent/Material	Company
SDS	Sigma
Acrylamid 30%	Carl Roth
Tris/HCl	Roth
Glycerin	Roth
2-Mercaptoethanol	Sigma Aldrich
Bromphenolblau	Sigma Aldrich
Methanol	Roth
ϵ -Amino-n-caproic acid	Sigma Aldrich
polyvinylidene fluoride membrane	Millipore
Filter paper 3MM Whatman, Dassel, Germany	Filter paper 3MM Whatman, Dassel, Germany
Tween	Sigma Aldrich
APS	Merck Millipore
TEMED	Sigma-Aldrich
Triton X100	Sigma-Aldrich
ReBlot Plus Mild	Milipore
Kaleidoscope Pre-stained Standard	BioRad

Table 7: Components of agarose gel to analyze RNA

Component	Company
Formaldehyde	Sigma Aldrich
MOPS	Sigma Aldrich
Sodium Acetat	Sigma Aldrich
EDTA	Roth
Agarose	Roth
RotiSafe	Roth
DEPC	Sigma Aldrich
Formaldehyde loading dye	Ambion

2.3.1 Fluorescence probes and antibodies

Table 8: List of antibodies used for flow cytometry analyses

Specificity	Clone	Company	Volume for 200,000 cells
HLA-DP PE	BRAFB6	Santa cruz	1 μ l
HLA-DQ FITC	Tu169	BD bioscience	1 μ l
HLA-DR APC	L243	BD bioscience	1 μ l
HLA-ABC PE	G46-2.6	BD bioscience	1 μ l
DC-SIGN PE	FAB161P	R&D	1 μ l
CD1a PECy7	HI149	BD bioscience	1 μ l
ILT-3 APC	ZM4.1	BioLegend	2 μ l
ILT-2 PE Cy 7	GHI/75	BioLegend	2 μ l
TIM-3 PE Cy 7	F38-2E2	BioLegend	2 μ l
BTLA PE	MIH26	BioLegend	2 μ l
CD80 FITC	L307	BD bioscience	2 μ l
CD86 FITC	2331	BD bioscience	2 μ l
CD83 FITC	HB15e	BD bioscience	2 μ l

CD4 FITC	RPA-T4	BD bioscience	1 μ l
CD4 V450	RPA-T4	BD bioscience	1 μ l
CD25 APC	BC96	BioLegend	1 μ l
FoxP3 PE	PCH101	eBioscience	5 μ l
CD14 FITC	M5E2	BD Bioscience	1 μ l
CD3 APC	UCHT1	BD Bioscience	1 μ l
CD45RA PE	HI100	BD Bioscience	2 μ l

Table 9: List of fluorescence probes used in flow cytometry

Substance	Company
MitSox	Invitrogen
Mitotracker	Invitrogen
DCFDA	Sigma Aldrich

Table 10: List of antibodies used for western blot analyses

Specificity	Clone	Company	Dilution
Rabbit anti-LC3B	EPR16883	Abcam	1:500
Rabbit anti-PKC	M110	Abcam	1:1000
Rabbit anti-Rab9	EPR13272	Abcam	1:1000
Mouse anti-MHC II	EPR11226	Abcam	1:10000
Rabbit anti-actin	G250	Cell signaling,	1:1000
Goat anti-rabbit HRP	P0448	Dako, P0448	1:2500
Goat anti-mouse HRP	P0447	Dako, P0447	1:2500

2.4.1 Cell culture material

Table 11: Cell culture media and supplementaries

Supplementary	Company
RPMI	Gibco
AIMV	Gibco
Hepes buffer 1M	Sigma Aldrich
penicillin/streptomycin	Gibco
Glutamine	Gibco
Human sera	Bavarian Red Cross
Fetal calf sera	Sigma Aldrich

Table 12: List of cytokine used in cell culture

Cytokine	Company
IL-1b	Miltenyi Biotec
IL-2	Novartis
IL-4	Miltenyi Biotec
IL-6	Miltenyi Biotec
IL-7	Miltenyi Biotec
IL-15	Miltenyi Biotec
IFN γ	eBioscience
TNF α	PromoCell
GM-CSF	Sanofi
PGE2	Sigma Aldrich

Table 13: Other substances

Substance	Company
Phosphat buffered saline (PBS)	Sigma Aldrich
Pancoll	PAA
HANKs Buffer	Sigma Aldrich

Table 14: Material for magnetic-activated cell separation

Component	Company
LS columns	Miltenyi Biotec
Pre-separation filters	Miltenyi Biotec
QuadroMACS separator	Miltenyi Biotec
CD4 magnetic Beads	Miltenyi Biotec
CD8 magnetic Beads	Miltenyi Biotec
CD45RA magnetic Beads	Miltenyi Biotec

Table 15: Material and reagents used for ELISpot

Reagent/Material	Company
ELISpot Platte	Milipore
Capture Antibody (Anti-human IFN γ -Mab1-D1K)	Lophius
Detection Antibody (Ak 7B61)	Lophius
Streptavidin ABC solution vectastain	Vector Laboratories
PBS powder	Biochrom
Tween	Sigma Aldrich
Ethanol	Roth
BSA	Sigma
Peroxide	Sigma
3-Amino-9-Ethyl-carbazole	Sigma

Table 16: Enzymes

Enzyme	Company
Restriction enzyme Xba I	New England Biolabs
Restriction enzyme Xho I	New England Biolabs
Restriction enzyme Spe I	New England Biolabs
T4 Ligase	New England Biolabs
Alkalic Phosphatase CIP	New England Biolabs

2.5.1 Kits

Table 17: List of kits

Kit	Company
mMESSAGE mMACHINE T7 Ultra Kit	Ambion
RNA-Recovery with RNeasy® Mini Kit-RNA cleanup	Quiagen
DNeasy Blood and tissue	Quiagen
Intracellular FACS staining	BD, eBioscience
DNA methylation kit	Zymo research europa
IL-12, IL-10, TNF, IFN γ , IL-6 ELISA	R&D

cAMP determination kit	Cell signaling
ATP determination kit	Thermo fischer
DC protein assay (protein determination)	BioRad
ECL substrate solution	GE Healthcare
Cytofix/Cytoperm Fixation and Permeabilization Solution	BD

2.6.1 Software

Program	Company
CellQuestPro	BD
GraphPad Prism 6	GraphPad Software
Microsoft Office 2011	Microsoft Redmond
DatLab4	Oroboros instruments
PreSense	PreSens, Regensburg
FlowJo v9.5.3	FlowJo,LLC
ImageJ	National Health Institute
Clone manager	Sci-Ed Software
Soft Max	Molecular devices
Mendeley	Elsevier

2.2 Methods

2.2.1 IDH2_{Mut} specific stimulation of T cells

T cell stimulation was done with peptide (IDH2 R140Q specific) loaded APCs and DCs expressing mutant IDH2R140Q. For peptide stimulation, peptide antigens were predicted with online tools and loaded on APC.

2.2.1.1 In silico Peptide prediction

Online tools (SYFPEITHI, BIMAS, NetMHCpan) were used to predict peptide epitopes specific for mutated isocitrate dehydrogenase 2. We focused on 8-10 meres spanning the mutated amino acid at position 140 where arginine is substituted with glutamine (R140Q). For all prediction tools amino acid sequence of the IDH2 R140Q protein was entered for peptide epitope prediction. In the following, the used platforms are summarized. Results of peptide prediction are summarized in Table 3.1.

2.2.1.1.1 SYFPEITHI

SYFPEITHI algorithm predicts T cell epitopes. In simple words, the algorithm gives scores to amino acid at each position of the possible peptide sequences based on known T cell receptor epitopes, natural ligands or binding peptides. Prediction efficacy depends on the amount of known binders to the selected HLA class I molecule. The higher the score, the more likely that the predicted peptide is a T cell epitope⁸⁸.

2.2.1.1.2 BIMAS

BIMAS algorithm predicts HLA peptide binding. It calculates half-time of dissociation to the selected HLA class I molecule. This is also made based on known peptide HLA class I molecule interactions. The higher the score, the stronger the predicted binding to the HLA class I molecule⁸⁹.

2.2.1.1.3 NetMHCPan

NetMHCpan server uses artificial neural networks trained with quantitative binding data of more than 150 different HLA molecules. The binding of peptides with a length of 8-14 amino acids can be predicted to HLA class I molecules (HLA-A, B, C, E and G alleles), while the prediction of 9mer peptides are the most accurate. As a result an IC₅₀ is calculated, the lower the value the higher the affinity to the selected HLA molecule⁹⁰.

2.2.1.2 IDH2 R140Q specific Peptides

Peptides which had a high probability to be presented on HLA class I molecules were purchased from JPT Peptide Technologies. In addition, peptides overlapping the mutated site at position 140 (R140Q) were designed and purchased also at JPT Peptide Technologies. Peptide sequences are shown in Table 19.

Table 19: Peptide sequences of IDH2 and IDH2 R140Q specific peptides

IDH2	IDH2 R140Q	Company
IRNILGGTVF	IQNILGGTVF	JPT Peptide Technologies
IRNILGGTV	IQNILGGTV	JPT Peptide Technologies
TIRNILGGTV	TIQNILGGTV	JPT Peptide Technologies
SPNGTIRNI	SPNGTIQNI	JPT Peptide Technologies
-	QNILGGTVF	JPT Peptide Technologies
-	TIQNILGGT	JPT Peptide Technologies
-	GTIQNILGG	JPT Peptide Technologies
-	NGTIQNILG	JPT Peptide Technologies
-	PNGTIQNIL	JPT Peptide Technologies
-	SPNGTIQNI	JPT Peptide Technologies
-	KSPNGTIQN	JPT Peptide Technologies
-	WKSPNGTIQ	JPT Peptide Technologies

2.2.1.4 Preparation of IDH mRNA

In the second stimulation protocol the coding region of wild type IDH2 including an HIS tail was bought in a production vector at Gene ART. The insert containing the coding region and the HIS tail was transferred in pGEM4Z-65A vector for *in vitro* mRNA transcription⁹¹. Nucleotide exchange with the quickchange kit revealed the corresponding sequence of IDH2 R140Q. Both constructs were used to transfect DCs for T cell stimulation (IDH2 R140Q) or reactivity assays. In another approach the insert was further modified with a signal peptide and the DC lamp1 gene (purchased) and processed like described in the following.

2.2.1.4.1 Digestion

Plasmid was digested to isolate the coding region of the IDH2 gene from the vector. For this 50 µl DNA was mixed with 7 µl cutsmart buffer (10x), the restriction enzymes Xba and Xho 3 µl each and 7 µl water. Mixture was incubated 16 h at 37°C.

2.2.1.4.2 Agarose gel

After digestion an agarose gel was run to check if digestion was successful. For that 6 g of agarose was mixed with 60 ml TRIS-Acetate-EDTA (TAE, 40 mM Tris-acetate and 1 mM EDTA, pH 8.3) buffer and heated in the microwave till it was dissolved. After solution came back to a temperature of 65°C 3 µl RotiSafe was added to stain DNA. After gel was hard gel was run at 100 V for 50 minutes. Gel was images with gel imager typhoon.

2.2.1.4.3 PCR Purification with High pure PCR product purification kit

PCR purification was performed between enzyme incubation, to separate the enzymes from the DNA. PCR product was bound on a column containing silica in high-salt buffer and eluted with low-salt buffer elution buffer. 50 µl DNA reaction (e.g. after digestion or dephosphorylation) was transferred to the column and further processed like described in the manufactures' protocol Purified DNA was eluted with 50 µl elution buffer.

2.2.1.4.5 Dephosphorylation of phosphates on the ends of the linearized vector

Digested vector was incubated with alkaline phosphatase from calf intestinal (CIP). CIP nonspecifically catalyzes the dephosphorylation of 5' and 3' ends of DNA and RNA phosphomonoesters, this prevents the re-ligation of the sticky ends of the vector with itself. For this reaction the following components were mixed and incubated for 2 h at 37°C.

Table 20: Dephosphorylation reaction

Component	Volume
Vektor	50 µl
10x Cut Smart Buffer	6 µl
Nuclease Free Water	1 µl
CIP	3 µl

After the incubation time 2 µl of fresh CIP was added and sample was incubated another 30 minutes at 55°C. After that another PCR purification was performed as mentioned above.

2.2.1.4.6 Ligation of insert in the vector

For ligation of dephosphorylated and purified vector and purified insert the following enzyme and solutions were used:

Table 21: Reagents for ligation

Reagent	Sample [μ l]	Control [μ l]
Vector	1	1
Insert	15	-
T4 Ligase buffer	2	2
Nuclease Free Water	1	16
T4 Ligase	1	1

The reagents were mixed and incubated 16 h at 16°C. During this time the ligase ligated the sticky ends of the vector and insert together, the product is a circular vector containing the insert.

2.2.1.4.7 Transformation of Plasmid DNA

To amplify the amount of insert containing plasmid, the construct was transformed in bacteria. Competent cells (JM109, E.coli) was thawed on ice and then mixed with 10 μ l of ligated plasmid containing IDH2 wild type coding region. Bacteria solution was incubated 30 minutes on ice and mixed now and then. Bacteria were incubated 45s at 42°C, to deliver the DNA plasmid into bacteria. After 1 minute incubation on ice bacteria were transferred in 1 ml LB (composition shown in Table 22) and incubated 40 minute at 37°C and 280 rpm shaking. After incubation solution was transferred in 1.5 ml tube and centrifuged 5minute at 4000 rpm. Flow through was discarded and pellet was resuspended in 50 μ l LB media and seeded on LB plates supplemented with Ampicilin (100 μ g/ μ l). Vector also contains an ampicillin resistance gene, which allow transformed bacteria to growth on these plates. Plate was incubated at 37°C overnight.

Table 22: Components of lysogeny broth (LB) media

Component	Amount for 1l
Yeast	5 g
Trypton	10 g
NaCl	10 g
Millipore Water	Up to 1 l after set pH to 7

2.2.1.4.8 Plasmid isolation out of bacteria

Depending on the amount of DNA needed Mini- or Midi preparation kits purchased from Qiagen were performed. The used method is based on alkali lysis ⁹². Buffer 2 containing SDS solves phospholipids and proteins out of the cell membrane. The high pH denaturates proteins, chromosomal DNA as well as plasmid DNA, this is neutralized by buffer 3. In

parallel high salt conditions lead to a precipitation of the denaturated protein, chromosomal DNA and cell debris with SDS. While plasmid DNA gets renatured and solved. Plasmid DNA binds to a silica membrane in a centrifugation column and gets washed. Plasmid DNA gets eluted with nuclease free water and stored at -20°C.

2.2.1.4.9 Concentration measurement with nano drop

If samples with suitable size of vector and insert were observed (checked with agarose gel), their concentration was measured. For concentration measurement of DNA or RNA the nano drop device was used, it measures absorbance of sample at different wavelengths and so determines the concentration and contamination with proteins, phenols or other contaminants.

Table 23: Values for DNA/RNA purity

ratio	Values
260/280	DNA sample: value of 1.8 is pure DNA RNA sample: value of 2.0 is pure DNA
260/230	without contamination 2.0-2.2 with contamination lower

For a measurement, 1 µl sample was transferred to the measuring chamber and spectra were measured. As an output you get the concentration and purity of the sample. The meaning of purity values is summarized in Table 23.

2.2.1.4.10 Sequencing of inserts

After measuring concentration of DNA construct, samples were sent to GATC for Light RUN sequencing. 5 µl of plasmid DNA (100 ng/µl) was mixed with 5 µl primer (5 µM) for sequencing (for sequence see Table 24). After receiving sequencing data from GATC, sequence identity was analyzed with Clone manager.

Table 24: Sequencing primer

Name	Sequence
for_pGEM4Z_S	CGCCCAGCTCTAATACGACTC
rev_pGEM4Z_S	GGAGCAGATACGAATGGCTAC

2.2.1.4.11 Mutagenese Quickchange

With QuikChange Site-Directed Mutagenesis Kit site directed mutagenesis was performed to exchange the nucleotide responsible for the exchange of arginine to glutamine in the amino acid sequence of IDH2 (IDH2 R140Q). A mutation site overlapping (15-20bp) primer was designed (total length 29bp, CCC CAG GAT GTT CTG GAT AGT TCC ATT GG) and used in a PCR cycling program. Addition of a restriction enzyme (DpnI) which degraded methylated template plasmid by sparing newly synthesized unmethylated mutated DNA.

Table 25: Reagents used for quickchange mutagenese

Component	Amount
5µl	10x reaction buffer
50 ng	Plasmid DNA
125 ng	Primer 1
125 ng	Primer 2
1 µl	dNTP mix
To 50µl	Nuclease Free Water

Reagents were mixed as described in Table 25 and transferred in PCR cyler. Cycling program for PCR was started as described in the following table.

Table 26: Cycler protocol for quickchange mutagenesis

Segment	Cycles	Temperature	Time
1	1	95°C	30 seconds
2	12–18	95°C	30 seconds
		55°C	1 minute
		68°C	2 minutes (minute/kb of plasmid length)

During the PCR program the mutation containing primer gets elongated to form a plasmid containing the mutated site. Addition of DpnI degraded methylated template vector, as a result all plasmid DNA contained the mutated site.

PCR product was used for transformation in XL-blue E. coli strand as described in section 2.2.1.2.6. Colonies were analyzed by miniprep and sequencing as described above.

Correct clone was duplicated with a midprep and used as a construct for *in vitro* synthesis and electroporation experiments.

Finally, the construct contained the following parts. Before the insertion site a T7 promotor was present to allow *in vitro* mRNA synthesis. The insert was ligated with the restriction enzymes XbaI and XhoI. Here the insert containing the mutated IDH2 R140Q is followed by a histidine tag to control expression. The construct was inserted into a pGEM4Z-65A vector backbone.

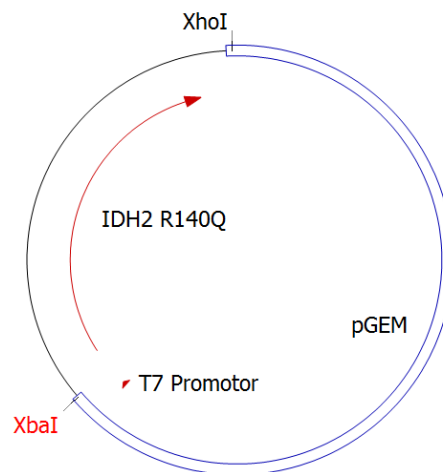


Figure 2.1: Map of pGEM4Z-65A vector containing the IDH2 R140Q coding region. Insert (IDH2 R140Q coding region) was ligated with XbaI and XhoI restriction sites into the pGEM4Z-65A vector. The pGEM4Z-65A vector also carried an ampicillin resistance which is not shown here⁹¹.

2.2.1.4.12 Linearization of vector

Genes inserted to vectors containing a T7 promotor were generated like described above. Before mRNA transcription the vector had to be linearized and purified. Vector was linearized with the restriction enzyme Spe I over night with the following reagents:

Table 27: Components for linearization of plasmid

Component	Amount
DNA	20 µg
SpeI	3 µl
Cutsmart 10x	1:10 dependent on total volume
Nuclease Free Water	up to the next

2.2.1.4.13 Phenol-Chlorophorm extraction

After linearization, DNA was purified by phenol-chlorophorm extraction to remove residual salts from buffers and proteins. Linearized plasmid DNA was filled up to 400 μ l with DEPC H₂O and mixed with 400 μ l Phenol/Chlorophorm/Isoamylalcohol solution by vortexing. Tube was centrifuged 5 minutes at maximal speed to achieve phase separation. Upper aqueous phase was transferred in a tube with 400 μ l Phenol/Chlorophorm/Isoamylalcohol and washed again. In total, five washing steps with Phenol/Chlorophorm/Isoamylalcohol solution were performed. Followed by 5 washing steps with 400 μ l Chlorophorm, after the last washing the upper phase was transferred in an RNase free tube and mixed with 40 μ l sodium acetate (3M), ethanol (100%) was added and tube was incubated 2-24 h at -20°C. Sample was centrifuged 30 minutes at maximal speed at 4°C. Supernatant was discharged and pellet was resuspended in 1400 μ l cold 70% ethanol and centrifuged as before. Supernatant was discharged, and pellet was air dried at room temperature. Pellet was resuspended in 40 μ l DEPC H₂O and concentration was measured with nano drop devise (2.2.1.2.8).

2.2.1.4.14 In-vitro transcription and purification of mRNA

Linearized and purified plasmid DNA was *in vitro* transcribed under RNase-free conditions. Prerequisite to use this mMACHINE T7 Ultra Kit is a T7 RNA polymerase promoter which is here already inserted in the pGEM4Z-65A backbone. Protocol was performed as described by the manufacture. Besides the 1 h incubation where the anti-reverse cap analog (ARCA) was build at the 5' end of the product was increased to 3 h. The cap analog is modified (OCH₃ group instead of a fourth 3'-OH group) which optimized the yield of functional mRNA. In general caps or also the poly A tail improve the stability of the mRNA *in vivo*. After that the DNA templet was digested with DNase and a Polyadenylation was performed, here the incubation time was increased to 1 h. After that 700 μ l RLT buffer and 500 μ l ethanol was mixed with the reaction mix and the mRNA was purified from enzymes and buffer with the RNeasy Mini Kit-RNA cleanup kit from Quiagen. RNA was eluted with 80 μ l RNase free water and stored at -80°C.

2.2.1.4.15 RNA gel

In vitro transcribed and purified mRNA was analyzed with an agarose gel, to check integrity, length and poly adenylation of RNA. 1.2 g of agarose was solved in 5 ml 10x MOPS (0.2 M MOPS, 20 mM sodium acetate and 10mM EDTA) buffer and 45 ml of DEPC water was added to get a 1.2% gel. Agarose was solved in the microwave and cooled down to 65°C

before 900 μ l, Formaldehyde and 3 μ l RotiSafe was added under the safety hood. Agarose solution was cast in a chamber under the hood and incubated till it was solid. Gel was equilibrated 30 minutes in running buffer (1X MOPS buffer, 2% Formaldehyde in DEPC water). Samples were prepared by mixing 2 μ l RNA sample to 1 μ l loading buffer (Formaldehyde loading buffer from mMESSAGING mMACHINE kit) and 10 μ l DEPC water. Sample mixtures were heated to 65°C for 5 minutes and chilled on ice before gel loading. Gel was ran 45 minutes at 100 V. Gel was imaged with typhoon advice.

2.2.1.5 General cell culture

All cells used were cultivated at 37°C 5% CO₂ and about 100% humidity. Cells were only handled sterile under the laminar flow and counted with Neubauer counting chambers and trypan blue. Trypan blue solution was used to exclude dead cells which appear blue in phase contrast microscopy because the dye is not able to move across intact cell membrane. Culture media supplemented with phenol red was used. Phenol red is a pH indicator; it turns reddish if the solution has a neutral pH and gets yellowish if pH drops. Cells produce acids during metabolism, for energy production necessary for cell proliferation. The color of the media, remaining growth area and cell number was used to decide if the cells had to be sub-cultured. In general if not mentioned cells were centrifuged at 1500 rpm for 5 minutes.

2.2.1.5.1 Counting of cells

Cells were resuspended and 50 μ l cell suspension was mixed with the same volume of trypan blue. This results in a 1:2 dilution. This solution was transferred into a Neubauer chamber and 2 big squared were counted. Cell number counted was divided by 2 and multiplied with 10⁴ and the dilution factor 2.

2.2.1.5.2 Thawing of cells

Long time storage of cells was done in the nitrogen tank at -150°C. Cells were thawed in the water bath at 37°C till half of cell suspension was thawed. Then cells were put in 20 ml media and centrifuged. Pellet was resuspended in fresh culture media and seeded according to their cell number.

2.2.1.5.3 Freezing of cells

Cells were harvested and centrifuged. Pellet was resuspended in 1 ml FCS with 10% DMSO per cryo tube. Cell suspension was aliquoted into the cryo tubes and put in a freezing container filled with 100% isopropanol to assure a slow and gentle (cooling rate 1°C/minute)

cell freezing without ice crystals which could destroy the cells. Freezing container was stored at -80°C overnight and then cells were frozen and put on their storage place in the nitrogen tank.

2.2.1.6 Isolate Peripheral blood mononuclear cell from blood samples of healthy donors

As a source of peripheral blood mononuclear cells (PBMCs) residual cells from platelet donations of healthy donors from the transfusion medicine of the University Hospital Regensburg were used and preceded like following.

2.2.1.6.1 Pancoll separation

Human blood was diluted 1:2 with PBS. Mixture was carefully added dropwise on 15 ml Pancoll, to avoid mixing of the two phases. Tubes were centrifuged 20 minutes at 2200 rpm without break. After centrifugation peripheral blood mononuclear cells (PBMC) were separated from granulocytes and red blood cells (Figure 2.2).

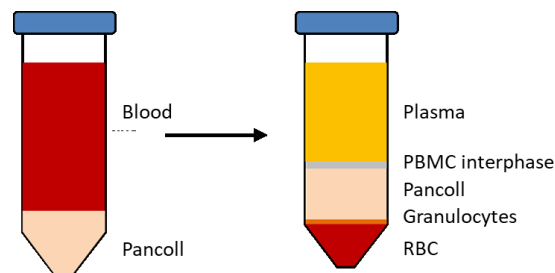


Figure 2.2: Phase separation after pancoll density separation. Diluted blood was put on top of pancoll solution. Then the tube was centrifuged, and the different phases separated. In the lowest phase red blood cells (RBC) accumulate, the layer on top is enriched for granulocytes. The transparent layer on top consists of plasma diluted with PBS, the next white interface is enriched for PBMCs and the layer underneath is made up by pancoll.

The white interphase containing PBMCs was put in another tube and washed twice with 50 ml PBS (10 minutes and 5 minutes 1500 rpm) and resuspended in 40 ml PBS for counting. Cells were aliquoted and frozen like described in 2.2.1.3.3 and stored in the nitrogen tank or used fresh in experiments.

2.2.1.6.2 Isolation of CD8 positive cells from PBMCs by Magnetic-activated cell separation (MACS)

As a starting population for T cell stimulation to generate IDH2_{Mut} specific T cell by peptide stimulation CD8 T cells were used. CD8 T cells were isolated from PBMCs (isolated like described in 2.2.1.3) of healthy donors. PBMCs were resuspended in 640 μl MACS buffer

(PBS supplemented with 2mM EDTA and 0,5% BSA). After adding 160 μ l anti-CD8 beads the mixture was incubated 20 minutes at 4°C. Mixture was mixed again after 10 minutes. In this time the bead bound CD8 specific antibody bind to CD8 on the surface. As a result, CD8 positive T cells are labeled with the magnetic beads. Cells were washed with 5ml MACS buffer to remove unbound beads. LS column was put in MACS separator and pre-separation filter was put on top. For equilibration 3ml of MACS buffer was put on the filter and column. Pellet was resuspended in 600 μ l MACS buffer and put on the pre-separation filter. CD8 positive cells are labeled with magnetic beads and remain in the column because of the magnetic force. Non-labeled cells leave the column as flow through. Flow through was collected in a tube and used as a source of antigen presenting cells for re-stimulation of T cells. Column was washed three times with 3 ml MACS buffer. This was done to wash unlabeled CD8 negative cells away and put out of the separator on a new tube. The cells were eluted with 5 ml MACS buffer by removing the column out of the magnetic field from the MACS separator and put on a 15 ml tube. Column was eluted two times with 5 ml MACS puffer, to get 10 ml CD8 positive cells. Cells were counted and seeded $1.5 \cdot 10^6$ cells/ml in a 24-well plate (2 m per well). 25 U/ml IL2 was added and the cells were seeded together with APCs.

2.2.1.6.3 Isolation of CD4 and CD8 positive cells from PBMCs

Electroporated cells were used to stimulated CD4 and CD8 T cells. The protocol is the same as described in 2.2.1.4.2 but less cells were used because CD4 T cells are more abundant in the blood than CD8 positive cells and anti-CD4 beads instead of anti-CD8 beads. About 20% of PBMCs are CD4 positive, while only 10% are CD8 positive, so only about a half of the starting cell number was used and CD4 specific beads. In the same way bulk CD4 T cells were generated for allogenic mixed lymphocyte reactions (MLR) with DCs matured and differentiated with or without D-2-HG.

2.2.1.6.4 Isolation of CD45RA positive cells from PBMCs

For allogenic MLRs to test the functional consequences of D-2-HG treatment also naïve enriched CD4 T cells were used. Therefore, a MACS was performed using CD45RA specific beads followed by FACS cell sorting of CD4 like described in the following chapter.

2.2.1.6.5 Fluorescent associated cell sorting

Enrichment of naïve T cell populations was done with fluorescent associated cell sorting. CD4 or CD8 positive cells isolated with MACS were stained with CD3 and CD45RA (55 μ l

each) in PBS supplemented with 2% FCS. CD45RA positive cells isolated the same way were stained with CD4-V450 antibody. After incubation of 30 minutes at 4°C in the dark, cells were washed with PBS supplemented with 2% FCS and filtered to remove cell clumps. Cells were resuspended in a concentration of 20×10^6 cells/ml in PBS supplemented with 2% FCS. Cells were sorted by Irina Fink (AG Edinger/Hoffman). Double positive population (CD3-APC/CD45RA-PE) or CD4 positive population was sorted in a tube containing 1 ml human sera. Human sera get diluted with the sorted cells solved in FACS flow. Cells were counted after cell sorting and seeded in the desired concentration.

2.2.1.6.6 Generating of mature FAST-DC for T cell stimulation

FAST-DCs were generated like described by Dauer et al. and Felzmann et al.^{93,94}. PBMC isolated from whole blood cells like described in 2.2.1.4 were seeded in a 6-well plate ($15\text{-}20 \times 10^6$ /well) and incubated 1.5 h in the incubator (37°C, 5% CO₂) in AIMV+1% HS. At this time, the monocytes should get adherent to the surface, while other cells like mainly lymphocytes should stay in suspension. After incubation wells were washed with warm PBS till only the adherent monocytes were left. Cells were cultured 500 IU/ml IL-4 and 1000 U/ml GM-CSF in AIMV+1% HS for at least 24 h. For maturation 1000 IU/ml IL-6, 10 ng/ml TGF- β , 10 ng/ml IL-1 β and 1 μ g/ml PGE₂ were added. After another 24 h the cells can be harvested with cold PBS and used for peptide incubation or electroporation.

2.2.1.6.7 Transfection of in vitro transcribed mRNA and T cell stimulation with DCs expressing IDH2 R140Q

Electroporation was performed to transfer *in vitro* transcribed mRNA of IDH2 R140Q into APCs adopted from Schaft et al.⁹¹. APCs should translate the mRNA in a protein and process and present it on their surface. First the cells were washed with RPMI and optiMEM both without phenol red or other supplementaries (1500 rpm, 5 minutes). Cell pellet was resuspended in 200 μ l optiMEM per electroporation sample (maximum 10×10^6 cells). *In vitro* transcribed mRNA (20 μ g) was put in an electroporation cuvette together with 200 μ l cell suspension. DCs were electroporated with 400 V for 5 ms (square-wave pulse). Cells were transferred in culture media provided in a 6-well plate and cultivated 16 h. After 16 h expression of IDH2 R140Q was confirmed by flow cytometric detection of HIS tag. Electroporated DCs were frozen in small portions and thawed on the day of T cell stimulation or T cell reactivity test with ELISpot. For T cell stimulation DCs were thawed and irradiated (70 Gy). DCs were seeded together with bulk or naïve enriched CD4 and CD8 T cells in 24-

well or 96-well plates. In 24-well plates 1.5×10^6 T cells were seeded together with 1.5×10^5 DCs, in 96-well plates 1×10^5 T cells were seeded with 1×10^4 DCs. AIMV was supplemented with 10% human sera and IL-7 (5 ng/ml), IL-12 (2 ng/ml) and IL-15 (5 ng/ml). T cells were re-stimulated every 7 days with electroporated DCs. On day 14 IL-12 was exchanged with IL-2. On day 14 the first IFN γ ELISpot was performed by using 20 μ l of T cell culture for each well of the IFN γ ELISpot well to test each well for reactivity.

2.2.1.6.8 T cell stimulation with Peptide loaded APCs

T cells were isolated from blood of healthy donors like described in 2.2.1.4.1. CD8 and CD4 T cells were isolated like described in 2.2.1.4.2 and 2.2.1.4.3 or further enriched for naïve T cells (2.2.1.4.4 and 2.2.1.4.5). T cells were seeded in 24-well plates in AIMV supplemented with 10% human sera and IL-7 (5 ng/ml), IL-12 (2 ng/ml) and IL-15 (5 ng/ml). For stimulation PBMCs and DCs were incubated with 10 mM peptide (IQN9/IQN10) for 4h at 37°C. PBMCs were irradiated with 35 Gy and DCs with 70 Gy and washed before seeding. In each well 1.5×10^6 T cells and 3×10^6 PBMCs or 1.5×10^5 DCs were seeded. Every 7 days T cells were re-stimulated with peptide loaded APCs like for the first stimulation. IL-12 was exchanged with IL-2 on day 14 of culture. On day 14+5 first functional analysis of T cells were done by IFN γ ELISpot and repeated on day 21+5 or 28+5. This protocol was adopted from Thomas et al. ⁹⁵.

2.2.1.6.9 Measurement of IFN γ secretion by ELISpot

Enzyme-linked immunosorbent spot (ELISpot) is an enzyme based assay to determine cytokine producing cells ⁹⁶. ELISpot plates were activated with 35%vol ethanol in water. After washing three times with PBS, plate was coated with first antibody against human IFN γ over night at 4°C. The antibody solution was discarded and the plate was washed three times with PBS supplemented with 0.05% SDS. To avoid unspecific binding the plate was blocked with culture media (AIMV supplemented with 10% HS) for at least one h at 37°C. As target cells autologous PBMCs were used they were pre-incubated with the peptides (10^{-6} M) 1h at 37°C. Responder T cells (15,000 cells/well) and target cells (50,000 cells/well) were seeded and incubated 20h at 37°C.

Plate was washed six times with washing buffer (PBS supplemented with 0.05% SDS) and incubated with a second antibody for 2h at 37°C. In this step the IFN γ was now between the first antibody coated on the plate and the second biotinylated antibody similar like an

sandwich ELISA. 30 minutes before incubation stops the streptavidin peroxidase solution was prepared (10 ml PBS supplemented with 0.001% Tween + 1 drop solution A + 1 drop solution B) and incubated 30 minutes in the dark at room temperature. After washing six times with washing buffer and tapped it dry the solution was added and the plate was incubated 1h at room temperature in the dark. Plate was washed with washing buffer and PBS three times each. Then the AEC-substrate solution (3-Amino-9-Ethyl-carbazole, for 500 ml 10 pills of dimethylformamid were solved in acetate buffer) supplemented with H₂O₂ (0.5 µl/ml) was incubated 8-10 minutes depending on the signal strength. In this step the AEC substrate solution was oxidized by the peroxidase. Plate was washed with tap water, the bottom was removed and the plate was air dried. Plate was analyzed with CTL ELISpot Reader.

2.2.3 Analyzing effect of D-2-HG metabolism and differentiation to monocyte-derived DCs

In the following methods are shown to analyze the effect of D-2-HG on DC differentiation, maturation and metabolism.

2.2.3.1 Isolation of monocytes by elutriation

PBMCs were isolated from leukapheresis products of healthy donors by density gradient centrifugation over a pancoll (2.2.1.4.1). Monocytes were isolated from PBMCs by countercurrent centrifugation (elutriation).

Elutriation was performed in a Beckman Avanti J-20XP centrifuge equipped with an elutriation centrifugation rotor and a flow chamber. All components were sterilized with 6% H₂O₂ for 20 minutes and washed twice with PBS. Pump was calibrated at 2500 rpm and 4°C with Hanks balanced salt solution (BSS). Pump was calibrated and PBMCs were loaded at the lowest flow rate (about 53 mL/min) after collecting one fraction the flow rate was increased to a maximum of about 130 mL/min. In the last fraction monocytes were enriched because there are the largest cells within the PBMCs, but there were also monocytes in the fractions before detectable. The first fraction was enriched for platelets, in the following fractions B and T cells and neutral killer cells were enriched. Monocyte enrichment was analyzed by CD14 antigen expression (only expressed on monocytes and macrophages), the purity was higher than 85%.

Monocyte fraction (last fraction) was centrifuged (8 minutes, 300×g, 4°C), resuspended in RPMI culture medium and counted. Monocyte yield was donor dependent, typically between 8-15% of total PBMCs.

2.2.3.2 Generation of monocyte-derived DCs

DCs were generated using the monocyte fraction gained by elutriation as described previously⁷¹. Briefly, monocytes were seeded in RPMI supplemented with 10% FCS, glutamine (2 mM), penicillin (100 U), streptomycin (100 µg/ml), HEPES (10 mM), IL4 (150 U/ml), GM-CSF (230 U/ml) at a concentration of 2×10^6 /well in a 6-well plate in 3 ml of medium or 7×10^6 in a T25 culture flask in 10 ml medium. D-2-HG was added immediately after seeding the cells once for the whole period of culture. Cells were cultured for 7 days to generate immature DCs. For maturation 100 ng/µl LPS was added for 24 hours. Peroxide (1 mM), vitamin C (2 mM), trolox (50 µM), pioglitazone (25 µM) and metformin (5 mM) were added together with D-2-HG directly after seeding of the cells.

2.2.3.3 Electron microscopic analyses of DCs treated with D-2-HG

After generating immature and mature DCs treated with or without D-2-HG like described in 2.2.2.2., DCs were harvested (1×10^7 cells per treatment) and washed with PBS and transferred in a 1.5 ml centrifugation tube. DCs were centrifuged at 300g for 5 minutes, pellet was fixed with Karnovsky-fixative for at least 2 h and further processed and analyzed in cooperation with the pathology department of the University Hospital Regensburg.

2.2.3.4 Phagocytosis Assay

Competent JM109 were transformed with pGEM4Z-65A vector carrying the GFP gene and an ampicillin resistance (see Transformation in section 2.2.1.2.6) and plated on LB plates containing ampicillin (100 µg/ml).

One colony was picked and transferred in 25 ml LB media containing ampicillin (100 µg/ml). Bacteria were incubated 10 to maximal 12 h at 37°C and 280 rpm. 500 µl of bacteria suspension was transferred in 49.5 ml LB media containing ampicillin (100 µg/ml) and incubated till the optical density was between 0.65 and 0.85 (165-195 minutes) at 600 nm. Suspension was transferred in 50 ml tube and span down (1500 rpm, 10 minutes). Pellet was resuspended in 2 ml phagocytose buffer (10% not heat inactivated human sera, 20% PBS, 70% BSS, 1 mM CaCl₂ and 0.5 mM MgCl₂) and incubated 30 minutes at 37°C and 180 rpm. In the meantime 250.000 cells per sample were resuspended in 500 µl phagocytose buffer and transferred in a 24-well plate. The plate was pre-warmed in the incubator (37°C, 5% CO₂). OD_{600nm} was measured in bacteria suspension (1:10 diluted in phagocytose buffer) and cell number was calculated according to the following equation:

$$\frac{\text{cellnummer}}{\text{ml}} = 8 \times 10^9 \times OD_{600nm \ 1:10 \ \text{diluted}}$$

$6,25 \times 10^6$ cells in 500 μ l phagocytose buffer were used per sample and transferred in 24-well plate. Here the MDDCs got in contact with the bacteria (1 MDDC to 25 bacteria cells). There was also a negative control where no bacteria cells were added. After 10 minutes of incubation in the incubator the cells were transferred in a FACS tube and spun down (1500 rpm, 10 minutes). Another set of samples were incubated 30 minutes to distinguish bacteria on the surface and inside the cell, because in 30 minutes all GFP expressed by phagocytized bacteria should be degraded and only the bacteria which stick to the surface will make a GFP signal. Pellets were resuspended in 200 μ l FACS buffer (PBS+5% FCS) and measured with the Calibur flow cytometer in the FITC channel.

2.2.3.5 Allogeneic mixed lymphocyte reaction

To investigate the stimulation capacity of DCs allogeneic mixed lymphocyte reactions (MLR) were performed like described previously⁷². Immature DCs generated like described in 2.2.2.2 were co-cultivated with allogenic CD8 or CD4 T cells isolated like described in 2.2.1.4.1, 2.2.1.4.2 and 2.2.1.4.3. T cells were seeded in a 96-well plate together with DCs generated in the presence or absence of D-2-HG in RPMI supplemented with 2 mM glutamine, 25 U/ml IL2 and penicillin streptomycin. 100,000 T cells were cultured with 10,000 DCs for one week. Activation of T cells was analyzed using flow cytometry. Cells were stained on day 4 of culture with antibodies against the IL-2 receptor CD25 and CD69 which are early activation marker of T cells. In addition, staining of FoxP3 was performed to analyze if regulatory T cells were generated. The staining was repeated on day 7, where also the cell number was counted.

2.2.3.6 Enzyme-linked immunosorbent assay (ELISA)

During the differentiation and maturation of monocytes to dendritic cells supernatants were collected for cytokine secretion measurement. Supernatants were stored at -20°C . An ELISA is a biochemical test to detect antigens in solution is analyzed by specific antibodies, one antibody is coated on the plate to capture the antigen, another specific antibody binds the analyte at another side to increase specificity of the detection the second antibody is coupled to an enzyme which reacts with the substrate which leads to a shift in its emission, this can be measured with a plate reader at 450 nm.

The plates were coated overnight with the capture antibody specific for the cytokine of interest in PBS. Plate was washed three times with 250 μ l wash buffer (PBS supplemented with 0.05% Tween 20). Residual liquid was removed and plate was blocked with 300 μ l reaction diluent (PBS supplemented with 1% BSA) for one h. After the plate was washed again and residual liquid was removed, the plate was loaded with standard and sample probes. A series of 1:1 dilutions were made from a 2000 pg/ml (or 1000 pg/ml) stock to 31.3 pg/ml and 100 μ l was pipetted in each well (duplicates) on the first two rows of the plate. Supernatant samples were loaded undiluted or 1:10 diluted in reaction diluent. Plate was incubated for 2 h and washed three times before 100 μ l of the detection antibody was added for 2 h. Plate was washed and incubated 20 minutes with 100 μ l streptavidin-HRP working solution. Plate was washed and incubated 20 minutes with the 100 μ l substrate solution, then the stop solution was added to the well. The plate was measured at 450 nm with a plate reader. Calibration curve and concentration of the samples was calculated by the software of the plate reader.

2.2.3.7 Measurement of cAMP level by ELISA

cAMP levels were measured in immature DCs (cultured for 7 days) differentiated in the presence or absence of 20 mM D-2-HG. iDCs were harvested and 1×10^6 cells were placed in tubes, centrifuge for 7 minutes at 1400 rpm, supernatants were discarded and DCs were washed two times in 1 ml of cold PBS. Cells were then lysed by adding 200 μ l 1x lysis buffer (included in the cAMP determination kit diluted in H₂O, stored at -20°C), incubated on ice for 10 minutes, centrifuged for 4 minutes at 1600 rpm and supernatants containing cAMP were collected and stored at -80°C. cAMP levels were measured by using the cAMP XP Assay according to manufacturer protocol.

2.2.3.8 Flow cytometric analyses

Flow cytometry allows the detection of extra- and intracellular molecules by binding the target of interest to an antibody conjugated to a fluorophore on a single cell level. The dye gets excited by a laser beam and the fluorescence signal is detected. Measuring the fluorescence intensity allows an estimation of the abundance of the molecule of interest, thus flow cytometry is a semi-quantitative method

2.2.3.8.1 Staining of surface molecules

Cells were harvested, transferred in polystyrene tubes and washed with PBS supplemented with 2% FCS (1500 rpm, 5 minutes). Supernatant was discarded and cells were stained with

antibodies coupled to specific fluorescence dyes for 20 minutes in the dark. Subsequently, cells were washed with 1 ml PBS supplemented with 2% FCS and resuspended in 250 μ l PBS supplemented with 2% FCS. Cells were measured using a BD Calibur. Data analysis was performed using the FlowJo software.

2.2.3.8.2 Intracellular staining

Intracellular FOXP3 staining was combined with staining of extracellular surface markers. Extracellular markers were stained first as described above, and subsequently cells were permeabilized by incubating cells in Fix-Perm solution for 20 minutes at 4°C. After washing twice FoxP3 antibody was added, incubated for 20 minutes at 4°C. Cells were washed twice and resuspended in PBS supplemented with 2% FCS for the measurement. To analyze intracellular expression of HLA class II molecules as well as the active form of mTOR DCs were washed with PBS supplemented with 2% FCS and incubated with Fix-Perm solution and further processed as described above.

2.2.3.8.3 Measurement of cytosolic ROS with 2',7'-Dichlorofluorescein diacetate

2',7'-Dichlorofluorescein diacetate (DCFDA) was solved in pure methanol to get a 400 μ M stock solution. Stock solution was freshly diluted 1:50 with media and 12.5 μ l were added to 500 μ l of cell suspension in a FACS tube. DCFDA comes as a AM ester which makes it cell permeable, unspecific esterases cleave this ester-bounds and release the dye in the cytosol where it can react with ROS. The more ROS is present in the cytosol the higher the fluorescent intensity of the cells. As an unstained control cells only were transferred in a FACS tube. Cells were incubated 20 minutes in at 37°C in the incubator. Cells were washed with cold PBS, resuspended in PBS supplemented with 2% FCS and immediately analyzed in the FL-1 channel of the BD Calibur flow cytometer. Data were analyzed with the FlowJo software.

2.2.3.8.4 Cystine staining

Cystine uptake was analyzed using a FITC coupled cysteine probe kindly gifted by Dr. Peter Siska who established a protocol to produce cysteine FITC ⁹⁷. Cells were washed with PBS and re-suspended in 250 μ l Krebs buffer (115 mM NaCl, 2 mM, KCl, 1 M NaHCO₃, 1 mM MgCl₂, 0.25% BSA) and incubated for 1h at 37 °C and 5% CO₂. To stain the cells 250 μ l of Krebs buffer containing 2 μ M cytine FITC was added 20 minutes at 37 °C and 5% CO₂ (final concentration 1 μ M cystine FITC). Cells were washed twice with cold PBS containing 2% FCS and analyzed in the FL1 channel of a FACS Calibur flow cytometer.

2.2.3.8.5 Measurement of mitochondrial ROS with MitoSox red

Mitochondrial superoxides were measured with the fluorescent MitoSox probe. MitoSox is cell permeable and has a cationic residue which targets into the mitochondria. Here MitoSox red gets oxidized by superoxide and exhibits red fluorescence. MitoSox red was solved in pure DMSO to get a 5 mM stock. Cells were incubated with 5 μ M MitoSox in buffer containing 135 mM NaCl, 1 mM MgSO₄, 20 mM HEPES, 0.4 mM KH₂PO₄, and 5 mM KCl for 10 minutes at 37 °C and 5% CO₂. Cells were washed with PBS containing 2% FCS and analyzed in the FL-3 channel of a FACS Calibur flow cytometer.

2.2.3.8.6 Staining of mitochondria with Mitotracker Green

MitoTracker green is a fluorescent dye which stains whole mitochondria volume. On day 7 DCs were harvested and 400,000 DCs were resuspended in 1 ml RPMI supplemented with 2 mM glutamine. Mitochondria were stained with 50 nM MitoTracker green solved in DMSO for 2 h at 37°C. Cyclosporine A (60.8 nM) inhibits mitochondrial permeability transition pore opening and for that was added during incubation to inhibit the transport out of mitochondria. Cells were washed with PBS supplemented with 2% FCS and resuspended in 200 μ l PBS supplemented 2% FCS for FACS measurement (FL-1). For the unstained control, the same amount of DMSO was added as added with MitoTracker staining.

2.2.3.9 Determining mitochondrial respiration by high-resolution respirometry

2.2.3.9.1 Oxygen measurement in whole cells

Oxygraph high resolution respirometry is a method to measure the oxygen consumption rate (OCR) in whole cells, like previously described⁹⁸. The system is closed so absolute values can be measured. The aperture has two measuring chambers to measure two samples simultaneously. On one side of the chamber there is a clark electrode which is an oxygen sensitive electrode. On the bottom of the chamber there is a stirrer, which provides a constant oxygen concentration in the whole chamber.

For storage the chamber was filled with 70% ethanol, before starting the measurement it was aspirated and the chamber was washed three times with Millipore water. Media was put in the chamber and measurement was started with open chambers to measure the maximal solubility of oxygen as it depends on air pressure it can vary from day to day. When the oxygen level is constant the monocyte suspension ($5-7 \times 10^6$ in 2.5 ml, fresh after elutriation or incubated over night in the fridge) in RPMI+10%FCS +IL4 +GM-CSF could be put in the

chambers and the actually cell number was determined. After the oxygen signal was stable (after 15-20 minutes) the substances (D-2-HG or media) were added, followed by the addition of LPS (1 ng/ml). Oxygen consumption was measured 1-1.5 h, then oligomycin was added. Oligomycin inhibits ATP synthase (complex V), after the signal was stable the cells were uncoupled with Carbonyl cyanide-p-trifluoromethoxyphenylhydrazone (FCCP). FCCP was added stepwise (0.5 μ M steps) till the signal did not increase by further addition. Complex II was inhibited with Rotenone before Myxothiazol was added (Inhibitor of complex I) which should set the oxygen consumption to a minimum. Concentration of inhibitors and FCCP are shown in the following table (Table 26). After the run the chamber was washed with Millipore water three times and incubated 20 minutes with 70% ethanol, 10 minutes with 100% ethanol and then stored in 70% ethanol.

Table 28: Substances used to modulate oxygen consumption

Compound	Final concentration in chamber
LPS	1 ng/ml
Oligomycin	2 μ g/ml
FCCP	1-7 μ M
Rotenone	0.5 μ M
Myxothiazol	0.5 μ M

2.2.3.9.2 Oxygen measurement in permeabilized cells

Oxygen concentrations can also be measured after adding specific substrates if the membrane of the cells assayed is destroyed with digitonin⁹⁹. For this oxygraph protocol the cells were resuspended in MIRO5 media (pH 7.1), which is a suitable media to stabilize mitochondria (for composition see following Table 29).

Table 29: Components of MIRO5 used for permeabilized cells in oxygraph

Compound	Final concentration
EGTA	0.5 mM
MgCl ₂ 6 H ₂ O	3 mM
Lactobionic acid	60 mM
Taurine	20 mM
KH ₂ PO ₄	10 mM
HEPES	20 mM
D-Sucrose	110 mM
BSA, Essentially Fatty Acid Free	1 g/l

As with the culture media in the protocol described in section 2.2.2.9.1 first the maximum oxygen saturation is measured with the MIRO5 media. If the oxygen consumption rate (OCR) is stable after adding the cells Malate is added. Malate stabilizes the mitochondria but does not increase OCR. Membrane permeabilization is done with digitonin. Digitonin acts as a cholesterol-complex agent, which binds cholesterol molecules located in the cell membrane. Complex formation leads to a reorganization of the cell membrane where pores are formed. Through these pores all substrates flush out of the cell and OCR decreases. Now defined substrates can be added and the increase of OCR can be measured. OCR was measured in the two chambers in parallel. In one chamber water was added as a vehicle control in the other D-2-HG solved in water, followed by the addition of ADP and MgCl₂ as a substrate for ATP synthase. Then other substrates of complex I like pyruvate and glutamate, or complex II succinate can be added (concentrations in Table 30). Cells were uncoupled with FCCP and inhibited with rotenone and myxothiazol, then Ascorbate and TMPD was added. TMPD is an artificial substrate of complex IV and leads to a high increase in OCR. Ascorbate is used to reduce TMPD, which gets easily oxidized. At last sodium azide is added to kill the cells and measure auto oxidation of the added substances. Chambers were cleaned like described in section 2.2.2.9.1.

Table 30: Substrates used to measure activity of different complexes of electron transport chain

Compound	Final concentration
Malate	2 mM
Digitonin	10 µg/10 ⁶ cells
ADP	5 mM
MgCl ₂	5 mM
D-2-HG	2-3 mM
Pyruvate	5 mM
Glutamate	10 mM
Succinate	10 mM
FCCP	1-7 µM
Rotenone	0.5 or 0.1 µM
Myxothiazol	0.5 µM
Ascorbate	2 mM
TMPD	0.5 mM
Sodium azide	100 mM

2.2.3.10 Analyze of pH value and oxygen concentration of DCs during differentiation from monocytes

With the PreSens technology pH and oxygen concentration was monitored on line during DC differentiation for 7 days. The tissue culture plates were coated with a sensor in the middle of the well.

The sensor can monitor either pH or oxygen non-invasively in living cells. An LED lamp excites the sensor, which emits fluorescence in response. Molecules like oxygen and protons quench the fluorescence signal and by this the concentration of this molecule can be measured in 24-well plates. 0.7×10^6 monocytes were seeded in 1 ml of RPMI culture medium in oxo or hydro dishes. DCs were treated with different concentrations of D-2-HG. DCs were cultured 7 days. Measurements were performed at 37°C, concentration was measured every 5 minutes.

2.2.3.11 Lactate and glucose determination

Lactate was determined in collaboration with the clinical chemistry of the University Hospital Regensburg. Glucose measurement was done with an enzymatic assay performed by Stephanie Färber (AG Kreutz, Internal Medicine III, University Hospital Regensburg).

2.2.3.12 Methylation analysis

During differentiation from monocyte to DC there are regions which get demethylated. Demethylated regions are associated with an active gene expression. Methylation analysis was performed by EpiTyping technology. With this method methylated CpG loci can be determined by mass spectrometry.

2.2.3.12.1 Culture and treatment of DCs for methylation analysis

For the d 0 sample monocytes were washed twice with cool PBS and cell pellet was frozen at -20°C. For the other time points monocytes were seeded on 6 well plates, per well 3×10^6 cells were seeded in 3 ml RPMI supplemented with 10% FCS, glutamine (2mM), penicillin (100 U) streptomycin (100 µg/ml), HEPES (10 mM), IL4 (150 U/ml), GM-CSF (230 U/ml). Four different treatments were cultured:

- 1) DC
- 2) 20 mM D-2-HG
- 3) 2 mM vitamin C
- 4) 20 mM D-2-HG and 2 mM vitamin C

DCs were harvested after 16 h, 66 h and 7 d. As with the d 0 monocytes, DCs were washed twice with cold PBS and the cell pellet was stored at -20°C.

2.2.3.12.2 Isolation of DNA with DNeasy Blood and tissue Kit from Qiagen and methylation analysis

For the isolation of DNA the DNeasy Blood and tissue Kit from Qiagen was used. Samples are first lysed using proteinase K. Buffering conditions to provide optimal DNA binding

Conditions. The lysate is loaded onto spin columns, during centrifugation, DNA is selectively bound to the membrane as contaminants pass through. DNA is then eluted in DNA was eluted by 200 µl Buffer AE and was further processed to analyze methylation status of DCs during differentiation in cooperation with the working group of Prof. Michael Rehli (Internal Medicine III, University Hospital Regensburg).

The genomic position of the analyzed CpG residues are summarized in Table 31 the corresponding amplicons have been described in reference ¹⁰⁰ and ¹⁰¹.

Table 31: Genomic position of analyzed CpG residues

Gene	Chromosomal (GRCh38/hg38)	Location	Amplicon (for bisulfite-treated DNA)
<i>CCL13</i>	chr17:34356259-34356559		Epi00109_CCL13.1 ^a
<i>STAT5</i>	chr17:42283625-42283783		Epi00104_STAT5A.2 ^a
<i>C9ORF78</i>	chr9:129839252-129839471		Epi00148_C9ORF78.3 ^a
<i>MMP7</i>	chr11:102530563-102530766		Epi00162_MMP7.1 ^a
<i>HOXB1</i>	chr17:48530488-48530489		Epi00193_HOXB1_01 ^a
<i>CD207</i>	chr2:70837911-70838410		Epi00116_CD207.2 ^a
<i>CLEC10A</i>	chr17:7079646-7080109		Epi00184_CLEC10A.1 ^a

2.2.3.13 Protein isolation

Monocytes (4×10^6) or DCs (2.5×10^6) were washed twice with cold PBS (5 minutes, 1500 rpm) and transferred to a 1.5 ml tube. Pellet was resuspended in 50 µl RIPA buffer (50 mM NaCl, 1.0% IGEPAL CA-630, 0.5% sodium deoxycholate, 0.1% SDS, 50 mM Tris, pH 8.0) and mixed thoroughly by vortexing for 1 minute. Tube was incubated 5 minutes at -20°C, thawed and mixed again. Tube was frozen in liquid nitrogen. Lysate was stored at -80°C or centrifuged immediately on high speed (13000 rpm) for 15 minutes. Supernatant was at -80°C.

2.2.3.14 Fractionized protein isolation

Lysates of cytosolic separated from other proteins were used to analyze the activity of protein kinase C (PKC). PKC is only active in the membrane, so the level of PKC in the cytosol compared to the membrane fraction give rise of PKC activity.

Buffer 1	Buffer 2
150 mM NaCl	RIPA Buffer
50mM HEPES	Protease Inhibitor Cocktail

Protease Inhibitor Cocktail	10 mM NaF (Phosphatase inhibitor)
10 mM NaF (Phosphatase inhibitor)	

DCs or monocytes were washed twice with cold PBS (1500 rpm, 5minutes) and counted. Pellet was resuspended in 100µl buffer 1 supplemented with 1 µl digitonin per million cells. Cells were mixed and incubated 10 minutes on ice, while mixing several times. Cell lysis was confirmed by trypan staining. Tube was centrifuged 10 minutes at 2000 g at 4°C. Supernatant containing the cytoplasmic proteins was transferred in a new tube and stored at -80°C. Pellet was resuspended in buffer 2 and mixed thoroughly by vortexing 1 minute. Tube was incubated 5 minutes at -20°C, thawed and mixed again. Tube was shock frozen in liquid nitrogen. Lysate was stored at -80°C or centrifuged immediately on high speed (13000 rpm) for 15 minutes. Supernatant and pellet was stored at -80°C.

2.2.3.15 Protein determination by Lowry

Protein determination was done like previously described by Lowry et al.¹⁰². Samples were thawed on ice. In the meantime, bovine serum albumin was diluted from a 30 mg/ml stock to 1.5 µg/µl (1:20). This first standard solution was further serial diluted 1:2 to get concentrations of 0.750-0.047 µg/µl. Samples were diluted 1:10. 5 µl sample and standard was transferred in a well of a flat button 96 well plates. In each well 25 µl of a mixture of solution A containing the alkaline copper tartrate solution (1 ml) and solution S (surfactant 20 µl) and 200 µl solution B containing Folin reagent. Plate was incubated 15 minutes at room temperature while shaking. In this time proteins react with the copper and reduce Folin reagent by the loss of oxygen atoms. This results in a color reaction from yellow to blue. This shift in the absorption spectrum was measured at 650 nm.

2.2.3.16 Analyzing protein of interest by western blot

2.2.3.16.1 SDS gel electrophoresis

Protein samples were separated by sodium dodecyl sulfate polyacrylamide gel electrophoresis (SDS-PAGE) with a discontinuous gel composed of a stacking and separating gel layers, which differed in salt and acrylamide (AA) concentration. The stacking gel contained of only 5% AA and therefore was used to concentrate the sample on the edge to the separation gel containing a higher but varying concentration of AA depending on the protein size to detect.

Required Buffers and solutions

- 1) Separating gel buffer 1.5 M Tris/HCL (pH 8.8)
- 2) Stacking gel buffer 0.5 M Tris/HCl (pH 6.8)
- 3) SDS sample buffer (2 x): 20% v/v Glycerin, 125mM Tris/HCL, 4% SDS, 10% 2-Mercaptoethanol, 0.02% Bromphenolblue
- 4) Laemmli buffer (5×): 40 mM Tris/HCL, 0.95 M Glycine, 0.5% SDS

	Separating Gel				Stacking Gel
	7.5%	10%	12%	15%	5%
Stacking Gel Buffer	-	-	-	-	2.5 ml
Separating Gel Buffer	2.5 ml	2.5 ml	2.5 ml	2.5 ml	-
SDS (10%)	0.1 ml	0.1 ml	0.1 ml	0.1 ml	0.1 ml
AA (30%)	2.5 ml	3.3 ml	4.0 ml	5.0 ml	1.665 ml
Millipore Water	4.9 ml	4.1 ml	3.4 ml	2.4 ml	5.735 ml

First the separation gel was produced and transferred between the glass plates in a gel caster, followed by the stacking gel containing the comb where the samples are loaded. 10-20 µg protein was loaded, and gel was run in laemmli buffer at 80 V. The volts were increased to 100 V and 120 V in the separation gel. The gel ran 1.5-2 h.

2.2.3.16.2 Western blot

After SDS-PAGE separated proteins were transferred on a polyvinylidene fluoride (PVDF) membrane using a three-buffer semi-dry system (Towbin et al. 1979). On the membrane one specific protein was detected with a corresponding antibody.

2.2.3.16.3 Protein transfer on membrane

Required buffers:

Buffer A: 0.3 M Tris (pH 10.4), 20% methanol in water

Buffer B: 25 mM Tris (pH 10.4), 20% methanol in water

Buffer C: 4 mM ε-amino-n-caproic acid (pH 7.6), 20% Methanol in water

The membrane was cut to gel size, activated with 2-propanol and incubated in buffer B. Three whatman filter pre-wet with buffer A were placed on the anode followed by three filter pre-

wet with buffer B. On top the membrane was put covered by the SDS-PAGE gel. Three whatman filter pre-wet with buffer C were put above the gel. In between air bubbles were removed. Protein transfer was conducted for 50-60 minutes depending on the size of the protein of interest.

2.2.3.16.4 Detection of protein of interest

After protein transfer membrane was blocked with 5% milk in wash buffer for 1 h at room temperature during shaking. Membrane was incubated over night with the first antibody recognizing the protein of interest at 4°C under continuous shaking. Antibodies and dilutions are summarized in Table 10. On the next day membrane was washed three times for 15 minutes. Membrane was incubated with the secondary antibody tagged with horse radish peroxidase (HRP) recognizing the constant domain of the first antibody for 1 h at room temperature under continuous shaking. After another three washes membrane was developed with ECL solution. It contains a substrate, which gets converted by HRP light. This light signal was detected by a chemiluminescence imager.

2.2.3.16.5 Elimination of antibodies bound on membrane

As a loading control actin was detected on all membranes, for that the antibodies were removed by a re-blot solution. Membrane was incubated 15 minutes with the re-blot solution at room temperature on the shaker. Membrane was washed three times, blocked and further processed like described above.

3 Results

3.1 Generation of IDH 2 R140Q specific T cell

In this part of the project the aim was to generate IDH2 R140Q specific T cells. For this, two main approaches were used one was the stimulation of T cells with autologous IDH2 R140Q peptide loaded DCs the other the stimulation with autologous DCs expressing mutant IDH2 R140Q protein upon mRNA electroporation.

3.1.2 HLA binding prediction by *in silico* programs

To find IDH2 R140Q-derived peptides for specific T cell stimulation online available *in silico* tools were used to predict peptide binding to specific HLA molecules. Algorithms for HLA class I binding prediction are in general more reliable than HLA class II specific ¹⁰³, so the focus was on HLA class I restricted peptides, which mostly consist of 8-10 amino acids. The programs BIMAS ⁸⁹, SYFPETHI ⁸⁸ and NET MHC Pan ⁹⁰ were used for prediction of 9- or 10-mers binding to HLA class I molecules.

Table 3.1: Result scores of *in silico* HLA binding prediction

Amino acid sequence (one letter code)	HLA restriction	BIMAS	SYFPETHI	NET MHC Pan
IRNILGGTVF	B*15:01	0.7	13	2843
IQNILGGTVF	B*15:01	274.0	23	12
IRNILGGTV	B*15:01	0.0	1	25522
IQNILGGTV	B*15:01	11.4	11	1437
TIRNILGGTV	A2	0.0	20	7075
TIQNILGGTV	A2	1.2	20	2559
SPNGTIRNI	B7	8.0	18	255
SPNGTIQNI	B7	8.0	18	562

Scores were calculated for peptides overlapping the mutated amino acid of the IDH2 R140Q mutation, each for the wild type (black) and mutated sequence (red) (Table 1). Peptides with the mutated sequence having a better score than the wild type sequence were selected for T cell stimulation (Table 1). Peptides which bound stronger to HLA molecules are more likely to stimulate T cells because they are presented for a longer time. The 9mer carrying the IDH2 R140Q mutation at position 2 (IQNILGGTV) showed the highest increase in HLA binding probability compared to the wild type sequence and all other peptides,

respectively (e.g. BIMAS wild type 0.0 compared to 11.4 (mutated)). Only the 10-mer with an additional phenylalanine (F) at the C-terminus showed better scores (e.g. BIMAS wild type 0.7 compared to 274.0(mutated)). T cell stimulation experiments were done with all peptides shown in Table 1. However, only with the peptides IQNILGGTV (IQN9) and IQNILGGTVF (IQN10) loaded on APC a specific T cell recognition was seen, so the focus will be on them.

3.1.3 T cell stimulation with peptide loaded antigen presenting cells

3.1.2.1 T cell stimulation with peptide loaded PBMC

Bulk CD8 T cells of an HLA B*15:01 positive donor were stimulated with IQN9 or IQN10-peptide loaded autologous peripheral blood mononucleated cells (PBMCs), to gain a IDH2 R140Q specific T cell population. In Figure 1 results of an IFN γ ELISpot assay are shown. In the IFN γ ELISpot assay CD8 T cells were stimulated with autologous PBMCs loaded with different concentrations of the mutated peptides IQN9 or IQN10 (IDH2 R140Q specific) or the wild type peptides IRN9 or IRN10 (negative control). T cells stimulated with IQN9-peptide loaded PBMCs secreted IFN γ when they were co-cultured with IQN9 peptide loaded PBMCs during the assay incubation time of 20h. In contrast these T cells showed reactivity against the wild type IRN10- and the IQN10-peptide (IDH2 R40Q specific) to the same extent (Figure 3.1A). Also, T cells stimulated with IQN10 peptide loaded PBMCs only showed activation by IQN10 loaded PBMCs (Figure 3.1B).

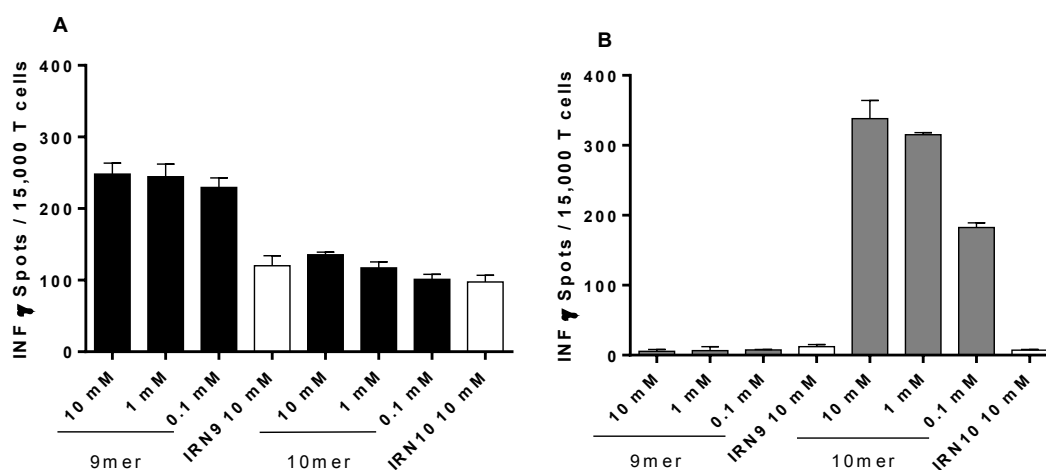


Figure 3.1: CD8 T cells (HLA-B*15:01) stimulation with autologous IDH2 R140Q specific peptide loaded PBMCs. (A) On d35+5 of primary stimulation and weekly restimulation with IQN9 peptide loaded PBMCs, CD8 T-cell responders were tested for IFN γ ELISpot reactivity against PBMCs loaded with IQN9 or IQN10 (0.1-10 mM) or the corresponding wild type peptides (10 mM). E:T ratio in the assay was 0.3:1. Data are shown as means of duplicates from one experiment representative of four performed with different T-cell donors (wherein one donor showed no reactivity). Error bars represent the range. (B) On d35+5 of primary stimulation and weekly restimulation with IQN10 peptide loaded PBMCs, CD8 T-cell responders were tested for IFN γ ELISpot reactivity against PBMCs loaded with IQN9 or IQN10 (0.1-10 mM) or the corresponding wild type peptides (10 mM). E:T ratio in the assay was 0.3:1. Data are shown as means of duplicates from one

experiment representative of four performed with different T-cell donors (wherein one donor showed no reactivity). Error bars represent the range.

In 3 of 4 different HLA-B*15:01 positive donors a peptide specific recognition of IQN9 and IQN10 loaded PBMCs was detected. In contrast no peptide specific T cells could be generated in 4 different donors using the HLA-A2 and HLA-B7 restricted 9mers TIQNILGGTV and SPNGTIQNI, respectively (data not shown).

3.1.2.2 T cell stimulation with peptide loaded DCs

PBMCs consist of mainly two types of antigen presenting cells (APCs) DCs and B cells¹. DCs were generated by plastic adherence and the FAST-DC protocol and activated with a cytokine cocktail. DCs are professional APCs and should be more effective in stimulating T cells¹.

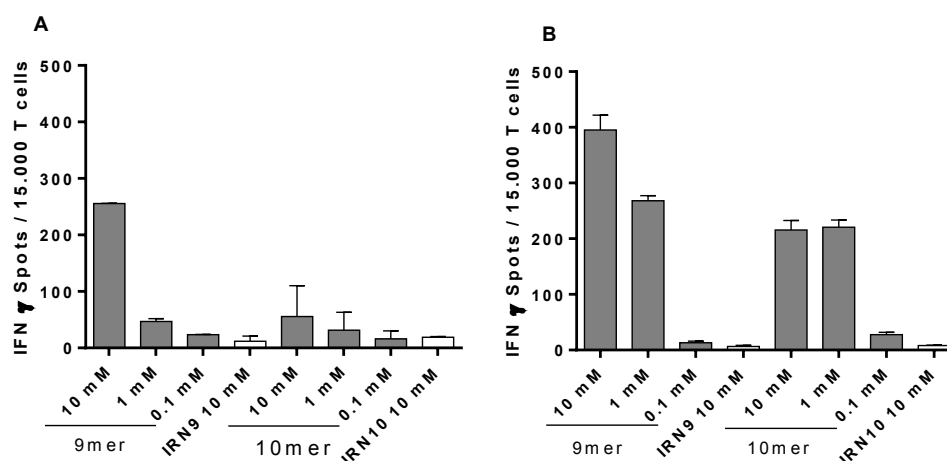


Figure 3.2: CD8 T cells (HLA-B*15:01) stimulation with autologous IDH2 R140Q specific peptide loaded DCs. (A) On d28+5 of primary stimulation and weekly restimulation with IQN9 peptide loaded PBMCs, CD8 T-cell responders were tested for IFN γ ELISpot reactivity against DCs loaded with IQN9 or IQN10 (0.1-10 mM) or the corresponding wild type peptides (10 mM). E:T ratio in the assay was 3:1. Data are shown as means of duplicates from one experiment representative of three performed with different T-cell donors (wherein one donor showed no reactivity). Error bars represent the range. (B) On d42+5 of primary stimulation and weekly restimulation with IQN9 peptide loaded DCs, CD8 T-cell responders from the same donor as in A were tested again for IFN γ ELISpot reactivity against DCs loaded with IQN9 or IQN10 (0.1-10 mM) or the corresponding wild type peptides (10 mM). E:T ratio in the assay was 3:1. Data are shown as means of duplicates from one experiment representative of five performed with different T-cell donors (two donors showed no reactivity). Error bars represent the range.

In Figure 3.2 results of an IFN γ ELISpot assay are showing the recognition of T cells stimulated with IQN9-peptide loaded autologous DCs. T cells of the same donor were tested on day 33 (Figure 3.2A) and 57 (Figure 3.2B) of culture to analyze the T cell specificity over time. For these assays 15,000 T cells were co-cultured with 5,000 IQN9/10 or IRN9/10 loaded autologous DCs for 20 hours. On day 33 of culture T cells recognized IQN9 better than IQN10-peptide loaded DCs, while the corresponding wild type-peptide (IRN9 and IRN10) loaded DCs did not activate T cells to secrete IFN γ (Figure 3.2A). Two weeks later the

specificity of the same T cells improved. For IQN9-peptide loaded DCs 1 mM peptide (IQN9) was enough to induce IFN γ secretion to levels comparable to the one seen with 10 mM peptide (IQN9) on day 33. Furthermore, T cells stimulated with IQN10 loaded DCs showed a higher reactivity against IQN10 loaded DCs, while IFN γ secretion against wild type peptide loaded DCs remained low (Figure 3.2B).

3.1.2.2.1 Stimulation with peptide pools in 96-well format

Because *in silico* prediction tools are based only on already known antigen HLA molecule pairs in some cases it does not depict the actual situation *in vivo*. Furthermore, different prediction tools results in different scores¹⁰³. And the promising peptide epitope candidate IQN9 is HLA-B*15:01 restricted, which is not a common HLA isotype¹⁰⁴. So, overlapping peptides were used for stimulation to find peptide epitopes which were not predicted *in silico* but processed as an antigen *in vitro*. The peptides used are listed in Table 2. They all cover the mutated amino acid glutamine (Q, depicted in red) which moves one position in each peptide. CD8 T cells were seeded in 96-well plates together with autologous DCs (E:T, 3:1) loaded with peptide mixtures 1, 2 or 3 (Table 3.2).

Table 3.2: Peptides used for peptide pool stimulation in 96-well format

Peptide #	Sequence	Peptide pool
A	QNILGGTVF	} 1
B	IQNILGGTV	
C	TIQNILGGT	
D	GTIQNILGG	} 2
E	NGTIQNILG	
F	PNGTIQNIL	
G	SPNGTIQNI	} 3
H	KSPNGTIQN	
I	WKSPNGTIQ	

Figure 3.3 shows an IFN γ ELISpot assay, in which the activation of T cells stimulated with one peptide-pool (1,2 or 3)-loaded DCs were tested against the same peptide-pool loaded DCs. As negative control unloaded DCs were used. T cell populations from well A1 and D4 (T cell populations (well) indicated below the bars) stimulated with peptide pool 1 showed recognition of the peptides with a low background. Also, T cells stimulated with peptide pool 2 recognized these peptides from peptide pool 2, but to a lower extent. T cells generated with peptide pool 3 showed the lowest reactivity (Figure 3.3).

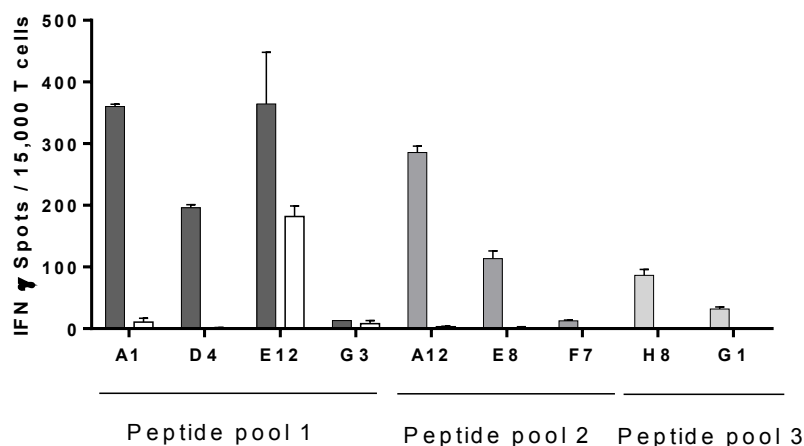


Figure 3.3: CD8 T cells stimulation with autologous IDH2 R140Q specific peptide pool loaded DCs. On d25+5 of primary stimulation and weekly restimulation with one of the three peptide pools loaded on autologous DCs, CD8 T-cell responders were tested for IFN γ ELISpot reactivity against DCs loaded with the same peptide pool (10 mM). On the day of the assay T cell culture was resuspended and 10 μ l T cell suspension was transferred in the assay plate to be tested against 5,000 peptide pool loaded DCs. Below the bars the T cell populations from different wells are indicated. Data are shown as means of duplicates from one experiment representative of three performed with different T-cell donors. Error bars represent the range.

During further culture reactivity was lost in all T cell populations. While 23 T cell populations (out of nine 96-well plates) showed peptide recognition in at least one IFN γ ELISpot, T cell populations reliably recognizing one of the IDH2 R140Q derived peptide could not be generated in 3 of 3 different donors (data not shown).

T cell populations of all stimulation cultures, which specifically and reliably recognized IQN9- and/or IQN10-peptide loaded DCs, were tested against DCs expressing IDH2 R140Q protein. However, no specific recognition of the IDH2 R140Q protein was observed.

3.1.2.3 Summary of stimulation with peptide loaded antigen presenting cells

In Table 3 the results of the peptide stimulation are summarized. It was only possible to stimulate T cells with the *in silico*-predicted HLA B*15:01 binding peptides (IQN9 and IQN10). But no T cell populations could be generated, which recognized endogenous processed IDH2 R140Q protein.

Table 3.3: Summary of results of stimulation with peptide loaded antigen presenting cells

Stimulation	HLA restriction	n	n peptide recognition	n endogen recognition
IQNILGGTV peptide	B15:01	7	5	0
TIQNILGGTV/SPNGTIQNI peptide	HLA-A2 and HLA-B7	4	0	0

Overlapping peptides pools 96 well plate	-	3	23	0
---	---	---	----	---

3.1.3 T cell stimulation with electroporated DC

In another approach CD4 T cells were stimulated with DCs expressing IDH2 R140Q protein upon mRNA electroporation. For expression control via flow cytometry a HIS tag was added on the C terminus of the amino acid sequence of IDH2 R140Q. For each experiment expression of the electroporated mRNA was confirmed by staining the HIS tag after overnight rest.

First, the kinetics of mRNA expression was measured after 4, 6, 8, 12, 16, 20 and 24 h to confirm expression of transferred mRNA for the first 24h. As an example, the expression of IDH2 wild type (blue) and IDH2 R140Q (red) 4 and 24h after electroporation are shown in Figure 3.4.

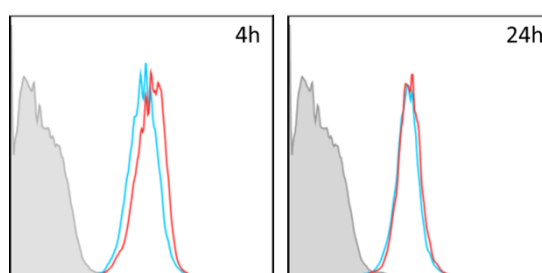


Figure 3.4: Transfection efficiency 4 and 24h after electroporation. After electroporation of IDH2 wild type or R140Q mRNA transfection efficiency was analyzed by flow cytometry. Data shown here are one representative histogram where IDH2 wild type transfected DCs are shown in blue and IDH2 R140Q transfected in red. Unstained DCs are shown in grey. Two histograms are shown at two different time points 4 and 24h.

Because it is unknown if the IDH2 R140Q protein is processed to a peptide antigen and if this peptide antigen would be presented on HLA class I or II molecules CD8 and CD4 T cells were used for stimulation with IDH2 R140Q expressing DCs. But CD8 T cell stimulations with IDH2 R140Q protein expressing DCs was not successful in 5 out of 5 donors (data not shown), the focus was on CD4 T cells. With CD4 T cells stimulation was done in 24 (data not shown) or 96 well plate formats and with bulk and naïve (enriched for CD3, CD4, CD45RA) T cells (Figure 3.5).

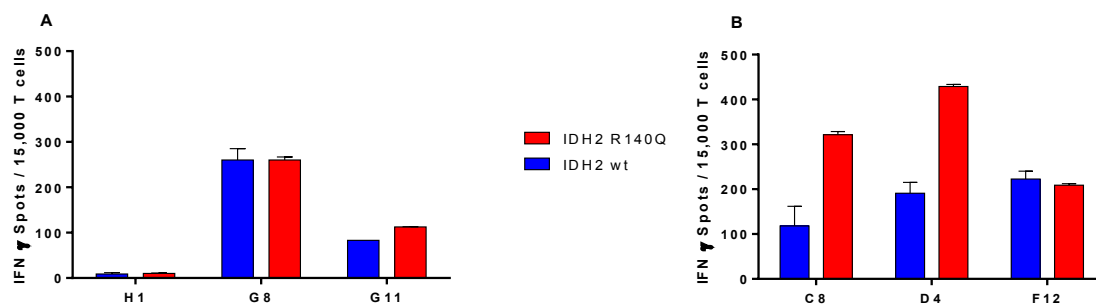


Figure 3.5: CD4 T cells stimulation with autologous IDH2 R140Q protein expressing DCs. (A) On d35+5 of primary stimulation and weekly restimulation with IDH2 R140Q protein expressing DCs, bulk CD4 T-cell responders were tested for IFN γ ELISpot reactivity against DCs expressing IDH2 R140Q protein. E:T ratio in the assay was 3:1. Below the bars the T cell populations from different wells are indicated. Data are shown as means of duplicates from one experiment representative of five performed with different T-cell donors. Error bars represent the range. (B) On d21+5 of primary stimulation and weekly restimulation with IDH2 R140Q protein expressing DCs, naïve CD4 T-cell (enriched for CD3, CD4, CD45RA) responders were tested for IFN γ ELISpot reactivity against DCs expressing IDH2 R140Q protein. E:T ratio in the assay was 3:1. Below the bars the T cell populations from different wells are indicated. Data are shown as means of duplicates from one experiment representative of three performed with different T-cell donors. Error bars represent the range.

Bulk CD4 T cell populations stimulated with autologous IDH2 R140Q expressing DCs in a 96-well plate format were not able to specifically recognize the mutated IDH2 R140Q protein in all five of the tested donors. An example is depicted in Figure 3.5A, where none of the cell populations secreted more IFN γ in the co-cultivation with IDH2 R140Q protein compared to IDH2 wild type expressing DCs. Naïve T cell populations showed in some tests a higher IFN γ secretion against IDH2 R140Q protein than IDH2 wild type protein expressing DCs (Figure 3.5B), but the reactivity was not stable in further experiments. We hypothesized that IDH2 R140Q is not sufficiently presented on the surface of DCs to stimulate a T cell reaction. To improve the processing and presentation of the IDH2 R140Q protein a signaling sequence was added (DC lamp1) known to improve targeting to the antigen processing pathway^{105–107}. However, also this modification did not result in T cell populations, which specifically recognize the IDH2 R140Q protein expressed by DCs (data not shown).

3.1.4 Stimulation of T cells with Influenza peptide

CD8 T cell stimulation with the IQN9- and IQN10-peptide was possible but based on our results these peptides were not processed from the IDH2 R140Q protein. To explain why these T cells even exist, a natural epitope close to the structure of the IQN9/10 peptide may occur¹⁰⁸. NCBI BLAST analysis of the IQN9 sequence resulted in a match on an influenza A peptide derived from the neuraminidase surfaceprotein of the virus. This peptide was used to stimulate T cells and to check reactivity of IQN9/10 stimulated T cells to the influenza A peptide (SQNILGTQE, Ifn A NA).

Bulk CD8 T cells were stimulated with autologous IQN9- or influenza A-peptide loaded PBMCs and tested in an IFN γ ELISpot for cross reactivity. In one donor T cells stimulated against IQN9-peptide loaded DCs showed recognition of IQN9- as well as influenza A-peptide loaded DCs. In the other case, were the influenza A (Inf A NA) peptide was used for T cell stimulation there was no specific recognition neither of the influenza A nor the IQN9-loaded DCs. The experiment was repeated with two other donors, but no IFN γ secretion against influenza A-peptide loaded target cells could be generated, neither with T cells stimulated with IQN9- nor influenza-peptide loaded DCs (Figure 3.6).

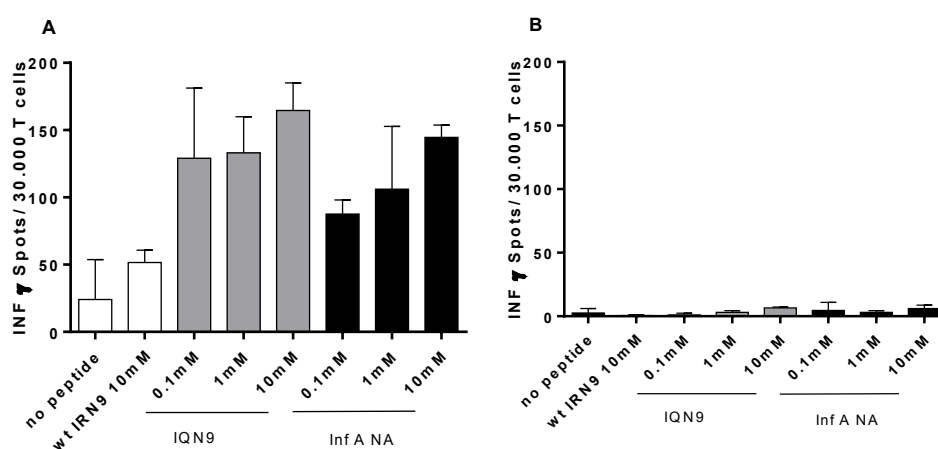


Figure 3.6: CD8 T cells (HLA-B*15:01) stimulation with autologous IDH2 R140Q or influenza peptide loaded DCs. (A) On d21+5 of primary stimulation and weekly restimulation with IQN9 peptide loaded DCs, CD8 T-cell responders were tested for IFN- γ ELISpot reactivity against DCs loaded with IDH2 R140Q (IQN9) or influenza A neuramidase (Inf A NA) peptide (0.1-10 mM). E:T ratio in the assay was 3:1. Data are shown as means of duplicates from one experiment of three performed with different T-cell donors (wherein no reactivity was seen in the other two donors). Error bars represent the range. (B) On d21+5 of primary stimulation and weekly restimulation with influenza A neuramidase peptide (Inf A NA) peptide loaded DCs, CD8 T-cell responders were tested for IFN- γ ELISpot reactivity against DCs loaded with IQN9 or Inf A NA peptide (0.1-10 mM). E:T ratio in the assay was 3:1. Data are shown as means of duplicates from one experiment of three performed with different T-cell donors (wherein no reactivity was seen in the other two donors). Error bars represent the range.

3.2 Effect of D-2-HG on metabolism and differentiation of monocyte-derived dendritic cells

The second part of my project was to analyze the effect of the oncometabolite D-2-HG on monocyte-derived DCs. As mentioned in the introduction metabolites secreted by cancer cells can modify the function of immune cells. Therefore influence of D-2-HG on the differentiation of monocytes into DCs was elucidated.

3.2.1 Uptake of D-2-HG in monocytes

Before the effects of D-2-HG were analyzed, 2-HG levels in monocytes were measured after 20 h incubation in the presence or absence of 10 mM D-2-HG. Monocytes were harvested, washed with PBS and further processed for liquid chromatography followed by mass spectrometry performed to determine the concentration of 2-HG in monocytes. Protein contents of cell pellets were also determined to normalize to μg of protein. These analyses were performed in cooperation with Prof. Peter Oeffner and PD Dr. Katja Dettmer at the Department of Functional Genomics, University Regensburg.

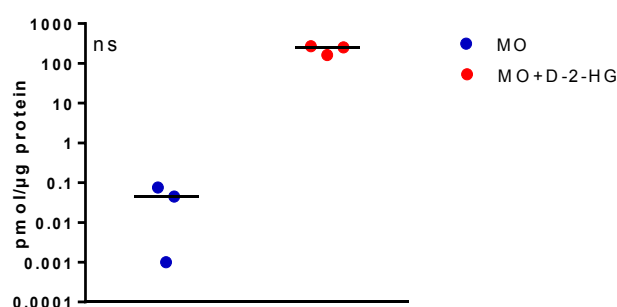


Figure 3.7: 2-HG concentration in cell pellets of monocytes (MO). Uptake of D-2-HG by monocytes was analyzed in the presence or absence of 10 mM D-2-HG for 20 h. Cells were washed with PBS and intracellular levels of D-2-HG were analyzed by mass spectrometry. Single values and median of 3 independent experiments with different donors is shown. Statistical analysis for group differences were performed with the Wilcoxon-Test (paired).

In untreated monocytes 2-HG content was beyond the limit of detection, showing that monocytes of healthy donors did not produce 2-HG (2-HG level 0.04 pmol/ μg protein). In monocytes treated with D-2-HG the 2-HG median levels were 252.9 pmol/ μg protein (Figure 3.7). The analysis was not specific for one enantiomer, but as D-2-HG was added, we concluded that most of the HG measured is D-2-HG and that D-2-HG entered the cell. So far, the mechanism of D-2-HG uptake of monocytes is not clear.

3.2.2 Changes of DC morphology upon D-2-HG treatment

After confirming the uptake of D-2-HG into monocytes, monocytes were seeded with or without 20 mM D-2-HG. After 7 days of D-2-HG treatment there was no influence on DC viability and cell yield determined by a cell counter (Figure 3.8A and B). Appropriate cursor settings for determining cell number and viability were established for DCs. But the mean diameter significantly increased with D-2-HG treatment (Figure 3.8C).

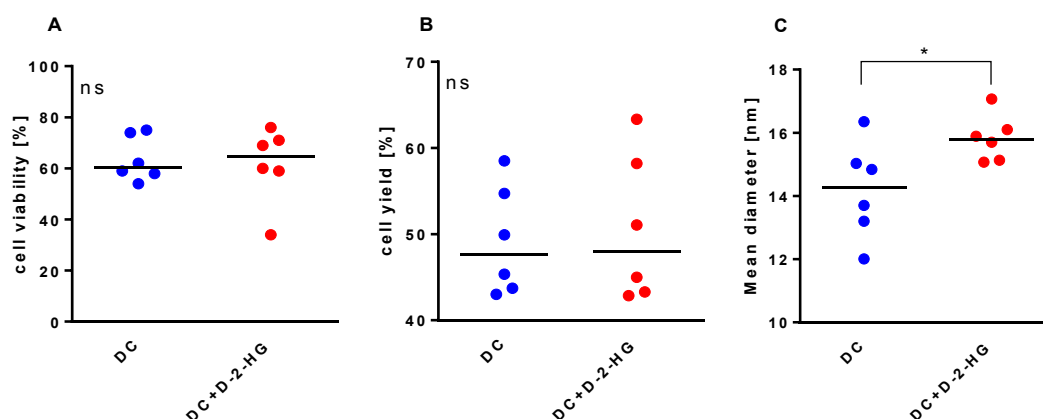


Figure 3.8: Viability (A), cell yield (B) and mean diameter (C) of D-2-HG treated DCs on day 7. DCs were differentiated in the absence or presence of 20 mM D-2-HG. Cell viability, yield and mean diameter were analyzed using the CASY cell analyzer system in. Cell yield was calculated with cell number of monocytes seeded on day 0. Single values and median of 6 independent experiments with different donors is shown. Statistical analyses for group differences were tested with Wilcoxon test (paired). (* $p \leq 0.05$ were considered significant, ns means not significant).

There was also no difference seen by bright-field microscopy on day 7, DCs from same donors had similar grades of adherence and cluster structures in both treatments (Figure 3.9).

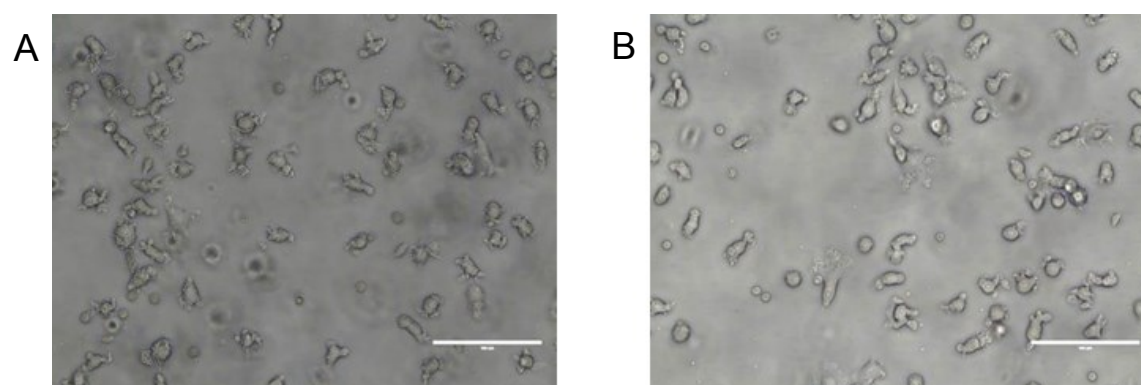


Figure 3.9: Bright field pictures of DCs (A) and DCs treated 7 days with D-2-HG (B). DCs were cultured 7 days in the presence or absence of D-2-HG [20 mM]. DCs were analyzed by light microscopy in bright field with a 40x magnification, bar represents 100 μm . This picture is one representative of 25 analyzed donors.

3.2.2.1.1 Dendritic cell structures analyzed by electron microscopy

DCs were differentiated in the presence or absence of 10 mM D-2-HG, on day 7 LPS was added for activation in one flask of each treatment. On day 8 DCs from each condition were harvested and fixed for electron microscopy (EM). Samples were further processed in cooperation with Prof. Brochhausen-Delius at the Department of Pathology of the University Hospital Regensburg.

First in smaller magnifications the shape of immature DCs (iDCs) treated with D-2-HG was compared to immature control DCs. In all three donors analyzed, less and shorter dendrites were visible in DCs treated with D-2-HG compared to control DCs. In most donors the dendrites were also (Figure 3.10).

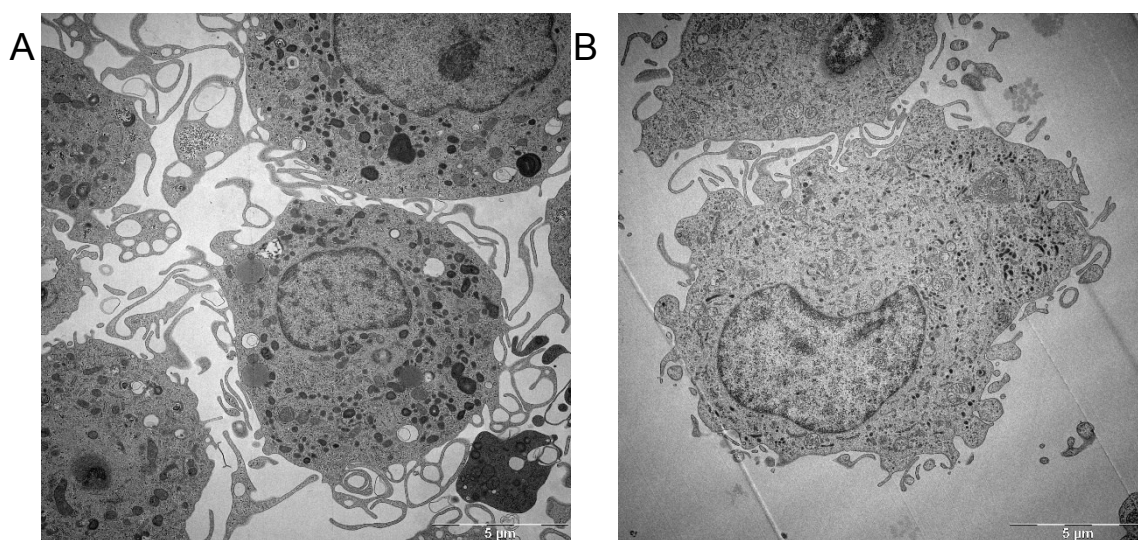


Figure 3.10: Electron microscope images of day 8 DCs treated with D-2-HG. DCs were cultured with D-2-HG (10 mM) (B) or without (A) for 8 days, harvested, fixed and further processed for electron microscopy. Pictures show one representative section of each group of DCs differentiated in the absence or presence of D-2-HG. EM analysis was performed with three different donors, for each donor 10 cells were analyzed with different magnifications. The magnification used here was 5000x, bar indicates 5 µm.

Next the effect of LPS on dendrite formation was analyzed. After activation of iDCs with LPS for 24h the number of dendrites increased in both groups (with or without D-2-HG). But there was still a difference in their appearance, dendrites of D-2-HG treated DCs were less and shorter as in the control cells (Figure 3.11).

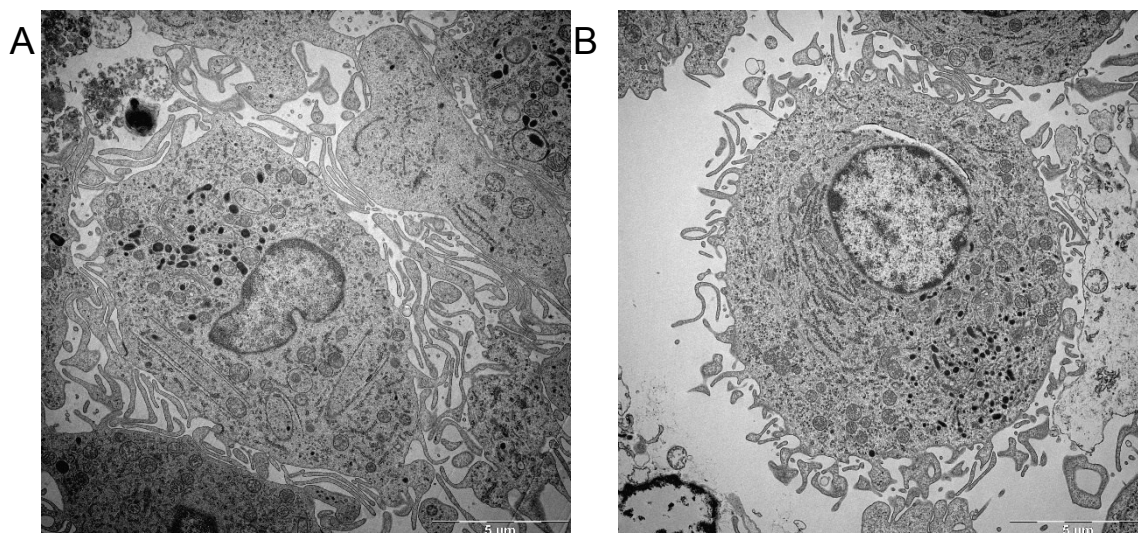
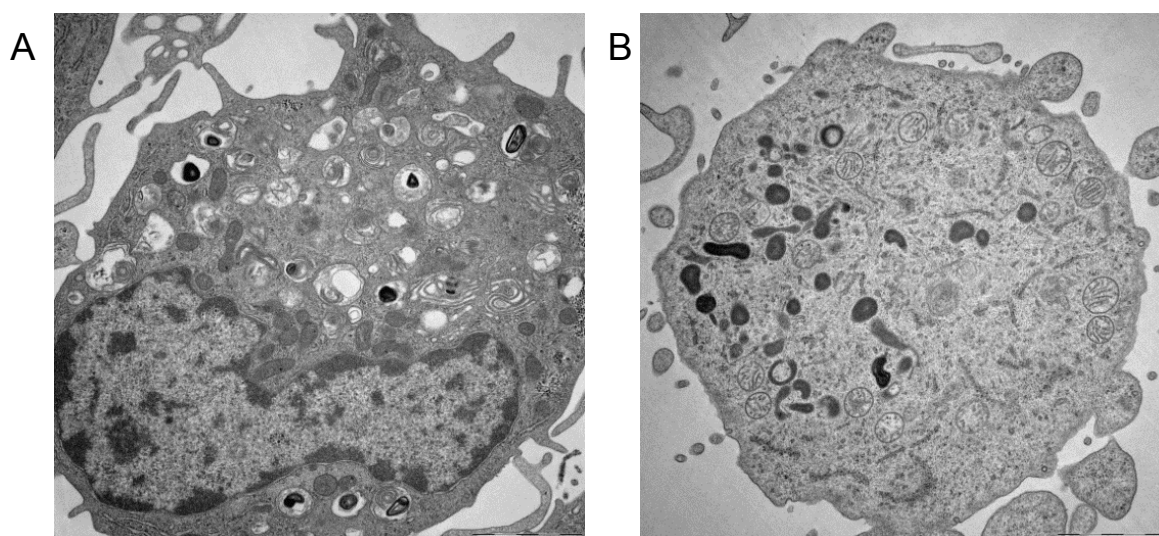


Figure 3.11: EM images of day 8 mature DCs treated with (B) or without (A) D-2-HG and activated with LPS. DCs were cultured with D-2-HG [10 mM] (B) or without (A) for 7 days and activated 24h with 100 ng/mL LPS, harvested, fixed and further processed for electron microscopy. Pictures show one representative section of each group of DCs differentiated in the absence or presence of D-2-HG. EM analysis was performed with three different donors, for each donor 10 cells were analyzed with different magnifications. The magnification used here was 5000x, bar indicates 5 μm .

3.2.2.1.2 Vesicle structure of D-2-HG treated DCs analyzed by electron microscopy

Another finding from the electron microscopy (EM) pictures was the differences in intracellular vesicles. In control DCs (Figure 3.12A) the vesicles were bigger with low electron density (bright) than in D-2-HG treated DCs (Figure 3.12B). Some of these vesicles contained small electron dense particles or membrane fragments. These vesicles get more dominant in control DCs treated with LPS.



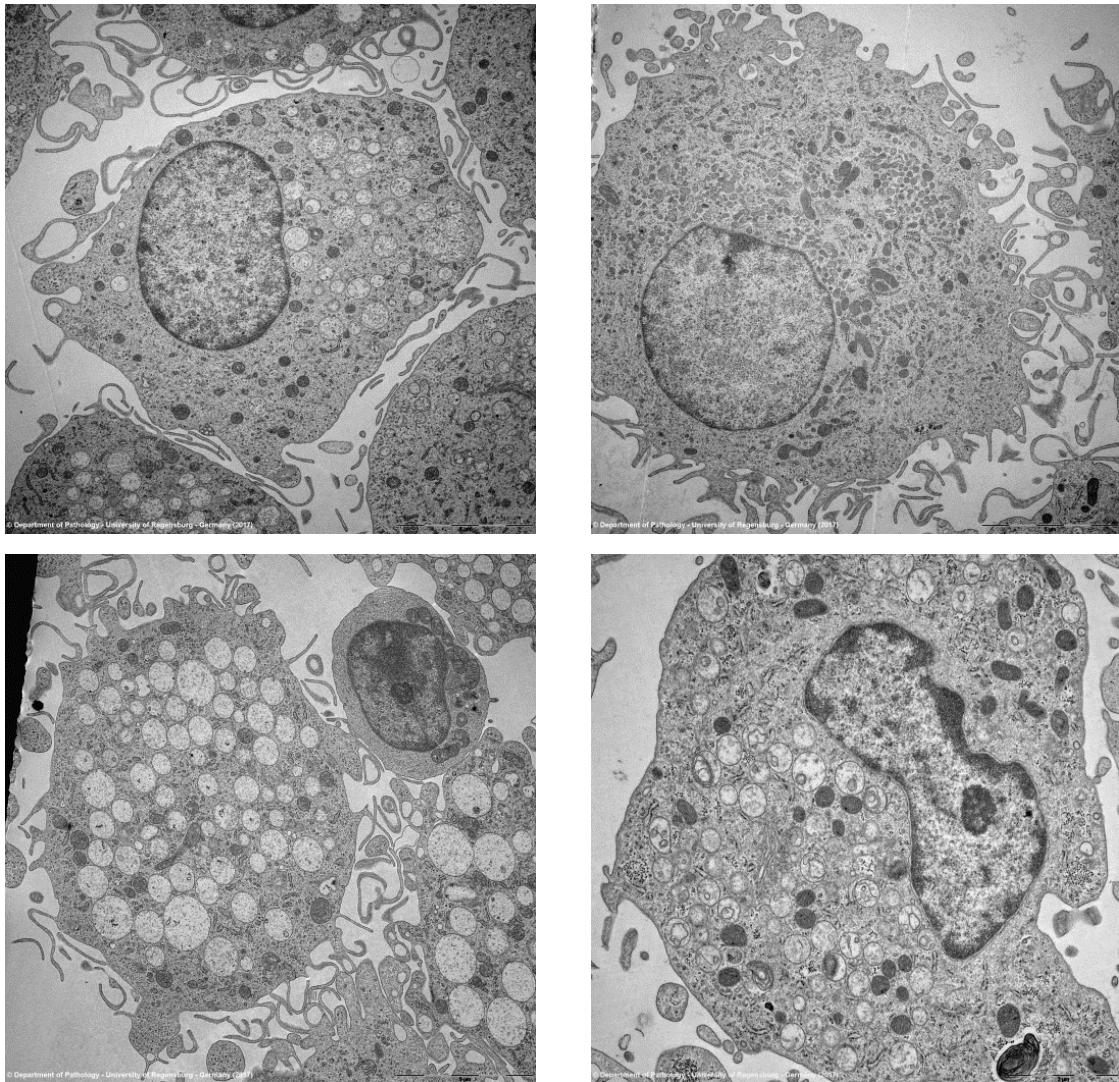


Figure 3.12: EM image of control (A) and D-2-HG treated DCs (B). DCs were cultured in the presents (B) or absence (A) of D-2-HG. On day 8 DCs of each group were harvested, fixed and further processed for electron microscopy. Pictures show one representative section of each group of DCs differentiated in the absence or presence of D-2-HG. EM analysis was performed with three different donors, for each donor 10 cells were analyzed with different magnifications. The magnification used here was 5000x, bar indicates 5 μ m.

In D-2-HG treated DCs these structures were less abundant. D-2-HG treated DCs contained more small vesicles with higher electron density (dark structures, Figure 3.12).

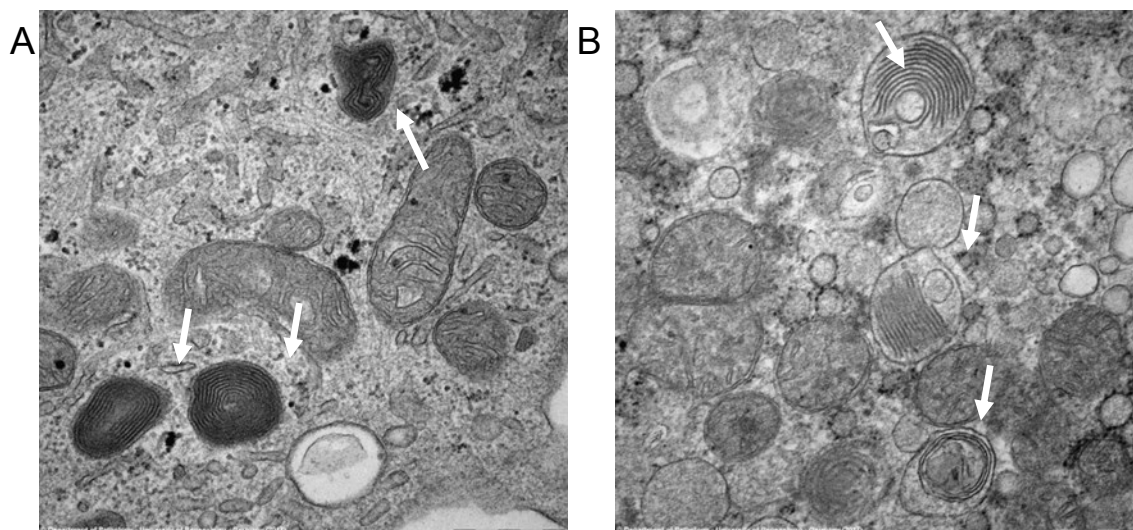


Figure 3.13: EM images of d8 DCs treated with D-2-HG. DCs were cultured in the presents (B) or absence (A) of D-2-HG. On day 8 DCs of each group were harvested, fixed and further processed for electron microscopy. Pictures show one representative section of each group of DCs differentiated in the absence or presence of D-2-HG. EM analysis was performed with three different donors, for each donor 10 cells were analyzed with different magnifications. Multi-laminar structures are indicated with arrows. The magnification used here was 40000x, bar indicates 500 nm.

In both donors, multi-membrane structures were visible as seen in Figure 3.13 indicated by the white arrows. In the control DCs (Figure 3.13A) multi-laminar structures were more electron dense and packed tighter than in the DCs treated with D-2-HG (Figure 3.13B). We saw difference in the abundance of the multi-laminar structures although both types could be seen in both treatments.

Differences in the structure of the vesicles may also have an influence on autophagy (microtubule-associated proteins 1A/1B light chain 3B, LC-3B) and late endosomes (Ras-related protein 9, Rab9) generation. Especially because these processes are important for antigen processing and presentation of DC as well as the multi-laminar vesicles.

3.2.2.3 Expression analyze of late endosome marker Rab9 by western blot

Rab9 is known to be present in late endosomes and can be used to analyze abundance of late endosomes. DCs differentiated in the presence or absence of D-2-HG were lysed with RIPA buffer and protein was isolated. 15 μ g protein was analyzed separated in a gel and transferred on a membrane to analyze Rab9 expression.

Rab9 was expressed in all three donors analyzed. In one donor there was a 50% reduction of Rab9 in D-2-HG treated DCs compared with control DCs of the same donor and normalized on actin expression. In the other two donors a slight decreased expression after

D-2-HG treatment was observed (Figure 3.14). Overall there was no significant effect of D-2-HG on the abundance of late endosomes.

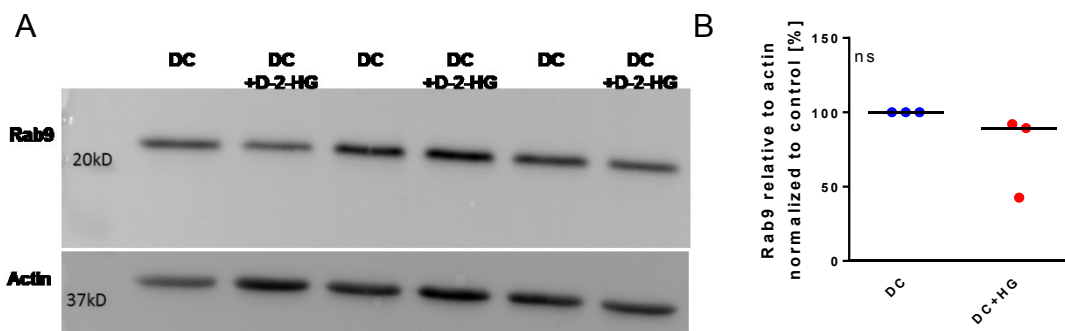


Figure 3.14: Rab9 expression analysis in DC treated with D-2-HG by western blot. DCs were harvested after 7 days of D-2-HG [20 mM] treatment. Whole protein was isolated and 15 μ g protein was loaded on a 14% SDS acrylamide gel. Membrane was stained with rabbit anti-Rab9 primary antibody (1:1000) and HRP linked anti-rabbit secondary antibody (1:2500). Antibodies were removed by membrane stripping and analyzed for actin with rabbit anti-actin (1:1000) and anti-rabbit (1:2500). Rab9 signal was measured after an exposure time of 51s. (B) Quantification was done by normalization on actin expression and expression of corresponding control DCs by ImageJ. Single values and median of 3 independent experiments with different donors is shown. Statistical analyses for group differences were tested with Wilcoxon test (paired). (* $p \leq 0.05$ were considered significant, ns means not significant).

3.2.2.4 Expression analyze of the autophagy marker LC-3B by western blot

After differences in the vesicle structure were observed in electron microscope pictures the amount of autophagosomes were analyzed by western blot detection of LC-3B. LC-3B is a protein involved in the formation of autophagosomes.

LC-3B was expressed in all donors. There are different forms of LC-3B which were detected by the antibody. The biggest form is pro-LC-3B (about 37kD) it gets converted in LC-3B I (band visible at about 15kD) and finally to LC-3B II (band visible at about 13kD). Expression in control DCs was in all donors higher than in D-2-HG treated DCs for LC-3B I and II. Overall expression of LC-3B I and II was about 50% decreased in D-2-HG treated DCs. Levels of pro-LC-3B were comparable in all treatments and donors (Figure 3.15).

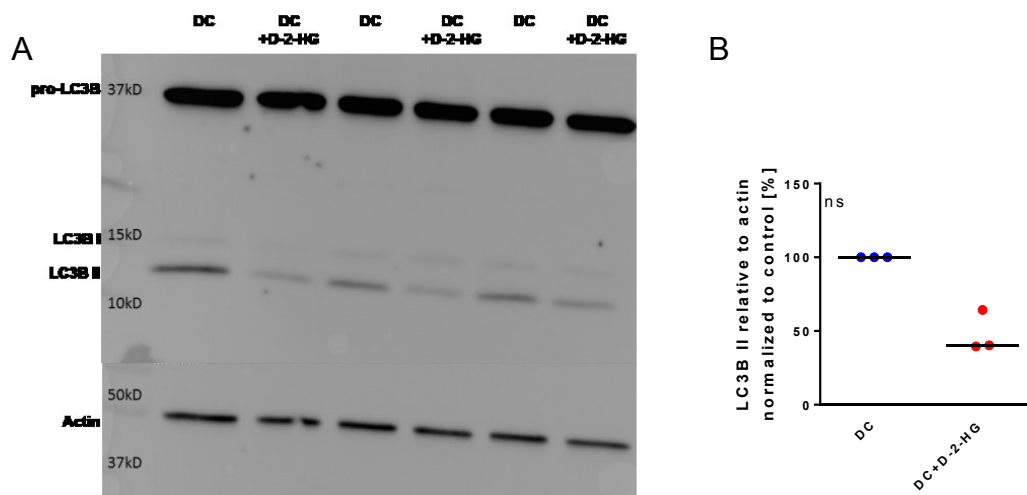


Figure 3.15: LC-3B expression analysis in DC treated with D-2-HG by western blot. DCs were harvested after 7 days of D-2-HG [20 mM] treatment. Whole protein was isolated and 15 μ g protein was loaded on a 14% SDS acrylamide gel. Membrane was stained with rabbit anti-LC-3B primary antibody (1:1000) and HRP linked anti-rabbit secondary antibody (1:2500). Antibodies were removed by membrane stripping and analyzed for actin with rabbit anti-actin (1:2500) and anti-rabbit (1:2500). LC3B signal was measured after an exposure time of 50s. (B) Quantification was done by normalization on actin expression and expression of corresponding control DCs. T Single values and median of 3 independent experiments with different donors is shown. Statistical analyses for group differences were tested with Wilcoxon test (paired). (* $p \leq 0.05$ were considered significant, ns means not significant).

In a second set of experiments monocytes were treated with Bafilomycin A1 (BafA1, autophagy inhibitor) in the presence or absence of D-2-HG for 7 days. In cell lysates of these treatments pro-LC-3B and LC-3B II as seen in the first western blot were not detectable. The only visible band was at the height of 15 kD, most likely corresponding to the LC-3B I. Analyses of these lysates did not reveal a strong reduction of the LC-3B signal as seen in Figure 3.15. Addition of BafA1 slightly increased the levels of LC3B.in the control cells as well as in the D-2-HG treated cells.

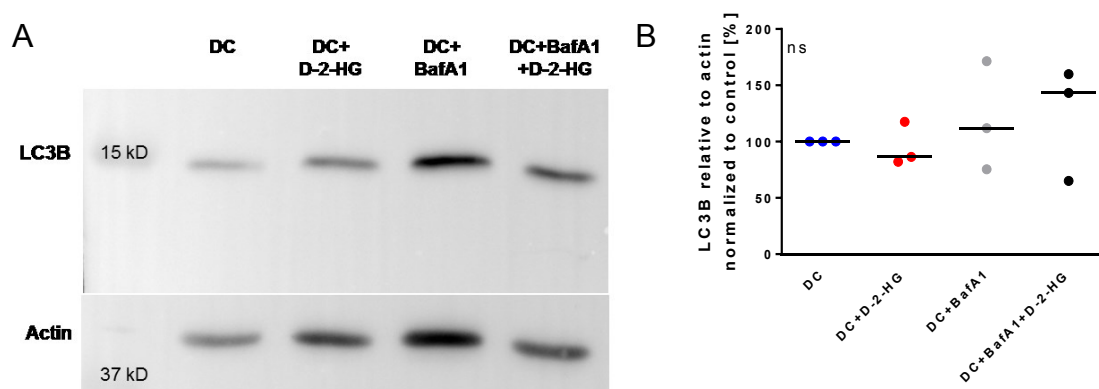


Figure 3.16: LC-3B expression analysis in DC treated with D-2-HG by western blot. (a) DCs were harvested after 7 days of D-2-HG [20 mM] treatment. Whole protein was isolated and 15 μ g protein was loaded on a 14% SDS acrylamide gel. Membrane was stained with rabbit anti-LC-3B primary antibody (1:1000) and HRP linked anti-rabbit secondary antibody (1:2500). Antibodies were removed by membrane stripping and analyzed for actin with rabbit anti-actin (1:2500) and anti-rabbit (1:2500). LC-3B signal was measured after an exposure time of 40s. (B) Quantification was done by normalization on actin expression and expression of corresponding control DCs. Single values and median of 3 independent experiments with different donors is shown. Statistical analyses for group differences were tested with Friedman test (paired). (* $p \leq 0.05$ were considered significant, ns means not significant).

3.2.2.5 HLA-class II expression of bafilomycin A1 treated DCs

After effects of D-2-HG on LC-3B (present in autophagosomes) abundance in DCs were observed, HLA class II expression was analyzed in BafA1 treated cells. We hypothesized, that reduced LC-3B levels could cause a decrease in HLA class II expression as autophagy is involved in the antigen processing machinery.

BafA1 treatment alone had no influence on HLA-DP (Figure 3.17A) expression and slightly reduced HLA-DR expression in 2 out of three donors. In combination with D-2-HG BafA1 had no positive effect, neither on HLA-DP, nor on HLA-DR expression (Figure 3.17B).

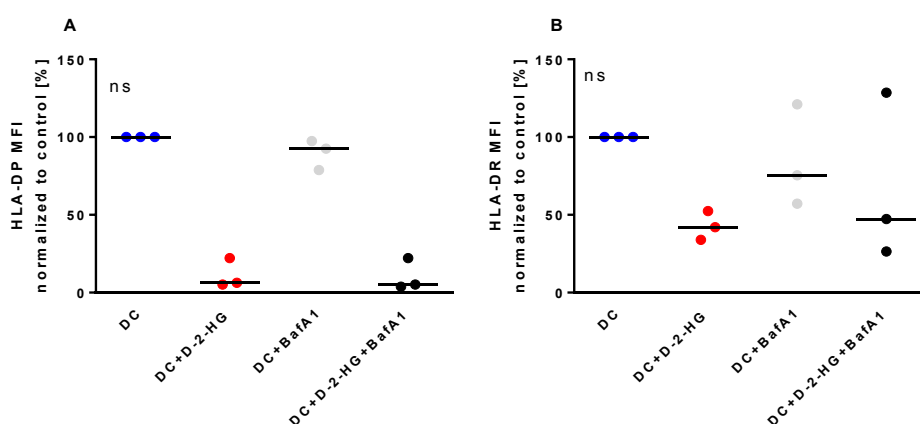


Figure 3.17: HLA-DP (A) and HLA-DR (B) expression of bafilomycin treated DCs. DCs were cultured in the presence or absence of 20 mM D-2-HG or 10 nM bafilomycin A (Baf A1) or both. HLA-DP (A) and HLA-DR (B) surface expression was analyzed by flow cytometry. Median (background corrected) intensity of the fluorescence signal (MFI) were used and results were normalized to the level in control. Single values and median of 3 independent experiments with different donors is shown. Statistical analyses for group differences were tested with Friedman test (paired). (* $p \leq 0.05$ were considered significant, ns means not significant).

3.2.3 Effect of D-2-HG differentiation and maturation of DCs

Next, the effects of D-2-HG on differentiation, maturation and activation monocyte derived DCs were analyzed by flow cytometry.

3.2.2.1 CD14 and CD1a expression of D-2-HG treated DCs

In a first set of experiments the expression of a panel of differentiation related surface markers was investigated.

CD14 (involved in LPS signaling response) is expressed on monocytes and macrophages but not on DCs¹⁰⁹. Expression of CD14 was high in monocytes but decreased during culture with IL-4 and GM-CSF in control DCs and D-2-HG treated cells. On day 7

DCs there was no expression of CD14 in all treatments, thus D-2-HG did not impact the differentiation related down-regulation of CD14 (Figure 3.18A).

CD1a, involved in lipid and glycolipid antigen presentation, is mainly expressed on DCs, but not on monocytes¹¹⁰. Hence, the expression should rise during DC differentiation. As expected there was a low expression of CD1a in monocytes but expression was significantly increases in DCs on day 7. In D-2-HG treated cells. However, expression increased only slightly to 19% of the level of control DCs (Figure 3.18B).

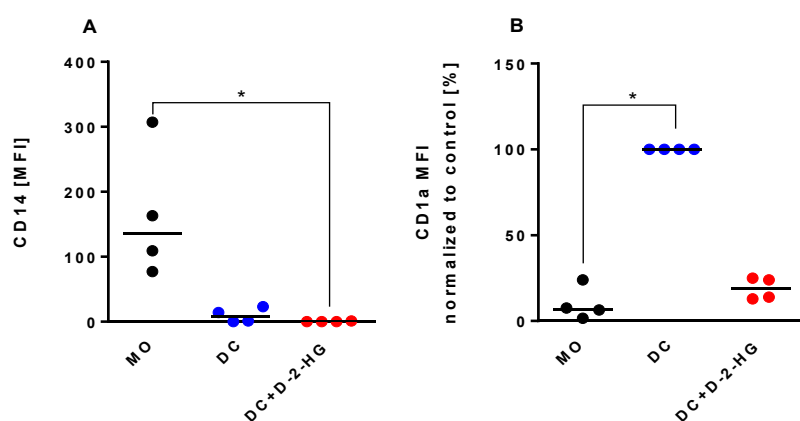


Figure 3.18: CD14 (A) and CD1a (B) expression of D-2-HG treated DCs. DCs were differentiated in the presence or absence of 20 mM D-2-HG. Monocytes (MO) were stained directly after isolation. On day 7 DCs were harvested and analyzed for CD14 (A) and CD1a (B) surface expression. Single values and median of 4 independent experiments with different donors is shown. For CD14 expression median (background corrected) intensity of the fluorescence signal were used and results were normalized to the level in control. For CD1a expression median (background corrected) intensity of the fluorescence signal is shown. Statistical analyses for group differences were tested with Friedman test (paired). (* $p \leq 0.05$ were considered significant).

3.2.2.2 DC-SIGN expression on D-2-HG treated DCs

Another marker for DCs is dendritic cell-specific, intercellular adhesion molecule (ICAM) -3 grabbing non-integrin (DC-SIGN), an adhesion molecule mainly expressed on DCs but also on some subpopulations of macrophages¹¹¹. DC-SIGN is involved in migration, antigen capture and T cell priming of DCs¹¹².

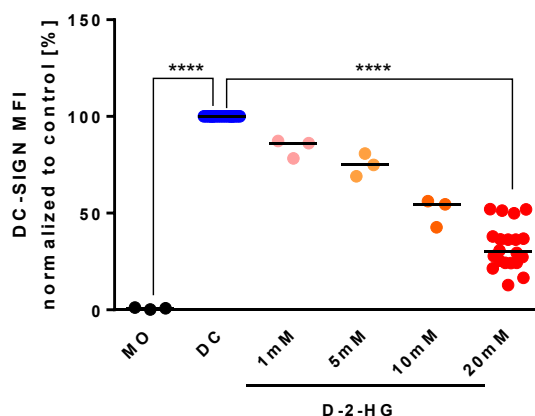


Figure 3.19: Surface expression of DC-SIGN after 7d incubation with D-2-HG. DCs were differentiated in the presence or absence of 1-20 mM D-2-HG. Monocytes (MO) were stained directly after isolation. On day 7 DCs were harvested and analyzed for DC-SIGN surface expression by flow cytometry. Single values and median of 3-20 independent experiments with different donors is shown. median (background corrected) intensity of the fluorescence signal were used. Statistical analyses for group differences were tested with Kruskal-Wallis test (paired). (* $p \leq 0.05$ were considered significant **** $p \leq 0.00001$).

DC-SIGN expression was absent on monocytes and significantly increase in untreated DCs on day 7. D-2-HG decreased the expression concentration-dependent (Figure 3.19), and 20 mM D-2-HG strongly reduced the expression compared to untreated control DCs (Figure 3.19).

3.2.2.3 HLA class I molecules of D-2-HG of DCs

Another class of surface molecules important for antigen presentation of DCs are HLA molecules. HLA class I molecules are expressed on an all nucleated cells and present antigens to CD8 T cells¹. The expression of HLA class I molecules was measured in immature and mature (activated with 100 ng/ml LPS) DCs in the absence or presence of D-2-HG, results are shown in Figure 3.20.

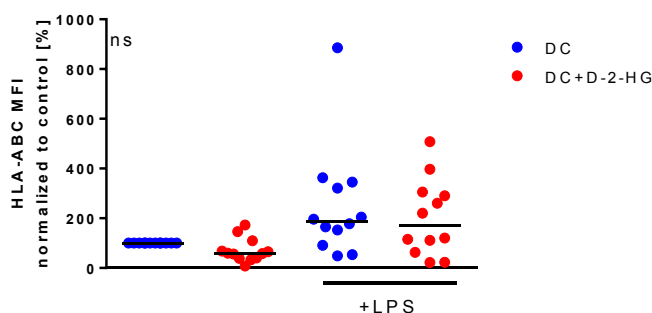


Figure 3.20: Impact of D-2-HG on surface expression of HLA-class I molecules after 7 days of culture. DCs were differentiated in the presence or absence of 20 mM D-2-HG. On day 7 DCs were activated with 100 ng/ml LPS for 24h. DCs were harvested and analyzed for HLA-class I surface expression with HLA-A, -B and -C specific antibody by flow

cytometry. Single values and median of 9 independent experiments with different donors is shown. Median (background corrected) intensity of the fluorescence signal were used and results were normalized to the level in control DCs. Statistical analyses for group differences were tested with Friedman test (paired). ($*p \leq 0.05$ were considered significant, no significance was found).

HLA class I expression increased after LPS incubation in D-2-HG treated and untreated DCs. The levels of HLA class I expression in D-2-HG treated DCs were comparable to untreated controls before and after LPS addition. Taken together, D-2-HG did not alter the expression and translocation of HLA class I molecules on the surface of DCs.

3.2.2.4 Surface expression of HLA class II molecules

Next, HLA class II molecule expression was investigated. HLA class II molecules also present antigens to T cells, but in contrast to HLA class I molecules HLA class II molecules present antigens to CD4 T cells¹. In contrast to HLA class I, HLA class II is more selectively expressed on antigen presenting cells under not inflammatory conditions¹.

The surface expression of HLA-DR, DP and DQ was analyzed on monocytes and DCs in the absence or presence of D-2-HG. Monocytes expressed low levels of HLA-DR molecules which increased during differentiation of untreated monocytes as well as in monocytes treated with increasing concentrations (1-20 mM) of D-2-HG. However, mean fluorescence intensity (MFI) of HLA-DR expression decreased with increasing D-2-HG concentrations. For 20 mM D-2-HG there was significantly less HLA-DR present on the surface compared to control DCs (Figure 3.21).

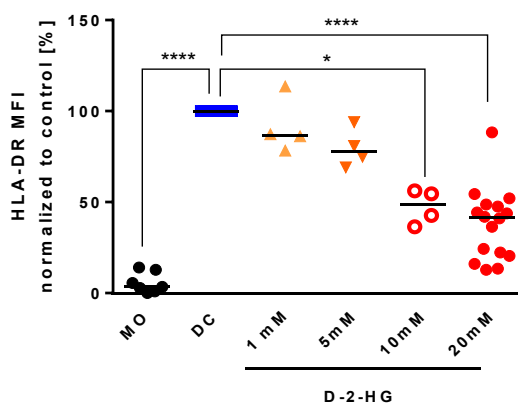


Figure 3.21: Analyses of HLA-DR expression of D-2-HG treated DCs (titration). DCs were differentiated in the presence or absence of 1-20 mM D-2-HG. Monocytes (MO) were stained directly after isolation. On day 7 DCs were harvested and analyzed for HLA-DR surface expression by flow cytometry. Single values and median of 3-4 independent experiments with different donors is shown. Median (background corrected) of fluorescence signal were used to normalize to control DCs. Statistical analyses for group differences were analyzed with Kruskal-Wallis test (paired). ($* p \leq 0.0505$ were considered significant, $****p \leq 0.00001$).

The expression of the two other HLA class II molecules HLA-DQ and -DP was also analyzed. Expression of HLA-DQ (Figure 3.22A) and -DP (Figure 3.22B) was also elevated

during differentiation from monocytes to DCs. This upregulation was blocked by D-2-HG. In some donors D-2-HG did not only limit the upregulation but even reduced the expression of HLA-DQ and DP below the level measured in respective monocytes. On days 4 only HLA-DR expression was elevated compared to the monocyte level (Figure 3.22C), the upregulation of HLA-DQ and -DP started later.

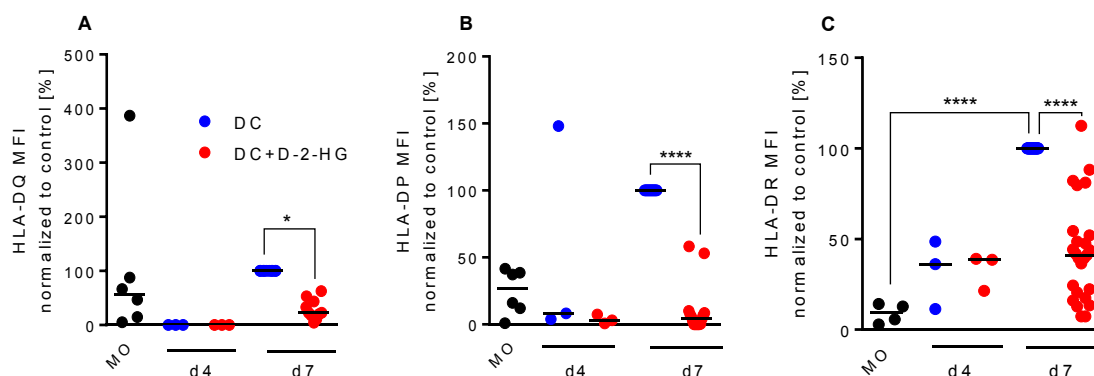


Figure 3.22: HLA-DQ (A), -DP (B) and -DR expression of D-2-HG treated DCs. DCs were differentiated in the presence or absence of 20 mM D-2-HG. Monocytes (MO) were stained directly after isolation. On day 4 and 7 DCs were harvested and analyzed for HLA-DQ (A, n=3-10), HLA-DP (B, n=3-15) and HLA-DR (C, n=3-25) surface expression. Medians (background corrected) of fluorescence signal were used to normalize to control DCs. Single values and median of 3-25 independent experiments with different donors is shown. Statistical analyses for group differences were analyzed with Kruskal-Wallis test (paired). (* p<0.05 were considered significant, *** p<0.001, **** p<0.0001).

3.2.2.4.1 Intracellular staining of HLA class II molecules

Since a reduced surface expression of HLA class II molecules was seen in D-2-HG treated DCs, it was checked if this was due to an inhibition of the HLA molecule transport to the surface or the result of reduced expression of HLA molecules. To answer this question, intracellular staining of HLA class II molecules was performed. HLA-DQ and -DP were not detected, so there is neither an intracellular HLA molecule storage nor a deficit in transport to the cell surface. For HLA-DR the intracellular staining showed similar results as the surface staining, D-2-HG treated cells showed less HLA-DR abundance than control DCs (Figure 3.23).

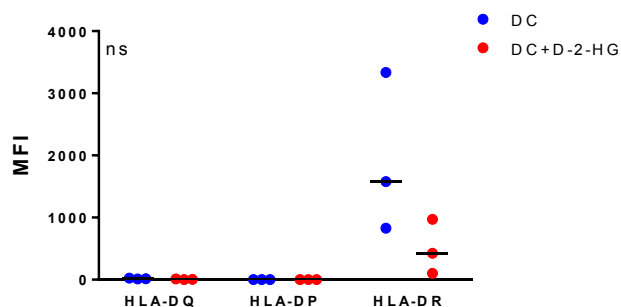


Figure 3.23: Intracellular staining of HLA class II molecules in D-2-HG treated DCs. DCs were differentiated in the presence or absence of 20 mM D-2-HG. On day 7 DCs were harvested and analyzed for intracellular HLA-DQ, HLA-DP and HLA-DR expression. Single values and medians (background corrected) of fluorescence signal are shown for three different donors. Statistical analyses for group differences were analyzed with Wilcoxon test (paired). (* $p \leq 0.05$ were considered significant, no significance was found).

3.2.2.4.2 Western blot analyses of HLA class II molecules

To confirm our results on the expression of HLA class II obtained by flow cytometry, the expression of HLA class II molecules was also determined by western blot. The antibody used binds to all three HLA class II molecules.

When compared to untreated controls, HLA class II expression was decreased in all lysates analyzed from D-2-HG treated DCs, but there were still HLA class II molecules detectable (Figure 3.24).

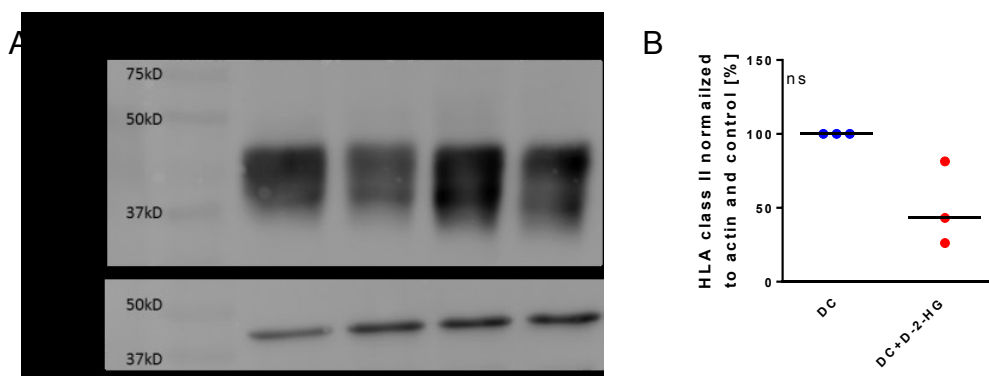


Figure 3.24: HLA class II expression analysis in DC treated with D-2-HG by western blot. (A) DCs were harvested after 7 days of D-2-HG [20 mM], protein was isolated with RIPA buffer. 10 μ g were loaded on a 12% SDS acrylamide gel. Membrane was stained with mouse anti-HLAII primary antibody (1:2000) and HRP linked anti-mouse secondary antibody (1:2500). Antibodies were removed by membrane stripping and analyzed for actin with rabbit anti-actin (1:2500) and anti-rabbit (1:2500). HLA class II signal was measured after an exposure time of 18s. (B) Quantification of three different donors was done by normalization on actin expression and expression of corresponding control DCs by ImageJ. Single values and median of 3 independent experiments with different donors is shown. Statistical analyses for group differences were analyzed with Wilcoxon test (paired). (* $p \leq 0.05$ were considered significant, no significance was found).

3.2.2.5 Expression of co-stimulatory molecules CD80/CD86

To analyze the effect of D-2-HG on DC activation the co-stimulatory molecules CD80 and CD86 were analyzed in immature DCs on day 7 as well as after LPS activation on day 8. CD80 and CD86 are co-stimulatory molecules which bind to CD28 on T cells leading to T cell activation ¹.

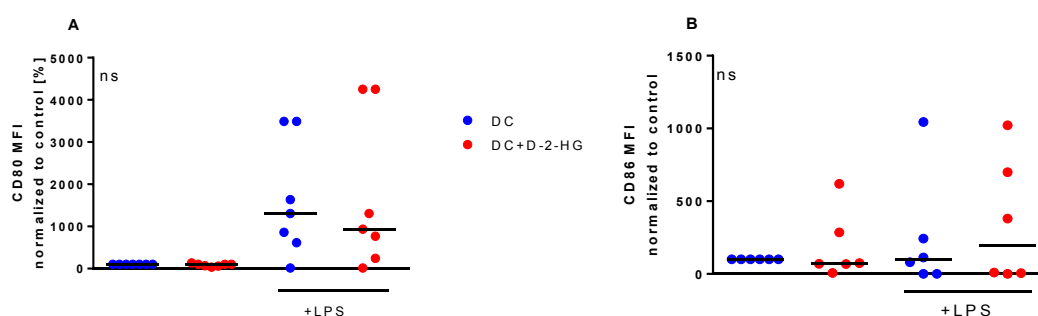


Figure 3.25: Expression of CD80 (A) and CD86 (B) in D-2-HG treated immature and mature DCs. DCs were differentiated in the presence or absence of 20 mM D-2-HG. On day 7 DCs were activated with 100 ng/ml LPS for 24h. DCs were harvested and analyzed for CD80 (A) and CD86 (B) expression by flow cytometry. Median (background corrected) intensity of the fluorescence signal were used. Single values and median of 7 independent experiments with different donors is shown. Statistical analyses for group differences were tested with Wilcoxon test (paired). (* $p \leq 0.05$ were considered significant, no significance was found).

Expression of CD80 and CD86 was low in immature DCs with or without D-2-HG. As expected LPS exposure induced the expression of CD80 and CD86 in both groups, but in DCs treated with D-2-HG and LPS the effect on CD86 was less pronounced and some donors had an even higher CD86 expression after D-2-HG treatment. Overall there was no significant effect on the expression of CD80 and CD86 (Figure 3.25).

3.2.3 Effects of D-2-HG on DC function

3.2.3.1 Effect of D-2-HG on cytokine production in DCs

After activation of D-2-HG treated or control DC for 24h with LPS supernatants were collected for measurements of cytokine concentrations. IL-12 levels of D-2-HG treated mature DCs were significantly lower than those in the untreated controls. In contrast for IL-10 there was a higher secretion in some of the tested donors in the D-2-HG treated DCs. Levels of IL-6 and TNF were comparable in both treatments (Figure 3.26). To summarize, DCs treated with D-2-HG showed less IL-12 secretion and a trend to a higher IL-10 secretion.

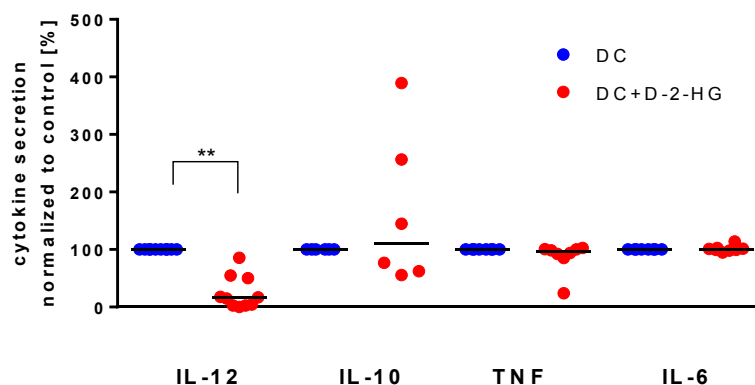


Figure 3.26: IL-12, IL-10, TNF and IL-6 secretion of mature DCs treated with D-2-HG. DCs were differentiated in the presence or absence of 20 mM D-2-HG. On day 7, DCs were activated with 100 ng/ml LPS for 24h. Supernatants were collected and analyzed for cytokine concentrations by ELISAs. Results from 7 different donors are shown. Cytokine concentrations of D-2-HG treated DCs were normalized to corresponding control. Single values and median of 6-10 independent experiments with different donors is shown. Statistical analyses for group differences were tested with Wilcoxon test (paired). (* $p \leq 0.05$ were considered significant, ** $p \leq 0.01$).

Taken together D-2-HG reduced the expression of MHC class II molecules and strongly impaired IL-12 secretion of DCs. Both effects could have a strong impact on the stimulation of T cells, especially of CD4 T cells, hence the stimulatory capacity of DCs differentiated in the presence or absence of D-2-HG was investigated on CD4 T cells.

3.2.3.2 Effect of D-2-HG on T cell stimulatory capacity of DCs

3.2.3.2.1 IFN γ secretion and proliferation of bulk and naïve enriched T cells

DCs cultured 7 days with or without D-2-HG were used as stimulators in an allogeneic mixed lymphocyte reaction (MLR) with naïve (CD4/CD45RA) or bulk enriched CD4 T cells in a DC to T cell ratio 1:10. For Stimulation of naïve enriched T cells, DCs were activated with LPS during MLR culture to stimulate production of pro-inflammatory cytokines like IL-12. For bulk CD 4 T cells DCs were activated with LPS for 24 hours and subsequently used in the MLR culture. After 5 days of MLR culture, supernatants were collected to analyze IFN γ secretion of T cells by ELISA. Results for bulk and naïve CD4 T cells are summarized in Figure 3.27A.

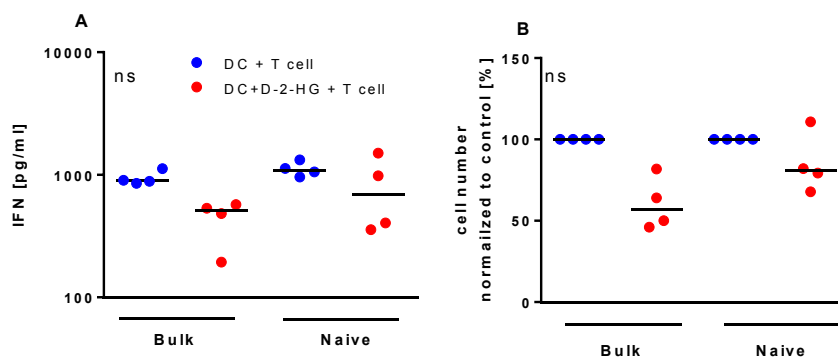


Figure 3.27: IFN γ secretion of bulk CD4 and CD4/CD45RA enriched T cells stimulated with allogeneic DCs treated without or with D-2-HG. Immature DCs differentiated in the presence or absence of 20 mM D-2-HG were cultured together with allogeneic naïve enriched T cells in a ration (1:10). (A) On day 5 supernatants were collected to analyzed IFN γ concentration by ELISA. (B) On day 7 T cell numbers were determined and cell numbers of T cells cultured with D-2-HG treated DCs were normalized to those obtained from T cells stimulated with untreated DCs. Single values and median of 4 independent experiments with different donors is shown. Statistical analyses for group differences were tested with Wilcoxon test (paired). (* $p \leq 0.05$ were considered significant, no significance was found).

IFN γ secretion of naïve enriched T cells stimulated with D-2-HG treated DCs was strongly affected in 2 of 4 donors tested and slightly reduced in one additional donor. The impact was stronger in the setup with bulk derived T cells, which could be related either to the application of bulk T cells or to the different stimulation protocol. IFN γ concentrations decreased from 894 pg/ml to 508 pg/ml. Although not statistically significant there was a strong trend to a reduced IFN γ concentration in both, bulk and naïve C T cells stimulated with D-2-HG treated DCs (Figure 3.27A).

On day 7 of MLR culture T cells were harvested and counted to analyze T cell proliferation. In the case of bulk CD4 T cells proliferation of T cells stimulated with D-2-HG treated DCs was reduced in all donors tested. By comparing the two medians a 43% reduction of proliferation was seen in T cells stimulated with D-2-HG treated DCs compared to T cells stimulated with control DCs ($p = 0,1250$, Figure 3.27B).

For naïve enriched T cells, there were less T cells in cultures with D-2-HG treated DCs compared to control DCs in 3 of 4 donors tested. But the reduction of T cell proliferation was not significant. In summary there was a reduction of about 20%.

3.2.3.2.2 Impact of D-2-HG on differentiation of regulatory T cells

In naïve T cells the expression of the activation marker CD25 and FoxP3 was analyzed by flow cytometry in addition. CD25 is a subunit of the IL-2 receptor which is only expressed on activated T cells¹¹³. In Figure 3.28 the percentage of CD25 expressing CD4 T cells is shown. On day 7 of MLR culture nearly all T cells (over 80%), were CD25 positive. There was no

striking difference in the CD25 expression of T cells stimulated with DCs differentiated in the absence or presence of 20 mM D-2-HG.

Regulatory T cells, which control the activity of conventional T cells also highly express CD25. To identify regulatory T cells, cells were stained intracellular for FoxP3. FoxP3 is an important transcription factor for the function of regulatory T cells¹¹³. The portion of CD4/CD25/FoxP3 positive cells was comparable in T cells stimulated with DCs differentiated in the absence or presence of D-2-HG. Frequency of T_{reg} was about 11% of all CD4 T cells (Figure 3.28).

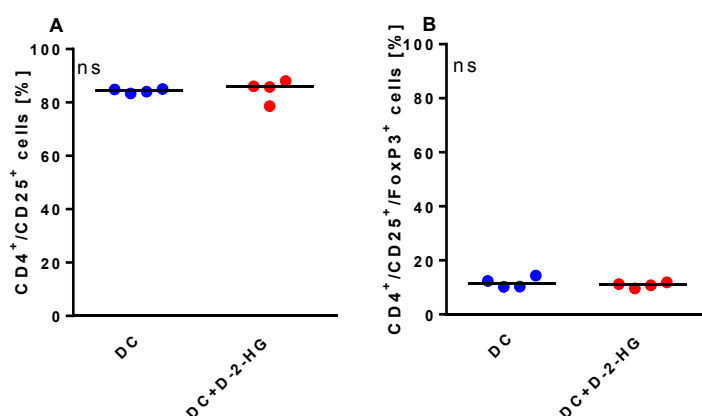


Figure 3.28: CD4/CD25 (A) and CD4/CD25/FoxP3 (B) positive T cells after 7 days of MLR with allogeneic DCs treated without or with D-2-HG. Immature DCs differentiated in the presence or absence of 20 mM D-2-HG were cultured together with allogeneic naïve enriched T cells in a ration (1:10). On day 7 T cells were analyzed for CD4, CD25 and FoxP3 expression. (A) Summarized data of CD4 and CD25 co-expressing cells of 4 different donors analyzed. (B) Median (background corrected) intensity of the fluorescence signal were used. Single values and median of CD4, CD25 and FoxP3 co-expressing cells of 4 different donors analyzed. Statistical analyses for group differences were tested with Wilcoxon test (paired). (* $p \leq 0.05$ were considered significant, no significance was found).

To sum up CD25 and FoxP3 expression was not influenced during stimulation with D-2-HG treated DCs, whereas a reduction in proliferation as well as IFN γ secretion by T cells in an allogenic MLR was detected.

3.2.3.3 Expression of inhibitory molecules on D-2-HG treated DCs

Activity of DCs can be modified by the expression of surface molecules. Stimulatory molecules can be less expressed and/or inhibitory molecules can be up-regulated. D-2-HG did not change expression of co-stimulatory molecules (CD80/CD86), next inhibitory molecules were analyzed.

Inhibitory molecules like programmed cell death ligand 1 (PD-L1), HLA-G, T cell immunoglobulin and mucin domain 3 (TIM-3), B- and T-lymphocyte attenuator (BTLA), Ig-like transcript 2 (ILT-2) and ILT-3 can be expressed on DCs and inhibit the activity of T cells.

To find out if the expression of these markers change during D-2-HG treatment they were analyzed on DCs after 7 days of culture.

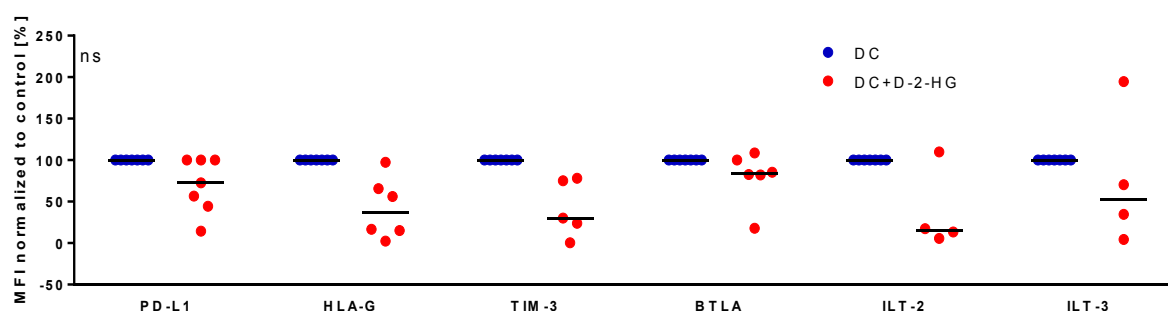


Figure 3.29: Expression of inhibitory molecules on D-2-HG treated DCs. DCs were differentiated in the presence or absence of 20 mM D-2-HG. On day 7 DCs were harvested and analyzed for the expression of inhibitory molecules PD-L1, HLA-G, TIM-3, BTLA, ILT-2 and ILT-3 by flow cytometry. Median (background corrected) intensity of the fluorescence signal were used. Single values and median are shown for 4-7 different donors. Statistical analyses for group differences were analyzed with Wilcoxon test (paired). (* $p \leq 0.05$ were considered significant, no significance was found).

Expression of nearly all inhibitory molecules analyzed was less expressed in D-2-HG treated DCs. PD-L1, BTLA and ILT-3 showed a slight, while HLA-G, TIM-3 and ILT-2 showed a strong decrease in their expression (Figure 3.29). In conclusion D-2-HG did not induce the expression, but rather reduce the surface expression of inhibitory molecules in DCs. Therefore the reduced HLA class II and IL-12 secretion caused the reduced stimulatory capacity of D-2-HG treated DCs rather than the expression of inhibitory molecules.

3.2.3.4 Effect of D-2-HG on phagocytosis activity of immature DCs

One important function of immature DCs is the uptake and presentation of antigens. Immature DCs can kill and take up pathogens (like bacteria) and present parts of the pathogen on the surface to T cells. To investigate functional consequences of D-2-HG treatment, phagocytosis activity of immature DCs was analyzed on day 7 of DC culture before activation with LPS.

DCs were incubated 10 minutes with E.coli expressing green fluorescent protein (GFP), to allow phagocytosis of bacteria. The uptake was monitored by measuring fluorescence intensity of DCs after several washing steps. As background control, DCs were incubated for 2h with GFP expressing E.coli, in this time intracellular bacteria and GFP were phagocytized and degraded, so only the fluorescent signal of the bacteria on the surface of the DCs was measured. As a result, there was no difference in phagocytosis activity in D-2-HG treated DCs compared with untreated controls (Figure 3.30). Also, the signal of the background did not change with D-2-HG treatment. In control DCs a median of about 30% of the DCs were GFP positive, as mentioned above the levels of D-2-HG treated DCs were comparable.

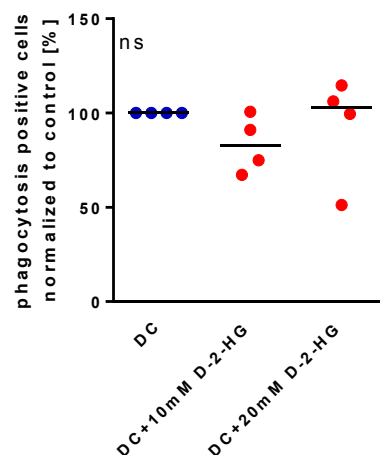


Figure 3.30: Phagocytose positive cells of D-2-HG treated DCs on day 7. Immature DCs differentiated in the presence or absence of 10-20 mM D-2-HG were used to analyze phagocytose activity. Percentages of green fluorescent DCs after incubation with GFP expressing E-coli were analyzed by flow cytometry. Single values and median of 4 independent experiments with different donors is shown. Statistical analyses for group differences were tested with Wilcoxon test (paired). (* $p \leq 0.05$ were considered significant, no significance was found).

3.2.4 Effect of D-2-HG on G protein receptor signaling

As mentioned above it is not yet clear how D-2-HG enters cells, but it was taken up by monocytes. Besides having intracellular effects D-2-HG could also impact signaling from the outside. To find out if D-2-HG is a ligand of G protein coupled receptors (GPCRs) protein kinase C (PKC) and cyclic AMP (cAMP) levels were analyzed in DCs.

Activation of $G_{q/11}$ (heterotrimeric G protein subunit) coupled receptors leads to an increase in inositol triphosphate which activates diacylglycerol and release calcium from the endoplasmatic reticulum. Both lead to an activation of PKC and translocation to the membrane¹¹⁴.

PKC levels were analyzed in lysates enriched for cytosolic and membrane proteins. In D-2-HG treated DCs PKC was more abundant in the cytosol and the membrane. In the donor shown here PKC (Figure 3.31A) was only detected in the D-2-HG treated DCs this was not true in the other two donors. In one of the three donors tested PKC was less abundant in D-2-HG treated DCs (Figure 3.31B). In the same donor also the inhibitory effect of D-2-HG was only seen in HLA-DQ and not for –DP and –DR (data not shown). Actin was present in both lysates and was used for normalization. For the membrane fraction it was a parameter of purity as it is no membrane protein (Figure 3.31B).

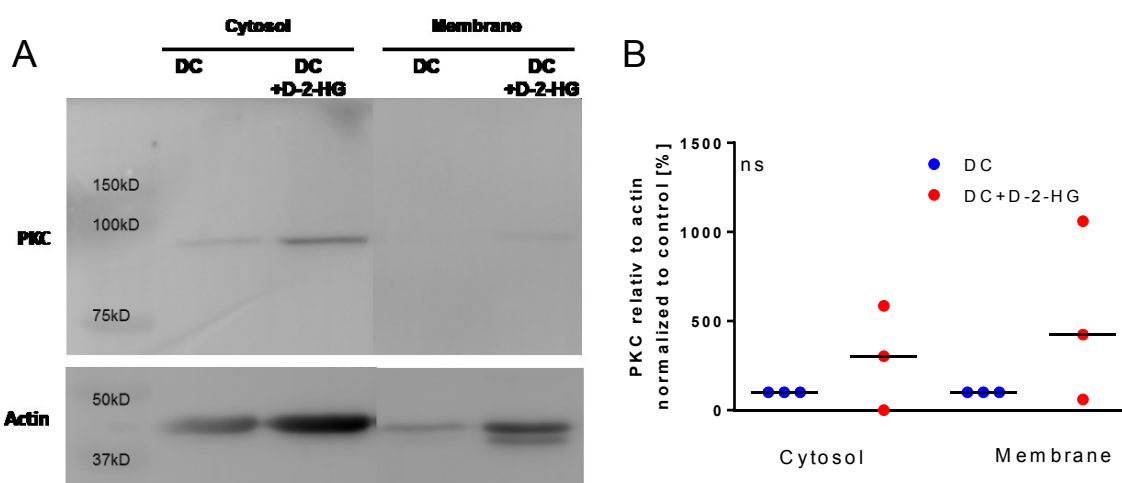


Figure 3.31: Western blot Analysis of PKC protein in cytosol and membrane fractions of DCs. (A) DCs were harvested after 7 days of D-2-HG [20 mM] treatment. Whole protein was enriched either for cytosolic or membranes proteins. 15 μ g protein was loaded on a 10% SDS acrylamide gel. Membrane was stained with rabbit anti-PKC (α,β,γ) primary antibody (1:1000) in and HRP linked anti-rabbit secondary antibody (1:2500). Antibodies were removed by membrane stripping and analyzed again for actin contents with rabbit anti-actin (1:1000) and anti-rabbit (1:2500). PKC signal was measured after an exposure time of 1 min 20s. Data are shown from one experiment representative of three performed with different donors. (B) Quantification of three experiments was done by normalization to actin expression and expression of corresponding control DCs by ImageJ. Single values and median are shown for 3 different donors. Statistical analyses for group differences were analyzed with Wilcoxon test (paired). (* $p \leq 0.05$ were considered significant, no significance was found).

As activation of G_i and G_s coupled receptors alters cAMP levels of the cells, cAMP level of DCs treated with D-2-HG were analyzed in parallel to the analyses of PKC translocation. Analyses of cAMP levels revealed slightly higher levels in D-2-HG treated DCs compared to the untreated control, but only in one donor an increase by 60% was detected (Figure 3.32).

Results of the analysis of GPCR signaling showed no significant impact of D-2-HG, further studies have to be performed to finally answer the question if D-2-HG is a ligand for GPCRs.

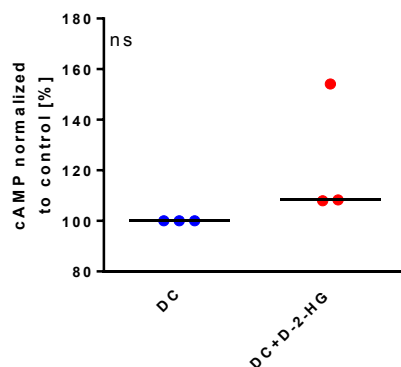


Figure 3.32: cAMP levels of D-2-HG treated DCs. 5×10^6 DCs differentiated in the absence or presence of 20 mM D-2-HG were lysed and cAMP measurement was performed. Single values and median of 3 independent experiments with different donors is shown. Statistical analyses for group differences were tested with Kruskal Wallis Test (paired). (* $p \leq 0.05$ were considered significant, here no significance was found).

3.2.5 Impact of D-2-HG on DC metabolism

As PKC is involved in calcium signaling and calcium is a regulator of metabolism also the impact of D-2-HG was analyzed. The transfer of calcium is important for oxidative phosphorylation (OXPHOS) and activated key decarboxylases of the TCA. Calcium also regulated the activity of pyruvate dehydrogenase and therefore provides sufficient amounts of pyruvate to either fuel the TCA or lactate production ¹¹⁵. During the last years it became evident, that also metabolic alterations play an important role in immune cell differentiation and activation. Reduced oxygen consumption but increased glycolytic activity have been shown in activated murine DCs and have been linked to their function ¹¹⁶. As mentioned in the introduction accumulation of metabolites or oncometabolites like D-2-HG may influence the metabolism of DCs and thereby their function due the high similarity to α -ketoglutarate.

3.2.5.1 Lactate production and glucose consumption of D-2-HG treated DCs

To characterize the glycolytic activity of DCs lactate secretion and glucose uptake was determined in supernatants of DCs differentiated in the presence or absence of D-2HG on day 7 of culture. DCs treated with D-2-HG produced more lactate than untreated control cells. Control DCs produced a median of 10.4 mM lactate, while D-2-HG treated DCs produced 16.9 mM. In addition, glucose consumption was also increased in DCs treated with D-2-HG (7.8 mM glucose in D-2-HG treated DC versus 5.6 mM in untreated DCs, Figure 3.33A, B).

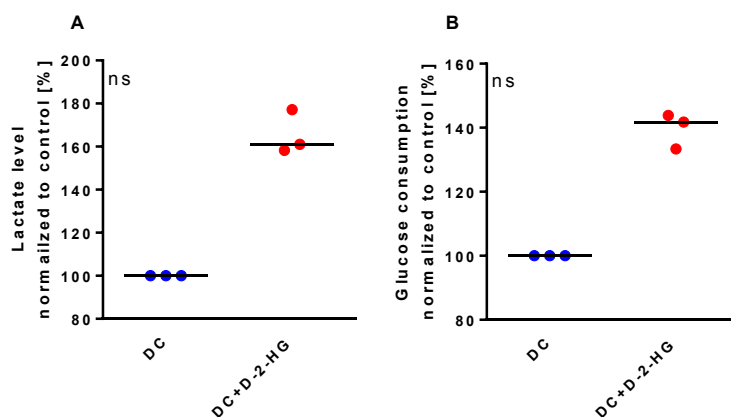


Figure 3.33: Lactate production (A) and glucose consumption (B) of D-2-HG treated DCs. DCs were differentiated in the presence or absence of 20 mM D-2-HG. On day 7 supernatants were collected to measure lactate (A) and (B) glucose concentrations. Glucose consumption was calculated by subtracting the remaining (measured) glucose from total glucose in the media. Concentrations measured in D-2-HG treated DCs were normalized to untreated control DCs. Single values and median of 3 independent experiments with different donors is shown. Statistical analyses for group differences were tested with Wilcoxon test (paired). (* $p \leq 0.05$ were considered significant, no significance was found).

In addition, pH values were monitored continuously during culture using the PreSens technology. Until day 2 the pH value was constant (7.4), beyond the pH dropped in D-2-HG treated DCs slowly until day 5 and remained constant at 6.6 after day 5. In control DCs pH values changed later in all donors tested (in one donor no pH drop was visible). In the donor shown in Figure 3.34 pH drop started at day 5 and continued until the end of the culture.

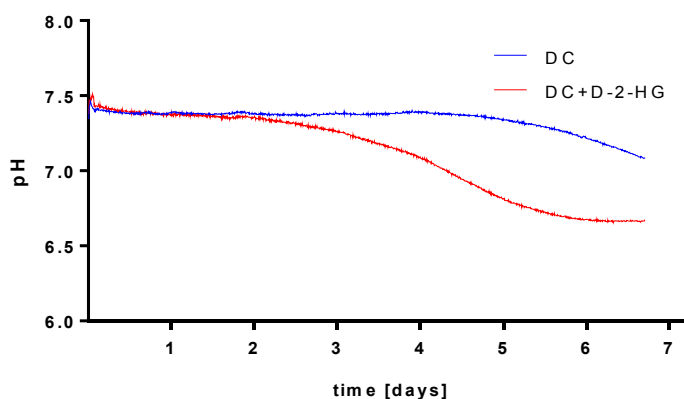


Figure 3.34: Online measurement of pH value during 7 days of culture. Monocytes were seeded in the presence or absence of 20 mM D-2-HG on 24-well hydro-dish, pH values were monitored during culture time by PreSens technology. One representative measurement out of 4 is shown.

3.2.5.2 Effect of D-2-HG on mTOR phosphorylation in DCs

Glucose metabolism can be regulated by different pathways, one is the mTOR pathway. The key protein is mTOR, which activity is regulated by phosphorylation on the serine residue 2448. To check a possible impact of D-2-HG on the activation status of mTOR,

phospho-mTOR was stained intracellularly in monocytes after overnight incubation with D-2-HG.

Phospho-mTOR staining was not changed by overnight D-2-HG treatment. In both conditions monocytes were positive for phospho-mTOR and signal intensities were comparable between control monocytes and D-2-HG treated monocytes as shown in Figure 3.35A. However, in one donor a difference in the isotype control staining was observed (Figure 3.35B). In donor 2 shown in Figure 3.35B mTOR signal was similar in both donors, but the isotypes were different (median for D-2-HG treated monocytes was 16 and for untreated monocytes 27). In conclusion, rapid changes in mTOR activity might not be involved in the early metabolic alterations. Furthermore, after 7 days of culture there were also no differences in the phospho-mTOR staining in DCs cultured in the absence or presence of D-2-HG (data not shown).

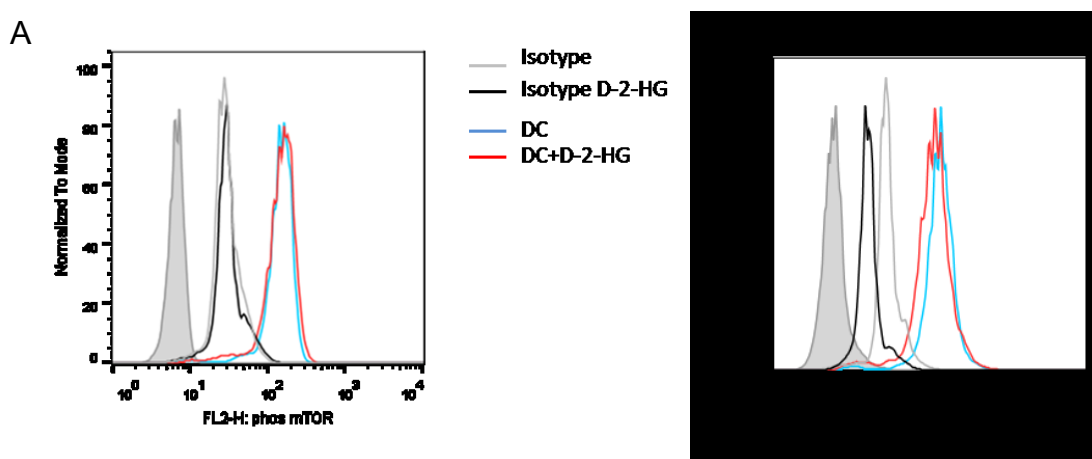


Figure 3.35: mTOR phosphorylation (Ser2448) of monocytes after overnight incubation with 20 mM D-2-HG. Monocytes were cultured overnight in the presence or absence of 20 mM D-2-HG. mTOR phosphorylation was measured by flow cytometry. One Histogram of population gates for living cells. Representative example of donor 1 (A) and donor 2 (B) analyzed.

3.2.5.3 Effect of D-2-HG on respiration of DCs

To analyze mitochondrial respiration in intact cells two different approaches were used. The PreSens technology allows the measurement of cellular oxygen consumption under culture conditions, whereas absolute values of oxygen consumption and functional parameters as maximum mitochondrial capacity can be determined high-resolution respirometry due to the possibility to apply substrates, inhibitors and uncouplers through a port.

Applying the PreSens technology revealed an immediate increase in cellular respiration upon the addition of D-2-HG, in all four donors analyzed. In Figure 3.36 one representative donor is shown.

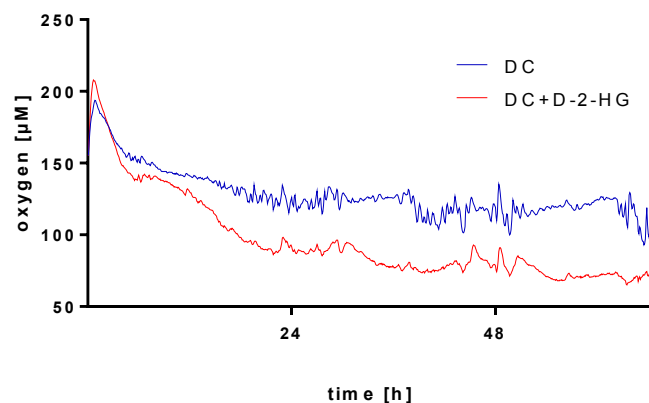


Figure 3.36: Oxygen concentration over time in DC cultures treated with D-2-HG. Monocytes were seeded in the presence or absence of 20 mM D-2-HG in 24-well oxy-dish, oxygen concentrations were monitored during culture time by PreSens technology. One representative measurement out of 4 is shown.

To further investigate alterations in mitochondrial activity high resolution respirometry was used. DCs were transferred into the oxygraph chambers at a density of approximately 5×10^5 . After determining basic respiration (ROUTINE) a protocol applying the mitochondrial ATP synthase inhibitor oligomycin to determine LEAK respiration, followed by titrating the uncoupler FCCP to measure the maximum capacity of the electron transfer system (ETS) and a subsequent administration of the mitochondrial respiratory complex I inhibitor rotenone and complex III inhibitor myxothiazol was used^{117,118}.

All respiratory parameters analyzed were normalized to cell number and expressed as pmol/s/ 10^6 cells. To compare the impact of D-2-HG between different donors respiratory parameters of D-2-HG treated DCs were further normalized to values of control DC of the same donor. In the course of differentiation from monocytes to DCs ROUTINE respiration increased independent of the treatment, however, the increase was much more pronounced in cells treated with D-2-HG. Already monocytes cultured overnight and cells differentiated for 4 days in the presence of D-2-HG showed slightly higher ROUTINE respiration compared to untreated control cells. On day 4 D-2-HG treated DCs had an 166% increased oxygen consumption rate, on day 7 the value rose to 185% of control levels (Figure 3.37).

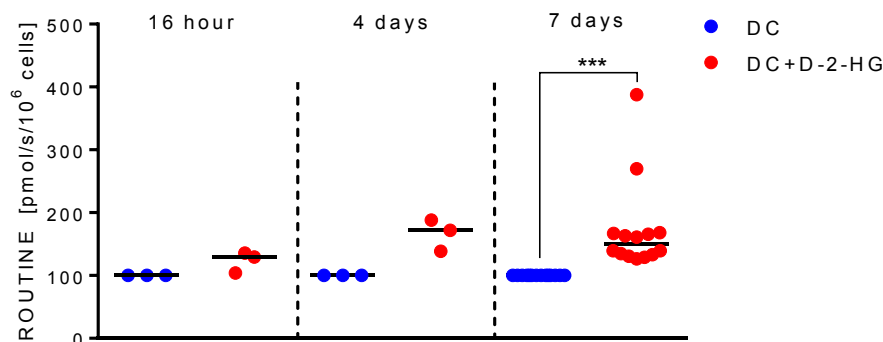


Figure 3.37: Oxygen consumption of D-2-HG treated DCs after 16 hours, 4 and 7 days. Oxygen consumption was measured by high resolution respirometry after overnight incubation (MO), 4 and 7 days. Monocyte or DCs were placed in oxygraph chambers in culture medium. ROUTINE respiration was measured (basal respiration) stabilization of respiration signal (basal respiration). Single values and median of 3-14 independent experiments with different donors is shown. Statistical analyses for group differences were tested with Wilcoxon test (paired). (* $p \leq 0.05$ were considered significant, *** $p \leq 0.001$).

To elucidate the possibility that D-2-HG might serve as a substrate D-2-HG was applied to permeabilized DCs. In this protocol the cell membrane was disrupted with digitonin. By permeabilization of the cell membrane, mitochondria can be analyzed without performing a time-consuming mitochondria isolation⁹⁹. The application of different substrates (glutamate, malate, pyruvate, succinate) allows the determination of the maximum mitochondrial capacity. To investigate whether D-2-HG has a direct impact on mitochondrial activity, D-2-HG was added to permeabilized DCs in the presence of saturating complex I and complex II substrates and ADP. In all donors tested there was increase in maximum OXPHOS after adding malate, pyruvate, glutamate, succinate and D-2-HG and ADP (solved in water) compared to adding water instead of D-2-HG (Figure 3.38A). Those data suggest that D-2-HG might serve as a mitochondrial substrate or immediately and directly turns on respiration. The same experiment was performed with the lymphocyte fraction gained by elutriation after overnight storage, to check whether this increase also is seen in other cell types. Overall, T cells consumed less oxygen than DCs. DCs had oxygen consumption rates of about 40 pmol/s/10⁶, T cells at most 8 pmol/s/10⁶. Moreover, in T cells D-2-HG addition did not lead to an increase in maximum OXPHOS (Figure 3.38B).

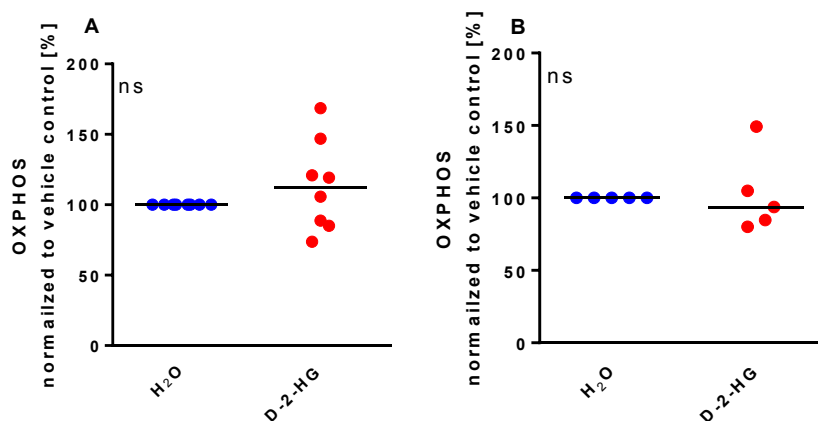


Figure 3.38: OXPPOS the presence and absence of D-2-HG in DCs (A) and T cells (B). (A) DCs were harvested on day 7 and placed in the oxygraph chamber wherein DCs were permeabilized with digitonine to analyze oxygen consumption of complexes of the respiratory chain. ROUTINE respiration after addition of water or D-2-HG together with substrates of complex I and II (malat, glutamate, pyruvate and succinate) was measured. Single values and median of 8 independent experiments with different donors is shown. (B) The same was done in T cells from lymphocyte fraction after overnight storage. Single values and median of 5 independent experiments with different donors is shown. Statistical analyses for group differences were tested with Wilcoxon test (paired). (* $p \leq 0.05$ were considered significant, no significance was found).

3.2.5.4 Determination of mitochondrial content in DCs

The higher oxygen consumption of D-2-HG treated DCs (Figure 37) could also be related to a long-term adaption and increase in respiratory complexes or even in elevated mitochondrial content. To test this hypothesis two additional parameters were analyzed; maximum ETS capacity in the uncoupled state as well as mitochondrial content. The latter was determined applying a cationic fluorescence dye mainly intercalating in mitochondria independent of their membrane potential.

In most of the analyzed donors the mitochondrial mass was increased in D-2-HG treated DCs on day 7 compared to untreated control DCs. Although not significant D-2-HG treated DCs had 44% more mitochondrial mass than untreated controls (Figure 3.39A).

Maximum ETS capacity can be measured by the addition of an uncoupling agent like Carbonyl cyanide-p-trifluoromethoxyphenylhydrazone (FCCP). FCCP destroys the proton gradient and thereby stimulate the complexes to maximal capacity. FCCP treatment resulted in an increased maximal capacity of ETS of D-2-HG treated DCs compared to the control DCs (Figure 3.39B).

So in summary one part of the increased respiration could be explained by an increased mitochondrial mass another part by the increased maximal capacity of ETC.

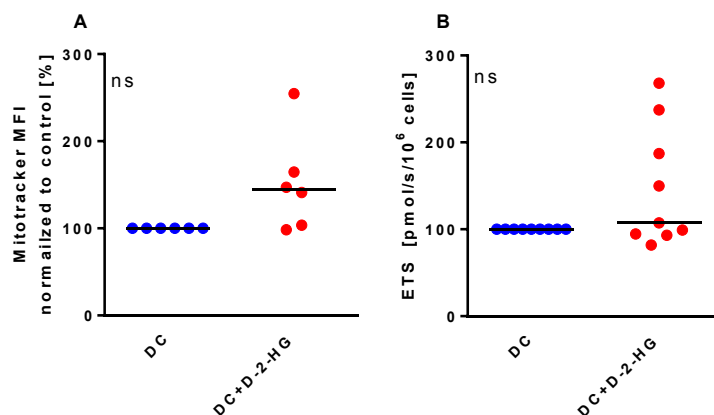


Figure 3.39: Mitochondrial mass (A) and maximum capacity of electron transport chain (B) of day 7 DCs treated with D-2-HG. DCs were differentiated in the presence or absence of 20 mM D-2-HG. (A) On day 7, mitochondrial mass was measured with Mitotracker Green by flow cytometry. Median (background corrected) intensity of the fluorescence signal were used. Single values and median of 6 independent experiments with different donors is shown. (B) DCs were placed in oxygraph chambers in culture medium on day 7 wherein maximum capacity of electron transport system (ETC) was measured after addition of carbonyl cyanide p trifluoromethoxyphenylhydrazone (FCCP) by high resolution respirometry oxygraph technology. Single values and median of 9 independent experiments with different donors is shown. Statistical analyses for group differences were tested with Wilcoxon test (paired). (* $p \leq 0.05$ were considered significant, no significance was found).

3.2.5.5 Measurement of ATP content of DCs

A higher respiration could result in a higher production of ATP, thus in higher ATP levels. To test this, ATP concentration was measured in D-2-HG treated DCs via bioluminescence. On day 7, D-2-HG treated DCs had significantly higher intracellular ATP levels (180%) compared to untreated controls (Figure 3.40A). A higher ATP production was already indicated calculating the effect of oligomycin on oxygen consumption. In D-2-HG treated DCs oligomycin exerted a stronger reduction in respiration, suggesting that more oxygen was used for ATP production (Figure 3.40B).

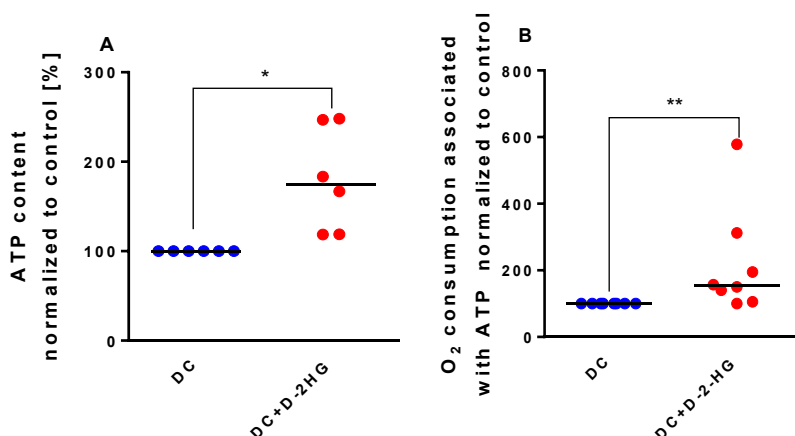


Figure 3.40: ATP content (A) and oxygen consumed to produce ATP (B) in D-2-HG treated DCs. DCs were differentiated in the presence or absence of 20 mM D-2-HG. (A) On day 7 ATP content was measured by luminescence. Signals of D-2-HG treated DCs was normalized to control. Median of 6 experiments with different donors is shown. (B) DCs were placed in oxygraph chambers in culture medium. Oxygen consumption was measured by oxygraphy. DCs were incubated with LPS for one hour, after that oligomycin (ATPase inhibitor) was added to inhibit ATP synthase. Difference in oxygen consumption before and after addition of oligomycin was used to calculate the oxygen used to produce ATP. Single values and median of 8 independent experiments with different donors is shown. Statistical analyses for group differences were tested with Wilcoxon test (paired). (* $p \leq 0.05$ were considered significant ** $p \leq 0.01$).

3.2.5.5.1 Effect of mutant IDH1/2 protein expression on respiration of DCs

Because a higher respiration rate in D-2-HG treated DCs was observed, DCs expressing wild type or mutant IDH1 and 2 (IDH1 R132H and IDH2R140Q) upon electroporation with *in vitro* transcribed mRNA were analyzed. To check if *in situ* produced D-2-HG by mutant IDH does mimic the effects of exogenous added D-2-HG.

After electroporation on day 7 of DC culture, DCs were stored overnight and stained intracellular with an anti-HIS antibody to check the expression of IDH proteins. An example for a corresponding histogram is depicted in Figure 3.4.

Electroporation itself did influence oxygen consumption of DCs. In most donors electroporation resulted in a decreased oxygen consumption (Figure 3.41A). Thus, DCs expressing wild type (wt) IDH were compared to DCs expressing mutant IDH. The expression of mutant IDH, IDH1 and IDH2 led to higher oxygen consumption (ROUTINE respiration) and higher maximal electron transport capacity (ETC), comparable to the effect of exogenously added D-2-HG (Figure 3.41B, C).

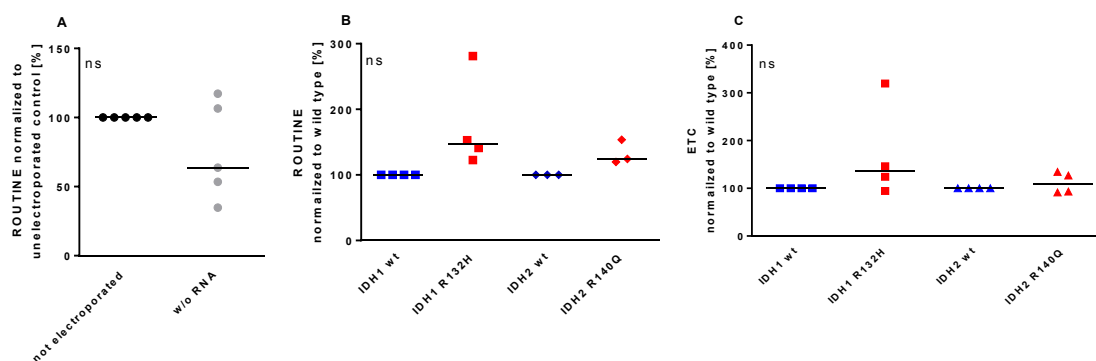


Figure 3.41: Oxygen consumption of DCs electroporated with IDH1 wild-type, IDH1 R132H, IDH2 wild-type or IDH2 R140Q. Immature DCs (day 7) were electroporated with *in vitro* transcribed mRNA coding for wild-type or mutated IDH1 and 2 (IDH1 R132H and IDH2 R140Q). DCs were placed in oxygraph chambers in culture medium. ROUTINE was measured after stabilization of respiration signal (basal respiration). Single values and median of 4 independent experiments with different donors is shown. Statistical analyses for group differences were tested with Wilcoxon test (paired). (* $p \leq 0.05$ were considered significant, no significance was found).

In parallel, monocytes were electroporated directly after isolation from PBMCs with mRNA coding for wild type and mutant IDH1 and 2 (IDH1 R132H and IDH2 R140Q). Transfection efficiency was comparable with the one in DCs but the viability after electroporation was lower. After 7 days of culture oxygen consumption was analyzed. Even after 7 days a negative impact of the electroporation was observed. DCs derived from electroporated monocytes consumed less oxygen compared to DCs derived from non-electroporated monocytes (data not shown). Nevertheless, expression of mutant IDH resulted in a trend towards increased respiration compared to monocytes expressing wild type IDH. Again, this was true for IDH1 and for IDH2 (Figure 3.42A). A higher effect of mutant IDH expression was seen in the maximum capacity of electron transport system. Here the median for IDH1 R132H expressing DCs reached 183% of wild type expressing cells. For IDH2 R140Q expressing DCs the effect was less pronounced (133%, Figure 3.42B).

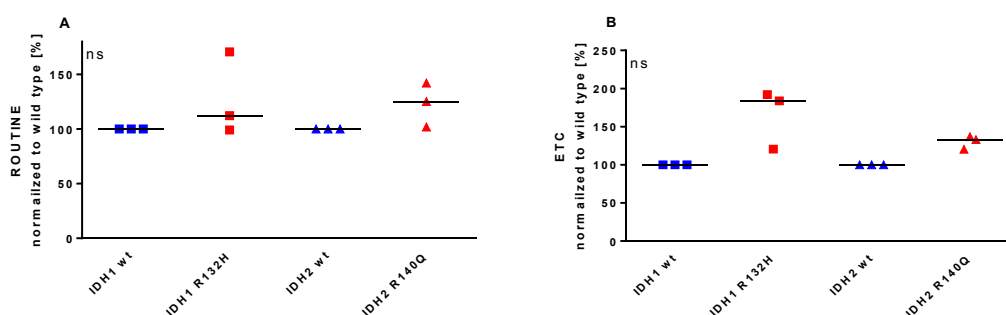


Figure 3.42: Oxygen consumption of DCs derived from monocytes electroporated with IDH1 wild-type, IDH1 R132H, IDH2 wild-type or IDH2 R140Q. Monocytes were electroporated with *in vitro* transcribed mRNA coding for wild-type or mutated IDH1 and 2 (IDH1 R132H and IDH2 R140Q) and differentiated for 7 days. DCs were placed in oxygraph chambers in culture medium. (A) ROUTINE respiration was measured after stabilization of respiration signal (basal respiration). (B) In the same experiments also, the maximum capacity of the electron transport system (ETC) was measured after the addition of FCCP. Single values and median of 3 independent experiments with different donors is shown. Statistical analyses for group differences were tested with Wilcoxon test (paired). (* $p \leq 0.05$ were considered significant, no significance was found).

Taken together, the expression of mutated IDH1 or IDH2 exerted similar effects on respiration as the addition of exogenously added D-2-HG, indicating that intracellular levels of D-2-HG are responsible for the observed alterations in respiration.

3.2.5.5.2 Effect of D-2-HG on mitochondrial structure of DCs

Basal respiration of D-2-HG treated DCs was significantly higher than in the control DCs and they showed a trend towards an increased mitochondrial mass. To further elucidate mitochondrial alterations, mitochondrial structure was analyzed by EM of DCs cultured in the absence or presence of D-2-HG and harvested after 8 days.

Only in one of three donors an effect of D-2-HG treatment on mitochondrial structure was observed. In all untreated control DCs mitochondria appeared well structured, with dense packed cristae and a dark (electron dense) mitochondrial matrix (Figure 3.43A). Compared to this, mitochondria in D-2-HG treated DCs of one donor seemed bloated with less dense cristae and a much brighter matrix. Also, the mitochondria itself were larger (Figure 3.43B). In the other two donors these differences were less pronounced.

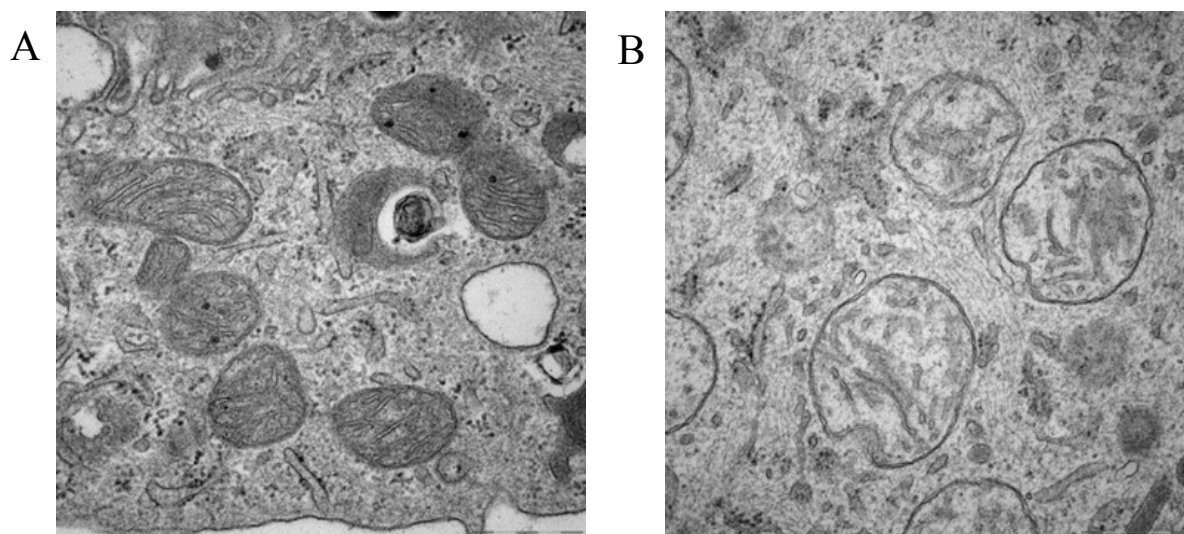


Figure 3.43: EM images of d8 DCs treated with D-2-HG (Donor1). DCs were cultured in the presents (B) or absence (A) of D-2-HG. On day 8 DCs of each group were harvested, fixed and further processed for electron microscopy. Pictures show one representative section of each group of DCs differentiated in the absence or presence of D-2-HG. EM analysis was performed with three different donors, for each donor 10 cells were analyzed with different magnifications. Multi-laminar structures are indicated with arrows. The magnification used here was 40000x, bar indicates 500 nm.

3.2.6 Effect of D-2-HG on reactive oxygen species of DCs

D-2-HG treated DCs showed a higher basal respiration (Figure 3.37), which could also lead to an increase in reactive oxygen species (ROS) levels. Complex I and III of the electron

transport chain can generate superoxides during transfer of electron along the different electron acceptors⁷⁵. Superoxide in the mitochondria can get converted to peroxide by superoxide dismutase (SOD), which then can translocate through the mitochondrial membrane into cytosol^{75,119}.

Determining residual oxygen consumption after inhibition of the respiratory chain applying rotenone revealed elevated oxygen consumption in D-2-HG treated DCs. After overnight (16h) D-2-HG incubation median of rotenone inhibited respiration was already increased to 145%, after 4 days of incubation the median peaks at 220% of control levels. After 7 days a significant increase of ROX was seen (Figure 3.44). This could hint to higher ROS levels produced in the mitochondria of DCs treated with D-2-HG.

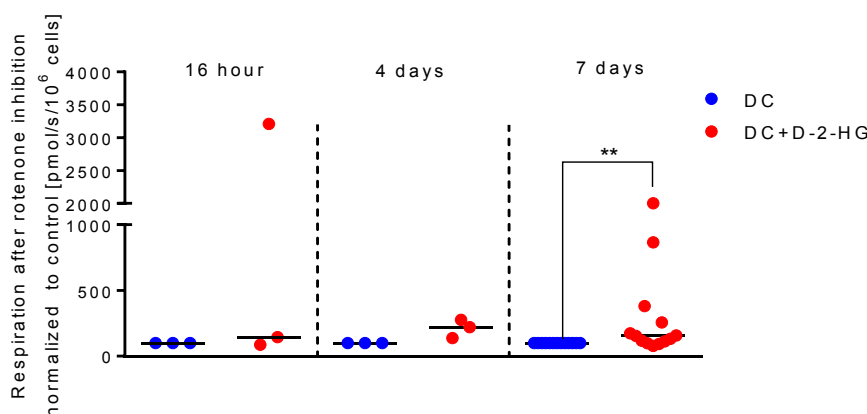


Figure 3.44: Oxygen consumption after inhibition of electron transport chain with rotenone in DCs cultured for 7 days in the presence of D-2-HG. DCs were differentiated in the presence or absence of 20 mM D-2-HG. On day 7 DCs were placed in oxygraph chambers in culture medium. Oxygen consumption was measured by oxygraphy. DCs were incubated with LPS for one hour, after that oligomycin (complex IV inhibitor), FCCP (uncoupler), rotenone (complex I inhibitor) were added. Single values and median of 3-14 independent experiments with different donors is shown. Statistical analyses for group differences were tested with Wilcoxon test (paired). (* $p \leq 0.05$ were considered significant ** $p \leq 0.01$).

3.2.6.1 Establishment of measurement of cytosolic ROS by DCFDA

2',7'-Dichlorofluorescein diacetate (DCFDA) was used to measure ROS abundance in the cytosol. DCFDA gets oxidized by ROS (all oxidants present) which induces a fluorescence signal¹²⁰. To establish the measurement, peroxide was added to DCFDA stained monocytes directly after elutriation. Peroxide can translocate through cell membranes and can be detected in the cytosol. In Figure 3.45 results are shown as a stacked histogram overlay. The grey histogram is the signal of DCFDA stained DCs without peroxide. Addition of 1 mM peroxide caused an increase in DCFDA signal after 5 minutes; the signal increased until 25 minutes

after addition and did not further increase after 30 minutes. The results showed, that the staining method worked properly. (Figure 3.44)

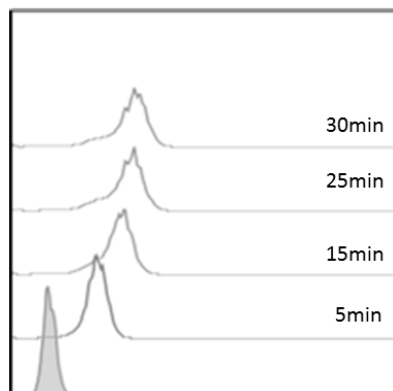


Figure 3.45: DCFDA staining of monocytes after addition of H_2O_2 . 1 mM peroxide was added to DCFDA stained monocytes. DCFDA signal was measured after 5-30 minutes incubation time. Filled grey curve is the signal of stained monocytes without H_2O_2 . Histograms of one performed experiment.

3.2.6.2 Short-term effects of D-2-HG on cytosolic ROS in DCs

After establishment of cytosolic ROS measurement, the short-term effect of D-2-HG on cytosolic ROS was analyzed in monocytes. Monocytes were stained with DCFDA, then 20 mM D-2-HG was added and fluorescence signals were measured after 5, 15, 25 and 30 minutes. As control, RPMI was added to DCFDA stained monocytes (Figure 3.46). Since addition of D-2-HG or RPMI did not increase the DCFDA signals, there was no immediate increase in cytosolic ROS, which does not exclude the possibility that ROS subsequently could emerge.

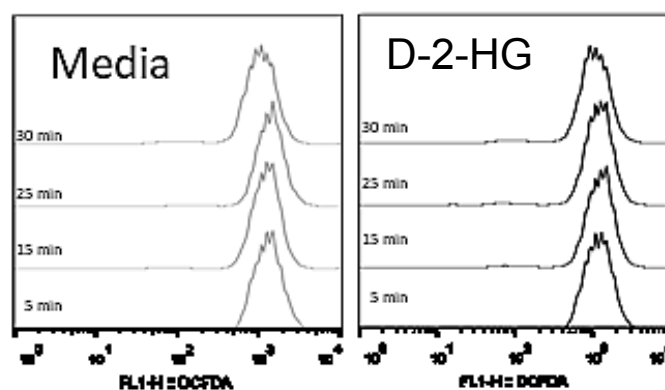


Figure 3.46: Short-term effects of D-2-HG on ROS levels in monocytes. 20 mM D-2-HG or media (control) was added to DCFDA stained monocytes. DCFDA signal was measured after 5-30 minutes incubation time. Filled grey curve is the signal of stained monocytes without H_2O_2 . Histograms of one experiment performed.

3.2.6.3 Short-term effect of D-2-HG on mitochondrial ROS of DCs

In parallel mitochondrial ROS levels were measured in monocytes by MitoSox red staining. MitoSox is a fluorescent dye which specifically detects superoxide in the mitochondria. Fluorescent signal was measured 5, 15, 20 and 30 minutes after the addition of 20 mM D-2-HG as a vehicle control RPMI was added. Both treatments did not change the MitoSox signal in the first 30 minutes of incubation (Figure 3.47). To control for methodological limitations, peroxide was used again as peroxide inhibits SOD and thereby leads to an accumulation of superoxide in the mitochondria. The addition of peroxide resulted in an increase in the MitoSox signal, confirming that the staining protocol worked (data not shown).

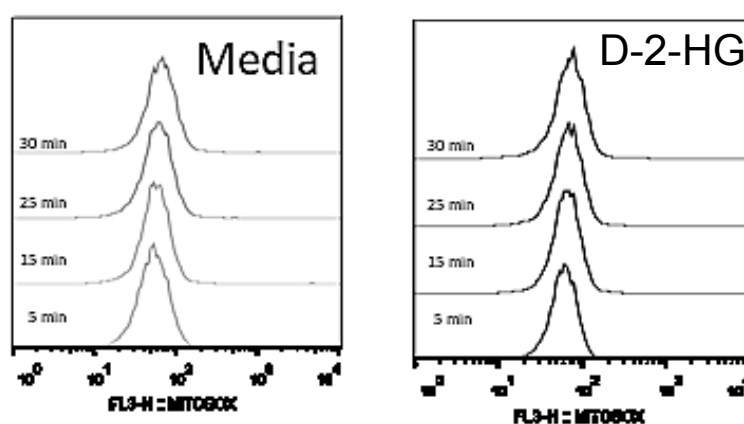


Figure 3.47: Short-term effect of D-2-HG on mitochondrial ROS in monocytes. 20 mM D-2-HG or media (control) was added to MitoSox stained monocytes. DCFDA signal was measured after 5-30 minutes incubation time. Filled grey curve is the signal of stained monocytes without H_2O_2 . Histograms of one experiment performed.

3.2.6.4 Long-term effect of D-2-HG ROS levels and cystine uptake in DCs

After investigating an immediate effect of D-2-HG on cytosolic ROS in monocytes, next the long-term effects of D-2-HG in DCs was measured after 7 days of culture. Herein, cytosolic ROS levels were significantly higher in D-2-HG treated DCs compared to untreated controls (Figure 3.48A).

Mitochondrial ROS was also measured in DCs treated with 20 mM D-2-HG for 7 days. Our hypothesis was that the increased respiration might also increase ROS levels in mitochondria. Indeed, mitochondrial ROS levels were increased in D-2-HG treated DCs compared to control DCs in 50% of all donors analyzed, nevertheless the effect was not significant (Figure 3.48B).

On day 7 DCs treated with D-2-HG had a higher amount of cytosolic and mitochondrial ROS compared to untreated DCs. To elucidate if this can be explained by

limited scavenging of ROS by glutathione, cystine uptake was measured after 7 days of D-2-HG treatment. Cystine is a dimer of cysteine and important for the production of glutathione¹²¹. Cystine uptake was reduced in four out of five donors analyzed (Figure 3.48C).

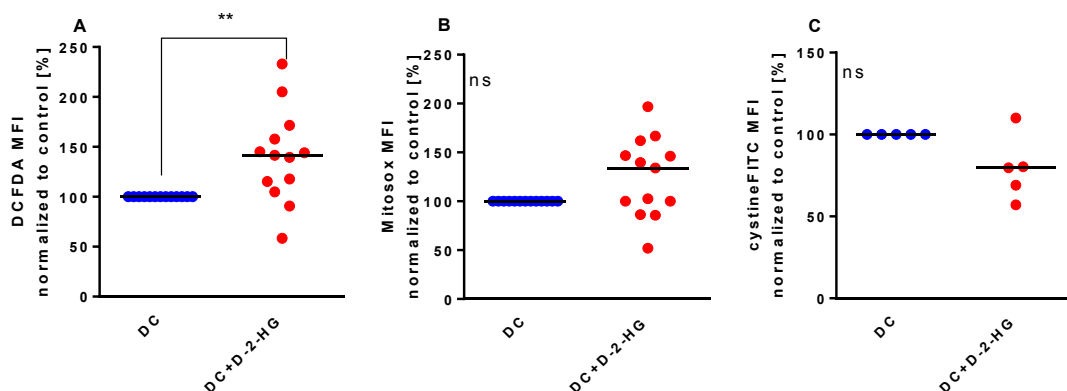


Figure 3.48: DCFDA, MitoSox and cystine staining of 7 days cultured DCs in the presence or absence of D-2-HG. DCs were differentiated in the presence or absence of 20 mM D-2-HG. On day 7 DC stained for (A) cytosolic ROS (DCFDA), (B) mitochondrial ROS (MitoSox) or (C) cystineFITC. Fluorescence signal was measured by flow cytometry. Median (background corrected) intensity of the fluorescence signal were used. Single values and median of 5-13 independent experiments with different donors is shown. Statistical analyses for group differences were tested with Wilcoxon test (paired). (* $p \leq 0.05$ were considered significant ** $p \leq 0.01$).

3.2.7 Effect of oxidants and antioxidants on HLA class II expression and ROS production of DCs

Since D-2-HG induced an increase in cellular ROS levels (Figure 3.48), we hypothesized that addition of peroxide could also mimic some of the effects of D-2-HG on DC differentiation, vice versa the addition of antioxidants might rescue the D-2-HG triggered phenotype.

3.2.7.1 Analyses of peroxide treatment on HLA-DP, -DR and CD1a expression on DCs

To mimic the effect of D-2-HG on ROS levels, peroxide was added during differentiation of monocytes into DCs (lower HLA class II expression, no CD1a expression). The effect of peroxide on HLA class II expression was analyzed on day 7. Here a lower expression of HLA-DP and HLA-DR was seen in the peroxide treated DCs compared to untreated control (Figure 3.49A, B). However, HLA-DQ expression was too low to analyze in these donors even in control DCs (data not shown). CD1a expression was also significantly decreased in D-2-HG treated DCs compared to untreated control DCs. With peroxide treatment CD1a expression was higher compared to control DCs (Figure 3.49C).

In summary peroxide treatment of DCs did only mimic the inhibitory effect of D-2-HG on HLA-DP expression.

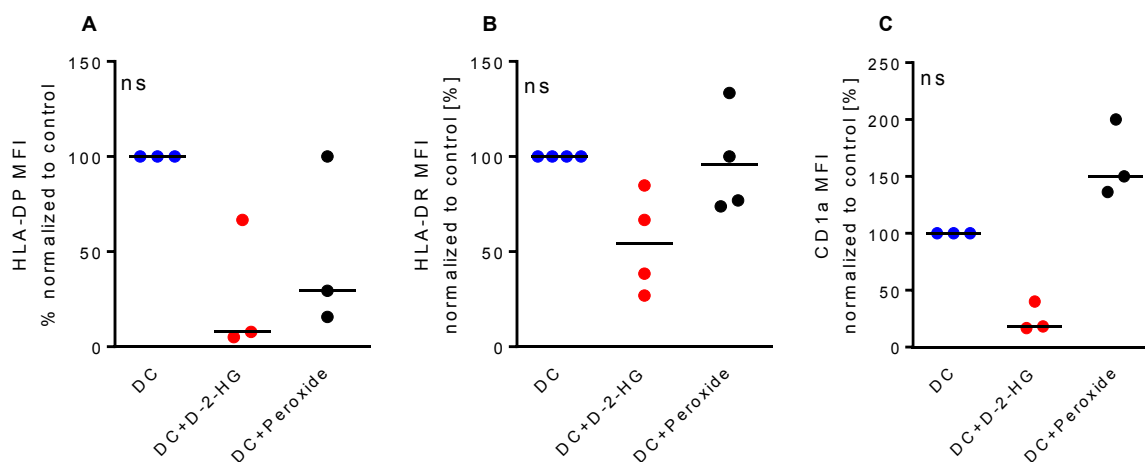


Figure 3.49: HLA class II expression of peroxide treated DCs. DCs were differentiated in the presence or absence of 20 mM D-2-HG or 1 mM peroxide. On day 7 DC stained for (A) HLA-DP, (B) HLA-DR and (C) CD1a expression. Fluorescence signal was measured by flow cytometry. Median (background corrected) intensity of the fluorescence signal were used. Single values and median of 3-4 independent experiments with different donors is shown. Statistical analyses for group differences were tested with Friedmann test (paired). (* $p \leq 0.05$ were considered significant, no significance was found).

3.2.7.2 Antioxidant treatment to rescue D-2-HG treated DCs

3.2.7.2.1 HLA class II expression on trolox and vitamin C treated DCs

Higher ROS levels were detected in D-2-HG treated DCs, in addition peroxide was able to mimic the effect of D-2-HG on HLA-DP expression. Both results suggested that an antioxidant might be able to rescue the effects of D-2-HG. In a set of experiments the water-soluble vitamin E derivative trolox (50 μ M) and vitamin C (2 mM) were used as rescue substances. As before, trolox and vitamin C were added to monocytes at the beginning of the culture in the presence or absence of D-2-HG.

Donors used for trolox treatment showed very low expression of HLA-DP and were excluded from the analysis of HLA class II expression. In one out of three donors with enough HLA-DP expression there was a positive effect of trolox treatment in the presence of D-2-HG (data not shown).

As seen before, D-2-HG treatment decreased HLA-DP and -DR expression. Vitamin C treatment lowered HLA-DP expression and HLA-DR expression of DCs (data not shown). All donors tested showed slightly higher expression of HLA-DR in vitamin C and D-2-HG co-treated DCs compared to DCs treated with D-2-HG alone (Figure 3.50A). Vitamin C in the presence of D-2-HG was able to rescue HLA-DP expression in 2 out of 4 donors tested (Figure 3.50 B). In the other 2 donors only, the D-2-HG effect was measurable. HLA-DQ

could not be analyzed in these donors because control DCs showed no expression (data not shown).

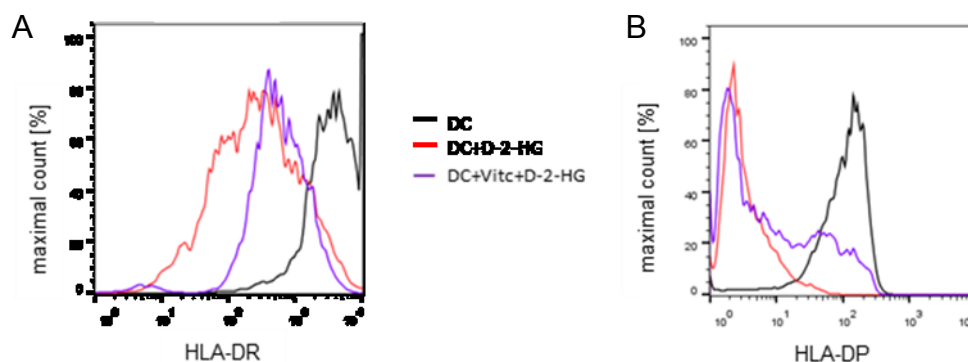


Figure 3.50: HLA class II expression after vitamin C treatment DCs. DCs were differentiated in the presence or absence of 20 mM D-2-HG or 2 mM vitamin C. On day 7 DC stained for (A) HLA-DP and (B) HLA-DR. Fluorescence signal was measured by flow cytometry. Representative histograms of one out of four donors are shown.

3.2.7.2.2 DC-SIGN and CD1a expression of trolox and vitamin C treated DCs

In parallel DC-SIGN and CD1a expression was analyzed in DCs treated with trolox, vitamin C in the presence or absence of D-2-HG as these surface markers were also reduced in D-2-HG treated DCs. Expression of DC-SIGN and CD1a was changed by trolox treatment. In one of three donors trolox treatment rescued DC-SIGN and CD1a expression of D-2-HG treated DCs (Figure 3.51A, B).

Expression of CD1a was not change neither by vitamin C treatment alone nor in the presence of D-2-HG. In contrast, DC-SIGN expression was increased in vitamin C treated DCs compared to untreated control DCs. Furthermore, in the presence of D-2-HG vitamin C treatment increased DC-SIGN to levels higher than levels of untreated control DCs (Figure 3.51A, B)

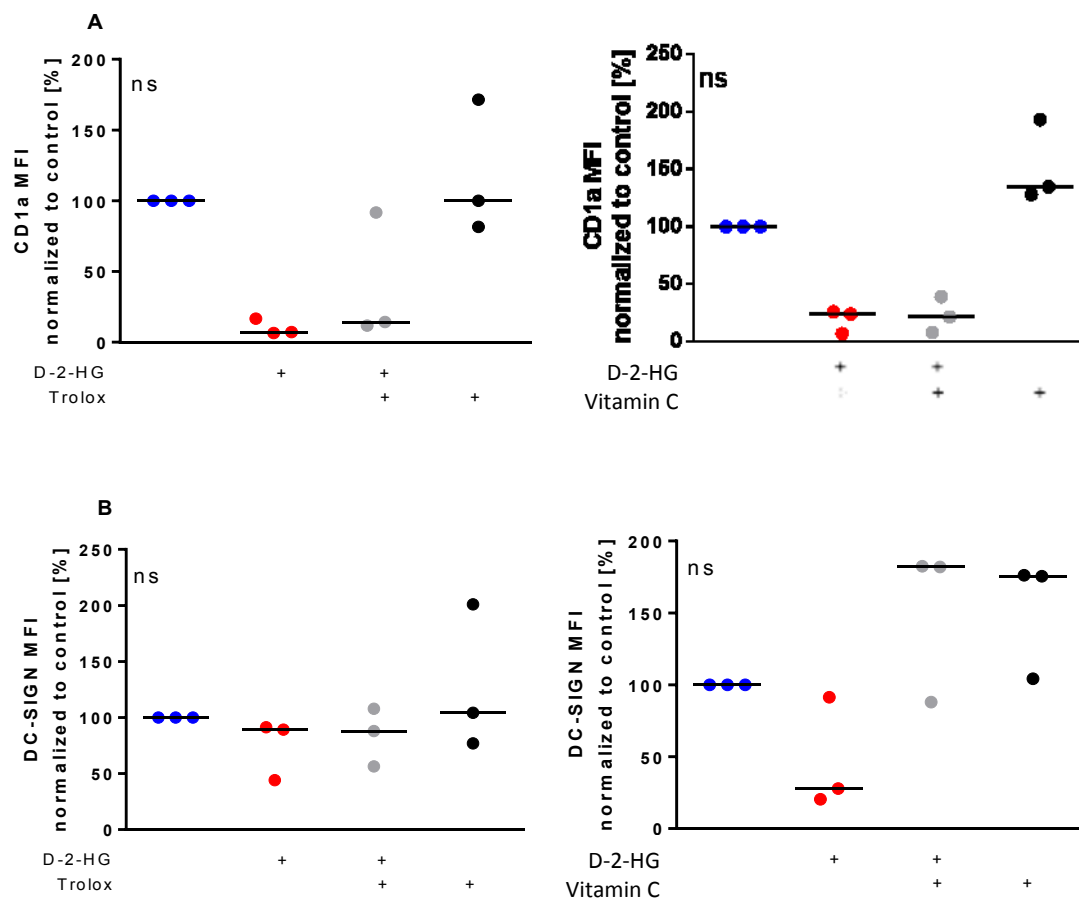


Figure 3.51: CD1a (A) and DC-SIGN (B) expression after trolox and vitamin C treatment. DCs were differentiated in the presence or absence of 20 mM D-2-HG, 50 μ M trolox or 2 mM vitamin C. On day 7 DC stained for (A) CD1a and (B) DC-SIGN. Fluorescence signal was measured by flow cytometry. Median (background corrected) intensity of the fluorescence signal were used. Single values and median of 3 independent experiments with different donors is shown. Statistical analyses for group differences were tested with Friedmann test (paired). (* $p \leq 0.05$ were considered significant, no significance was found).

3.2.7.2.3 IL-12 secretion of trolox and vitamin C treated DCs

DCs treated with trolox and vitamin C, in the presence of D-2-HG were activated on days 7 for 24h with LPS and IL-12 was analyzed in supernatants by ELISA. Trolox treatment alone lead to an increase in IL-12 secretion and was able to also increase IL-12 secretion in two of three donors tested. In the 3rd donor trolox treatment alone did also lower IL-12 levels, this was in contrast to the effects seen in the other donors and could be an explanation for the inconsistent results in the presence of D-2-HG (Figure 3.52A).

Surprisingly vitamin C treatment did lower IL-12 secretion of activated DCs and was not able to rescue the effects of D-2-HG when added in the presence of D-2-HG (Figure 3.52B).

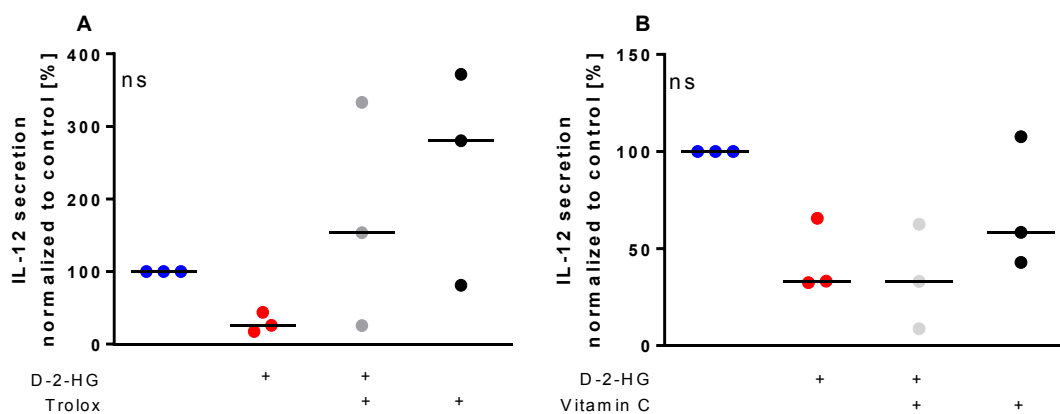


Figure 3.52: IL-12 secretion after trolox treatment. DCs were differentiated in the presence or absence of 20 mM D-2-HG, 50 μ M trolox (A) or 2 mM vitamin C (B). On day 7 DCs were activated with 100 ng/ml LPS, after 24h supernatants were collected to analyze IL-12 concentration by ELISA. Single values and median of 3 independent experiments with different donors is shown. Cytokine concentrations of D-2-HG treated DCs were normalized to corresponding control. Statistical analyses for group differences were tested with Friedmann test (paired). (* $p \leq 0.05$ were considered significant, no significance was found).

3.2.7.2.4 Reactive oxygen species of Vitamin C treated DCs

Also ROS levels were determined in vitamin C treated DCs after 7 days of culture. There was no effect seen on mitochondrial ROS in any of the treatments (D-2-HG, vitamin C, D-2-HG and vitamin C) (Figure 3.53A). Cytosolic ROS was increased in DCs treated with D-2-HG or vitamin C alone. The combination of both treatments had no additive effects on cytosolic ROS levels (Figure 3.53B).

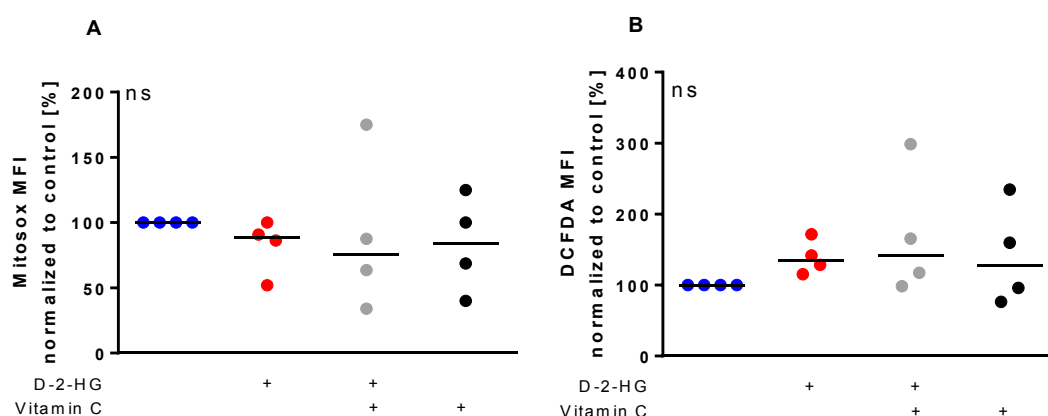


Figure 3.53: Mitochondrial (A) and cytosolic (B) ROS levels of vitamin C treated DCs. DCs were differentiated in the presence or absence of 20 mM D-2-HG or 2 mM vitamin C. On day 7 DC stained for (A) mitochondrial ROS (MitoSox) (B) or cytosolic ROS (DCFDA). Fluorescence signal was measured by flow cytometry. Median (background corrected) intensity of the fluorescence signal were used. Single values and median of 4 independent experiments with different donors is shown. Statistical analyses for group differences were tested with Friedmann test (paired). (* $p \leq 0.05$ were considered significant, no significance was found).

ROS levels in vitamin C treated DCs were analyzed because a decrease in ROS was expected, but as seen here there was no change of ROS levels with vitamin C treatment or even an increase. This could be explained by the fact that ROS level of DCs after 7 days of culture were analyzed and might not be stable. It is also known that the addition of vitamin C leads to an increase in extracellular ROS¹²². Because no reduced ROS level were seen with vitamin C treatment, ROS levels were not measured in trolox treated DCs.

3.7.8 Rescue experiments with modulator of metabolism

As D-2-HG induced an immediate and persisting increase in respiration (Figure 3.37, partially inhibiting DC respiration might rescue the inhibitory effects of D-2-HG on DC marker expression and IL-12 secretion. As anti-diabetic drugs are capable to reduce respiration, metformin and pioglitazone were selected. Metformin is an anti-diabetes drug, which has many targets in the cell, e.g. complex I of the respiration chain¹²³.

The anti-diabetes drug pioglitazone is a synthetic ligand of the peroxisome proliferator-activated receptor (PPAR) γ , which alters transcription of genes involved in carbohydrate and lipid metabolism. This leads to a metabolic shift towards glycolysis and an increased sensitivity to insulin¹²⁴. Moreover, it has been shown that pioglitazone reduces cellular respiration.

3.7.8.1 Respiration of metformin and pioglitazone treated DCs

In these set of experiments metformin (5 mM) and pioglitazone (25 μ M) were added to monocytes in the absence or presence of D-2-HG (20 mM) and cultured for 7 days. First the oxygen consumption of DC treated with metformin and pioglitazone in the presence or absence of D-2-HG was measured by high resolution respirometry.

Metformin treatment slightly reduced respiration of untreated as well as D-2-HG treated DCs when added on day 0 of culture. But in the presence of D-2-HG metformin was not able to reduce the respiration to control levels (Figure 3.54A).

In the presence of D-2-HG, pioglitazone was able to reduce the oxygen consumption to the levels of untreated DCs. Pioglitazone alone did not change the oxygen consumption (Figure 3.54B).

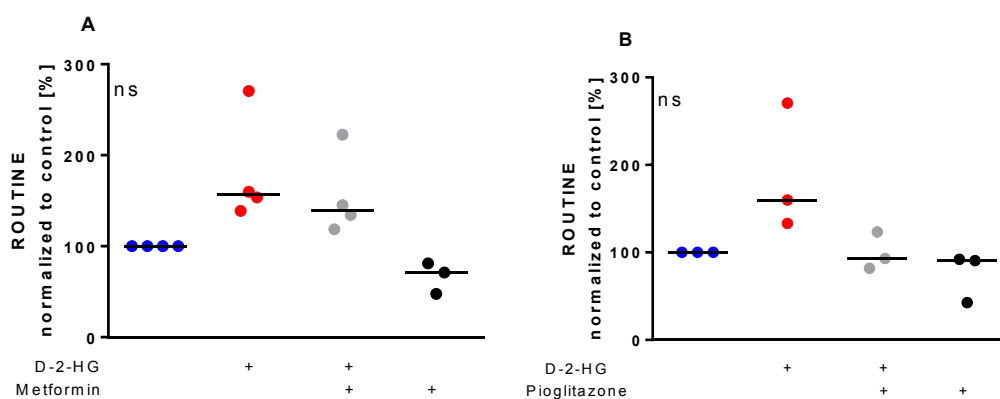


Figure 3.54: Basal respiration of DCs treated with metformin. Oxygen consumption was measured by high resolution respirometry after 7 days of treatment with (A) 5 mM metformin (Met), (B) 25 μ M pioglitazone (Pio) in the presence or absence of 20 mM D-2-HG. DCs were placed in oxygraph chambers in culture medium. ROUTINE respiration was measured (basal respiration). Single values and median of 3-4 independent experiments with different donors is shown. Statistical analyses for group differences were tested with Wilcoxon test (paired). (* $p \leq 0.05$ were considered significant, no significance was found).

3.7.8.2 HLA class II expression of metformin and pioglitazone treated DCs

In parallel, expression of HLA class II molecules in metformin and pioglitazone treated DC was analyzed. Metformin treatment did not normalize respiration of D-2-HG treated DCs and was not able to rescue the expression of HLA-DR or HLA-DP expression in the presence of D-2-HG. Metformin treatment alone partially lowered HLA-DP expression and increased HLA-DR expression (Figure 3.55A, B). Control DCs of these donors did not express HLA-DQ, so an analysis of HLA-DQ was not possible (data not shown).

Pioglitazone treatment alone decreased HLA-DP expression and increased HLA-DR expression. Pioglitazone treatment of DCs did not rescue the HLA-DP expression in the presence of D-2HG, but increased HLA-DR expression to levels above the levels of the untreated control DCs (Figure 3.55C, D). HLA-DQ could not be analyzed in these donors because control DCs showed no expression (data not shown).

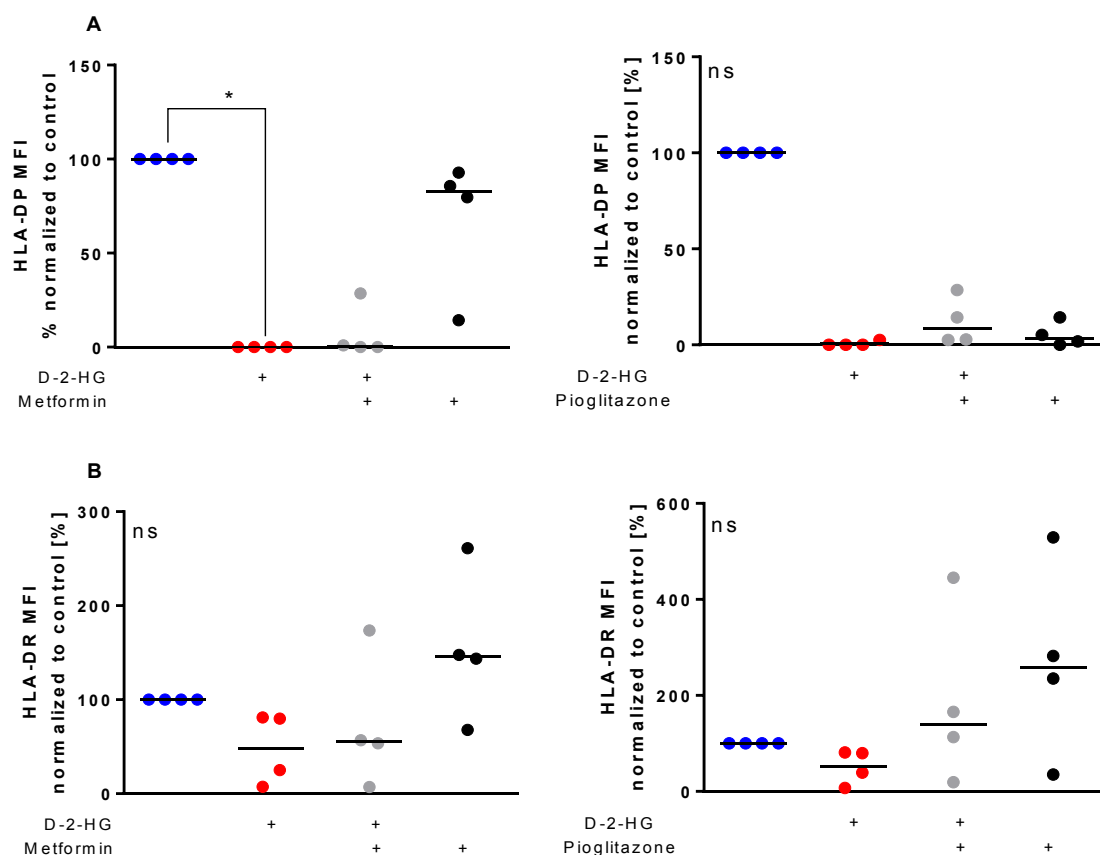


Figure 3.55: HLA-DP (A) and HLA-DR (B) expression on metformin treated. DCs were differentiated in the presence or absence of 20 mM D-2-HG, 5 mM metformin (met) or 25 μ M pioglitazone (pio). On day 7 DC stained for (A) HLA-DP and (B) HLA-DR. Fluorescence signal was measured by flow cytometry. Median (background corrected) intensity of the fluorescence signal were used. Single values and median of 3-4 independent experiments with different donors is shown. Statistical analyses for group differences were tested with Friedmann test (paired). (* $p \leq 0.05$ were considered significant).

3.7.8.3 DC-SIGN expression after pioglitazone treated DCs

CD1a and DC-SIGN expression was also reduced in D-2-HG DCs, because of that CD1a and DC-SIGN was analyzed after metformin and pioglitazone in the presence or absence of D-2-HG treated DCs after 7 days of culture.

In Figure 3.58A CD1a expression is shown. Metformin treatment decreased CD1a expression in all donors tested. In the presence of D-2-HG, metformin had no influence on CD1a expression. CD1a expression stayed low as seen in DCs treated with D-2-HG. Pioglitazone even further decreased CD1a expression as D-2-HG or metformin.

Metformin treatment increased DC-SIGN expression in two of three donors tested. In the presence of D-2-HG, metformin increased DC-SIGN expression in the same two donors. In DCs treated with metformin and D-2-HG DC-SIGN expression reached 94% of expression of untreated DCs. Pioglitazone treatment alone did reduce DC-SIGN expression in 2 out of 3

donors. In DCs treated with pioglitazone and D-2-HG, DC-SIGN levels were comparable with those of DCs treated with D-2-HG alone. To conclude this result pioglitazone was not able to rescue the effects of D-2-HG on DC-SIGN expression (Figure 3.58B).

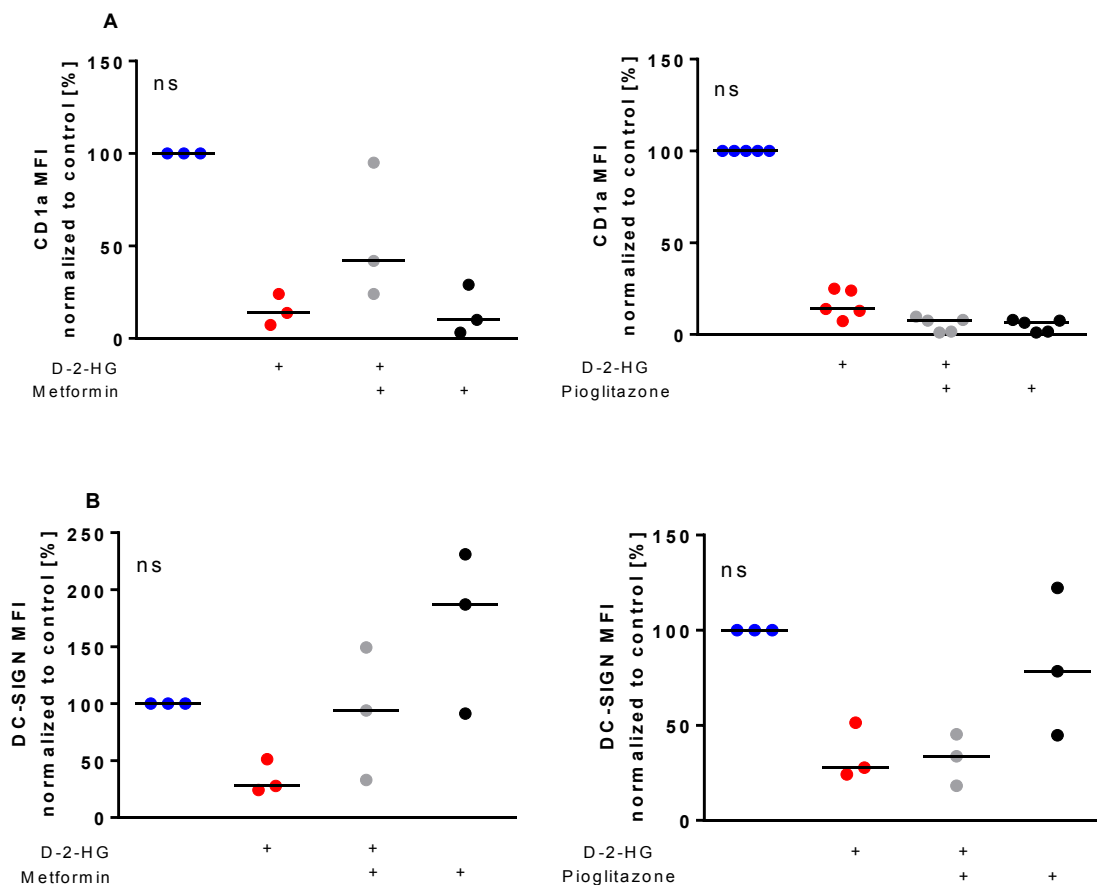


Figure 3.58: CD1a (A) and DC-SIGN (B) expression on metformin and pioglitazone treated DCs. DCs were differentiated in the presence or absence of 20 mM D-2-HG, 5 mM metformin or 25 μ M pioglitazone. On day 7 DC stained for (A) CD1a and (B) DC-SIGN expression. Fluorescence signal was measured by flow cytometry. Median (background corrected) intensity of the fluorescence signal were used. Single values and median of 3-5 independent experiments with different donors is shown. Statistical analyses for group differences were tested with Friedmann test (paired). (* $p \leq 0.05$ were considered significant, no significance was found).

3.7.8.4 IL-12 secretion of metformin and pioglitazone treated DCs

DCs treated with metformin and pioglitazone in the presence of D-2-HG were activated on days 7 for 24h with LPS and IL-12 was analyzed in supernatants by ELISA.

As previously shown also in these samples IL-12 secretion was decreased after D-2-HG treatment. Metformin alone also lowered IL-12 secretion. DCs treated with D-2-HG in combination with metformin did further decrease the levels of IL-12 (Figure 3.56A).

In the donors analyzed to evaluate the effect of pioglitazone treatment, the IL-12 secretion was low in control DCs. D-2-HG treatment reduced IL-12 secretion about 50%. Pioglitazone alone did even further reduce IL-12 levels. In supernatants of DCs treated with pioglitazone in the presence of D-2-HG IL-12 was nearly absent. In conclusion it was not possible to rescue IL-12 secretion with pioglitazone (Figure 3.56B).

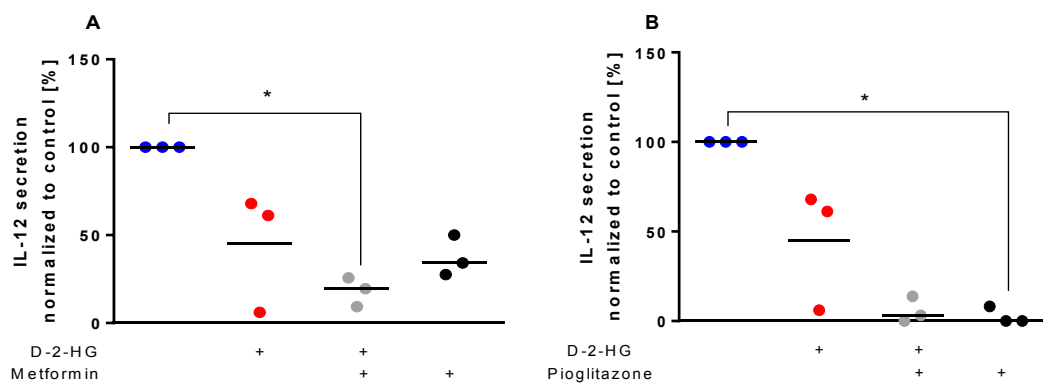


Figure 3.56: IL-12 secretion of DCs treated with metformin and pioglitazone. DCs were differentiated in the presence or absence of 20 mM D-2-HG, (A) 5 mM metformin (met) or (B) 2 mM vitamin C. On day 7 DCs were activated with 100 ng/ml LPS, after 24h supernatants were collected to analyze IL-12 concentration by ELISA. Single values and median of 3 independent experiments with different donors is shown. Cytokine concentrations of D-2-HG treated DCs were normalized to corresponding control. Statistical analyses for group differences were tested with Friedmann test (paired). (* $p \leq 0.05$ were considered significant).

3.7.8.5 ROS levels in metformin and pioglitazone treated DCs

On day 7 ROS levels were also analyzed in metformin and pioglitazone treated DCs. In these experiments the mitochondrial ROS levels in the D-2-HG treated cells were not increased compared to the untreated control.

Metformin treatment increased the levels of mitochondrial ROS in the presence or absence of D-2-HG (Figure 3.57A). Metformin treatment rescued the increased cytosolic ROS levels in the presence of D-2-HG, while metformin treatment alone had no influence on cytosolic ROS levels (Figure 3.57B).

Pioglitazone alone or in combination with D-2-HG had also no effect on mitochondrial ROS levels. As seen before (Figure 3.48), also in these experiments cytosolic ROS was increased in D-2-HG treated DCs. Pioglitazone alone lowered cytosolic ROS levels to 50% of control DCs. Pioglitazone in combination with D-2-HG reached similar levels as with pioglitazone alone (Figure 3.57A, B). In summary, pioglitazone was able to reduce cytosolic ROS in the presence or absence of D-2-HG.

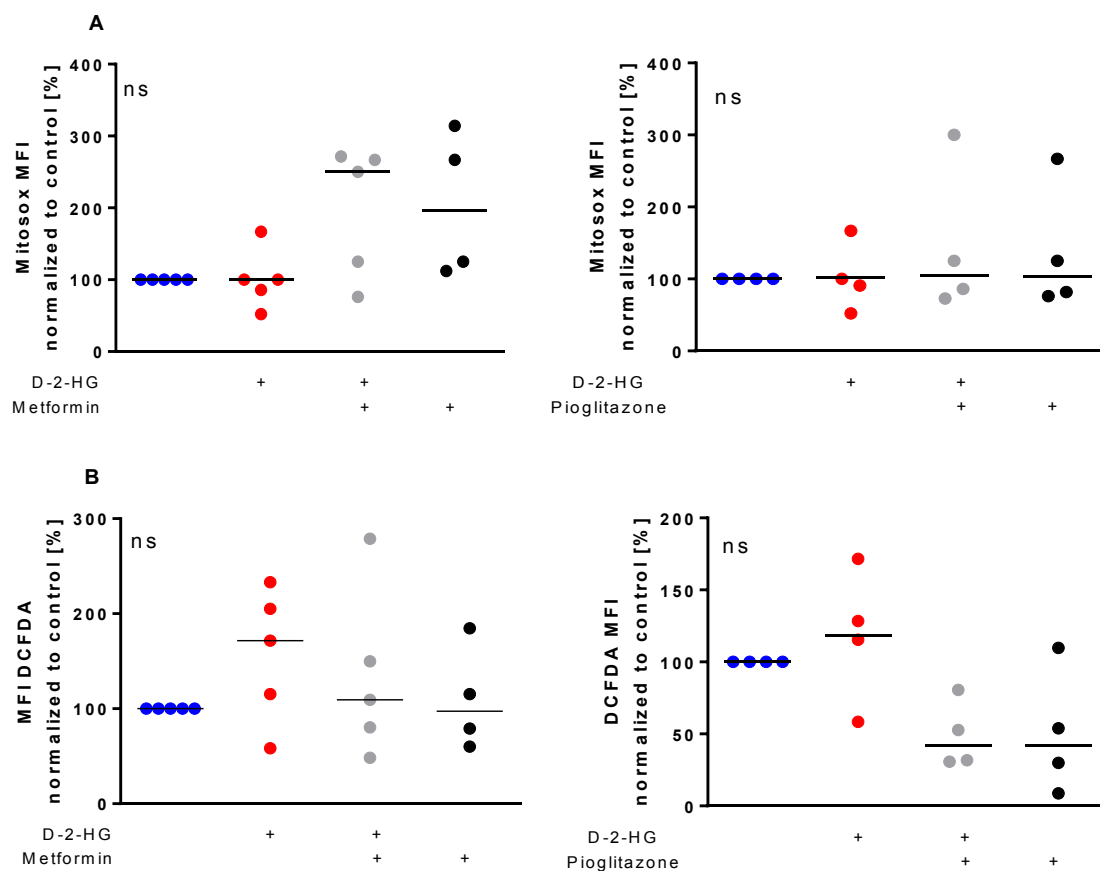


Figure 3.57: Mitochondrial (A) and cytosolic (B) ROS levels in metformin and pioglitazone treated DCs. DCs were differentiated in the presence or absence of 20 mM D-2-HG, 5 mM metformin or 25 μ M pioglitazone. On day 7 DCs were stained for (A) mitochondrial ROS (MitoSox) (B) or cytosolic ROS (DCFDA). Fluorescence signal was measured by flow cytometry. Median (background corrected) intensity of the fluorescence signal were used. Single values and median of 5 independent experiments with different donors is shown. Statistical analyses for group differences were tested with Friedman test (paired). (* $p \leq 0.05$ were considered significant, no significance was found).

In summary pioglitazone lowered the respiration and cytosolic ROS levels of D-2-HG treated DCs to levels comparable to untreated control DCs. Pioglitazone was able to partly rescue HLA-DR expression but had no effect on IL-12 secretion.

3.7.9 Methylation analysis of DC differentiation

Vitamin C rescued HLA-DR and DC-SIGN expression (Figure 3.50 and Figure 3.51). Furthermore, vitamin C is a co-factor of TET2 (demethylase) and is known to be able to restore TET2 activity^{125,126}. Methylated promoters are associated with low gene expression¹²⁷. To find out if these effects of vitamin C on HLA-DR and DC-SIGN expression were

changed by epigenetic regulation, vitamin C (2 mM) was added to monocytes at the beginning of the culture in the presence or absence of D-2-HG. DNA of monocytes (directly after elutriation), 16 h, 66 h and 7 days cultured DCs was isolated for each treatment (untreated, vitamin C, D-2-HG, vitamin C and D-2-HG).

In cooperation with the working group of Prof. Rehli methylation analyses were performed using epityper technology. This was done to address the question if D-2-HG also inhibits demethylation of loci getting demethylated during DC differentiation. DNA methylation analysis revealed a delayed demethylation pattern of D-2-HG treated DCs in loci which get demethylated during physiological DC differentiation, like C9ORF78, CD207, CCL13 and CLEC10A, which can be nicely monitored in methylation pattern of non-treated DCs from monocytes to 16 h, 66 h and 7 days cultured DCs changing from 100% methylated (blue) to lower methylation percentages (yellow). STAT5 is a gene locus which is demethylated later during DC differentiation, STAT5 was only in untreated and vitamin C treated DCs demethylated. Vitamin C alone did speed up demethylation in all genes analyzed compared to control DCs but was only in part able to counteract the inhibitory effect of D-2-HG. As expected the control genes MMP7 and HOXB1 did not change methylation status during DC differentiation (Figure 3.59).

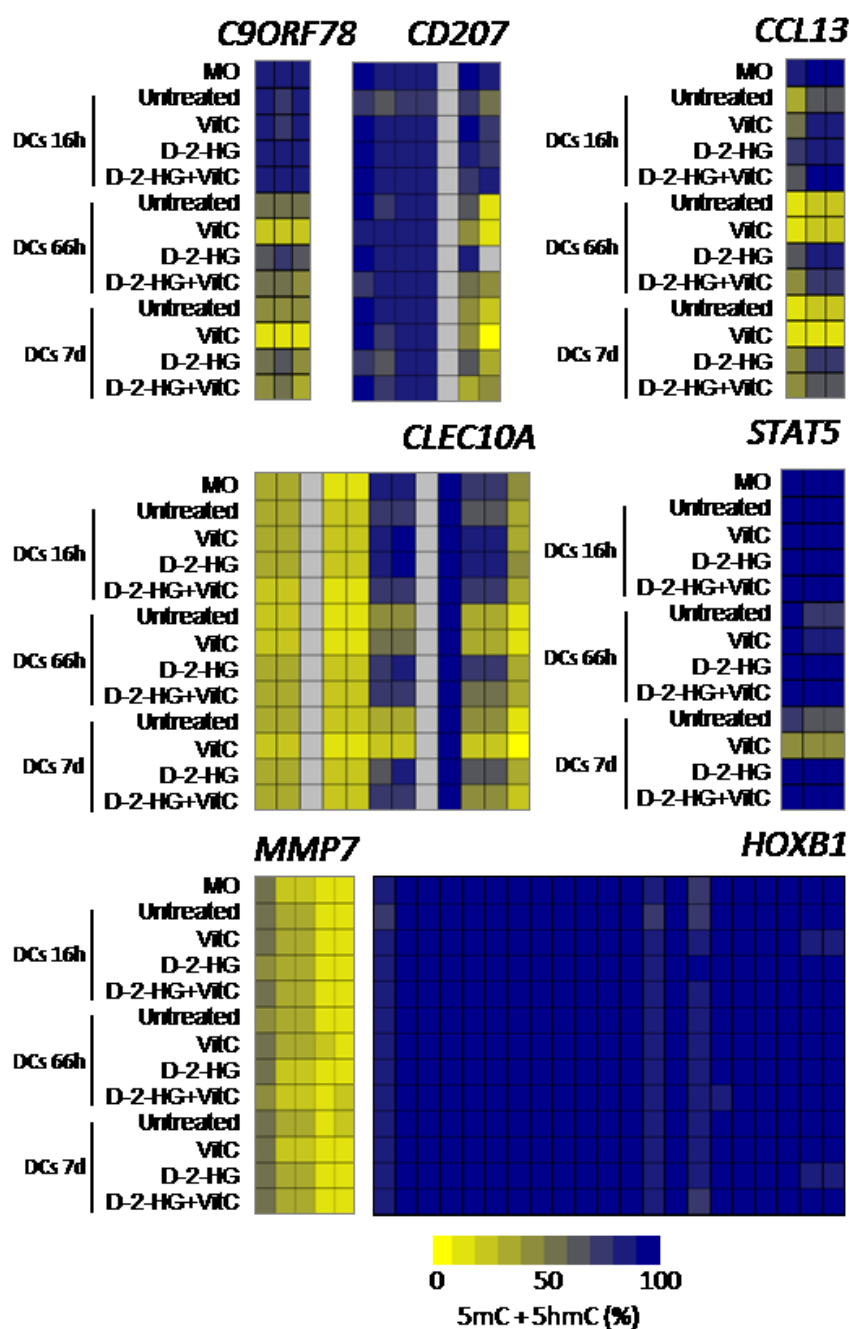


Figure 3.59: Methylation analysis of DC differentiation. MassARRAY analysis of bisulfite-converted DNA, at five loci showing active DNA demethylation during monocyte to DC differentiation (C9ORF78, CD207, CCL13, CLEC10A, STAT5), as well as for two control regions (MMP7 and HOXB1). Data are presented as heatmaps (mean of three different donors). The methylation ratio (including both 5mC and 5hmC) at single CpGs dinucleotides (individual boxes) is indicated by shades of yellow to blue (yellow: no methylation, dark blue: 100% methylation). Grey boxes indicate CpGs that were not detected by MALDI-TOF MS.

3.7.10 Primary AML blast from IDH mutated leukemias

3.7.10.1 RNA_{seq} data of primary AML IDH_{MUT} blasts from the cancer genome atlas

As mentioned before DCs treated with D-2-HG had a significantly lower surface expression of HLA-class II molecules (Figure 3.21 and Figure 3.22). To analyze if this is also true in primary AML blasts harboring IDH mutations (only separated in IDH1 and 2 mutation), we analyzed RNA sequencing data of the online available data base the cancer genome atlas (TCGA). Alleles of HLA genes, which are mainly expressed are selected and shown in Figure 3.60. For all genes, expression of HLA-class II genes was reduced in IDH1 mutated blasts compared to IDH non-mutated blasts. The gene for the HLA-DQA1 alpha chain was significant lower expressed in IDH1 mutated blasts compared to blasts expressing wild type IDH. For AML blasts with IDH2 mutation this effect was not observed (Figure 3.60).

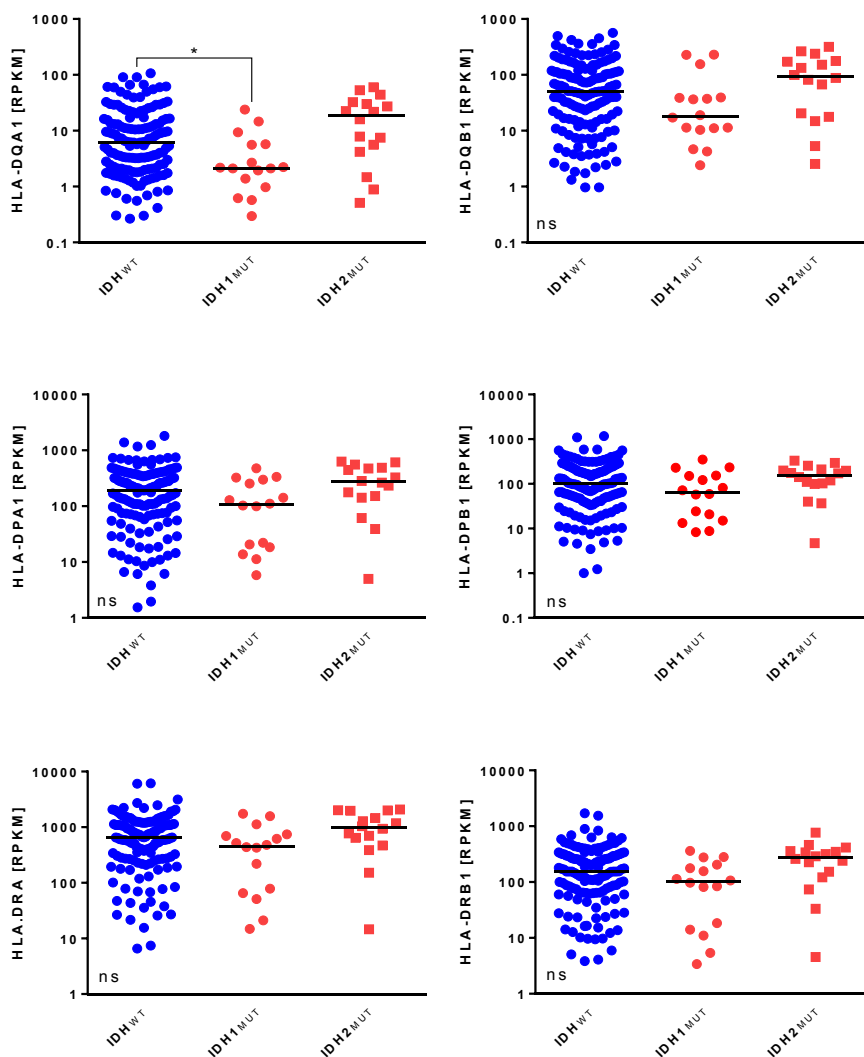


Figure 3.60: RNAseq Data of the Cancer Genome Atlas. RNA sequencing data were downloaded on the TCGA website. Medians of reads per kilobase million (RPKM) are shown of 158 IDH wild type and 16 IDH1 and 2 expressing blasts each.

RPKM means reads of RNA_{seq} were normalized to fragment length. Statistical analyses for group differences were tested with One-way Anova (unpaired). (*p≤0.05 were considered significant).

3.7.10.2 HLA class II protein expression of primary AML IDH_{MUT} blasts

RNA_{seq} data showed a lower HLA class II molecule mRNA levels in AML blasts with an IDH1 mutation. Surface expression of HLA class II molecules was analyzed in primary AML blasts. IDH mutated (IDH1 and IDH2 mutated blasts were combined) AML blasts had a significant lower surface expression of HLA-DP compared to AML blasts expressing wildtype IDH. For HLA-DQ the levels was comparable in both groups. HLA-DR was in tendency lower expressed in AML blasts expressing mutated IDH. The red dots represent IDH2 mutated, the triangles represent IDH1 mutated AML blasts. In contrast to the RNA_{seq} data, the surface staining of HLA class II molecules expression of blasts expressing mutated IDH1 were similar to those in IDH2 expressing blasts (Figure 3.61A, B, C).

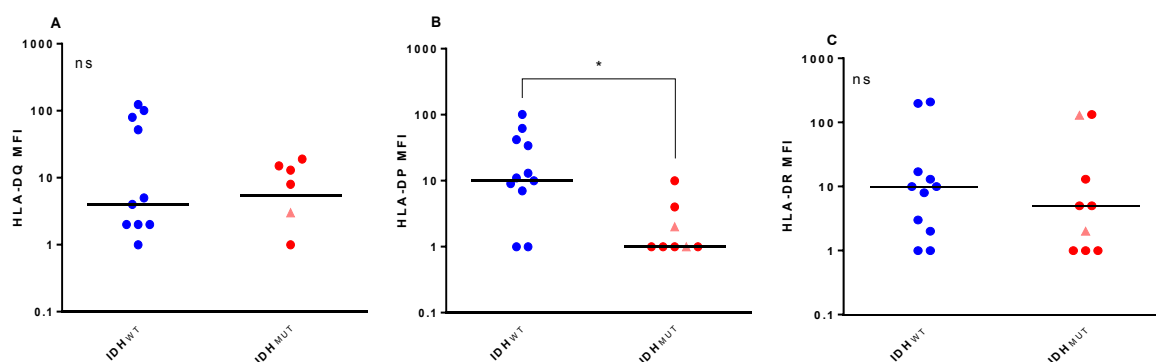


Figure 3.61: HLA-DP (A), -DQ (B) and -DR (C) expression of AML blasts with and without IDH mutation. AML blasts were thaw and stained for HLA-class II surface expression. Single values and median of 10 IDH wild type AML blasts and 9 IDH 1 (triangles) or 2 (dots) mutated AML blasts are shown. Median (background corrected) intensity of the fluorescence signal were used. Statistical analyses for group differences were tested with Mann Whitney test (paired). (*p≤0.05 were considered significant).

3.7.10.3 HLA expression on AML blasts analyzed by western blot

Surface staining of HLA-DR and HLA-DP molecules revealed a lower expression in IDH mutant compared with IDH wild type AML blasts. To confirm this data, protein lysates were produced and analyzed by western blot.

In line with the surface staining of IDH mutant blasts showing less HLA class II expression, also the total HLA class II signal was lowered in IDH mutant blasts. Signals of HLA class II specific antibody was normalized to actin signal (loading control). However, in one IDH wild type patient (#4) expression of HLA class II molecules was low, but in all other

wild type expressing donors HLA class II molecules expression exceeded those in IDH mutated blasts (Figure 3.62).

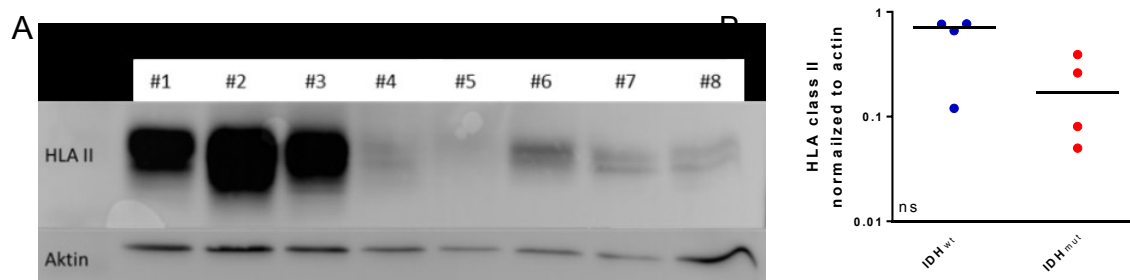


Figure 3.62: HLA class II expression of IDH mutant and wild type blasts analyzed by western blot. PBMCs from AML patients were thawed and proteins were extracted. 10 μ g were loaded on a 12% SDS acrylamide gel. Membrane was stained with mouse anti-MHCII primary antibody (1:2000) and HRP linked anti-mouse secondary antibody (1:2500). Antibodies were removed by membrane stripping and analyzed for actin with rabbit anti-actin (1:2500) and anti-rabbit (1:2500). HLA class II signal was measured after an exposure time of 18s. (B) Quantification of three different donors was done by normalization on actin expression and expression of corresponding control DCs by ImageJ. Statistical analyses for group differences were analyzed with Wilcoxon test (paired). (* $p \leq 0.05$ were considered significant, no significance was found).

4 Discussion

4.1 Generation of IDH2 R40Q specific T cells

4.1.1 T cell stimulation with peptide and protein of mutant IDH2 R140Q

T cell stimulation with IDH2 R140Q specific peptides IQN9 and IQN10 gave rise to T cells that specifically recognize these peptides with low background activity (Figure 3.1 and 3.2). But these T cells were not able to recognize DCs expressing IDH2 R140Q. This could be explained by the possibility that there is no peptide antigen presented on HLA molecules, which is specific for the amino acid exchange (R140Q) or even for the IDH2 protein. It is known that not all proteins expressed in a cell are presented on HLA molecules. Bassani-Sternberg et al. showed results of advanced mass spectrometry (MS) analysis wherein they analyzed the melanoma-associated immune-peptidome (up to 95,500 patient-presented peptides each) from 25 melanoma tissue samples. Out of 1,100 nonsense mutations in each patient only eleven mutated peptide ligands were found, wherein four were found to be immunogenic¹²⁸. In addition, the protein should be expressed in an adequate level. In animal experiments, irradiation of cancer cells cultures generated mutation specific T cells only for antigens overexpressed in tumor cells^{129,130}. We can exclude that the expression was an issue in our experiments because we saw sufficient expression (Figure 3.4) and mRNA electroporation is known to be a potent tool for T cell stimulation with foreign proteins¹⁰⁷. In summary, we concluded that IDH2 R140Q proteins are not guided to the antigen processing and presentation machinery and therefore IDH2 R140Q derived peptides are not presented on HLA molecules.

4.1.2 Peptide prediction with *in silico* algorithms

The results from *in silico* prediction tools showed a lower binding affinity (to HLA-B*15:01) for the IDH2 wild type (IRN9) peptide than for the mutated peptide (IQN9) (Table 3.1). Analysis of binding positions of 9mer amino acid peptides presented by HLA class I molecules to TCRs revealed positions 1-3 and position 9 as anchor positions with no contact to the TCR. While positions 4-8 were in close contact with the TCR¹³¹. Thus, position 2 where the mutated amino acid is located in the IQN9-peptide is most likely an anchor position, which explains the different binding affinities of IRN9 (wild type) and IQN9 (mutated) predicted by BIMAS, SYFPETHI and NET MHC Pan.

Amino acids at positions 4-8 which are possibly recognized by TCRs do not differ in the wild type and mutated peptide. T cells recognizing these amino acids would have been most probably already deleted in the thymus¹³². This is not the possibility in our experiments because it was possible to generate IQN9-peptide specific T cells. So, most likely there is an antigen with a similar amino acid sequence.

4.1.3 Influenza peptide is similar to mutant IDH2 R140Q derived peptide IQN9

To find this similar antigen, the sequence around the mutated amino acid glutamine (Q) was used for an NCBI BLAST (aligned input amino acid sequence to protein sequences in the NCBI data base) to find viral proteins with similar amino acid sequences. We were focused on viral proteins because it is known that TCRs specific for viral or bacterial peptides are also able to recognize structural similar self-antigens. This is called molecular mimicry^{108,133}. The most promising hit was the neuramidase protein of influenza A virus where 5 amino acids (QNILG) were identical to the sequence of IQN9-peptide. The enzyme neuramidase is located on the surface of the virus and so a component of influenza A vaccination. People who had an influenza infection or vaccination generate specific T cells against the surface molecules of the virus.

Stimulation with the influenza A peptide did not result in any specific T cell response, but IQN9-peptide stimulated T cells were able to recognize the influenza A peptide (Figure 8). It seemed that the influenza A peptide used in our stimulation experiment is not an endogenous processed peptide of the influenza A neuramidase protein. The physiological sequence of the peptide could be different in length or bind to an HLA molecule which was not expressed in the tested donors. The fact that IQN9-peptide stimulated T cells were able to recognize the influenza A peptide showed that influenza A specific T cells were generated. This was only possible in one of the three donors tested. This might be due to the different infections or vaccinations background of the analyzed donors. The donor who showed reactivity was yearly vaccinated against influenza viruses, vaccination frequencies of the other two donors tested is not known and might not be as regular.

It is estimated that 10^{12} T cells are present in the human body expressing less than 10^8 different TCRs so it is very unlikely that one TCR only recognize one specific antigen¹³⁴. Therefore, it is reasonable that TCRs only bind to the amino acids in the middle of a peptide to increase the peptides which can possibly be recognized by this TCR. Furthermore, this

could be a possible explanation why we could generate IQN9-peptide specific T cells but no T cell population recognizing the endogenously processed IDH2 R140Q protein.

4.2 Effects of D-2-HG on differentiation and metabolism of monocytes derived dendritic cells

Cancer associated D-2-HG produced by mutant IDH showed inconsistent impacts on cell metabolism^{13,72,123,135}. Dendritic cell (DC) differentiation and activation is accompanied with changes in their metabolism⁸⁰. In the second part of the project the impact of D-2-HG on the metabolism and differentiation of primary human myeloid cells was investigated.

4.2.1 Uptake of D-2-HG

Monocytes treated with D-2-HG had higher 2-HG level than monocytes only incubated with media (Figure 3.7). This is in line with experiments done with DCs (unpublished data) and two recently published paper wherein D-2-HG uptake was shown in T cells^{72,136}. Bunse et al. showed a higher D-2-HG uptake in DCs compared to T cells¹³⁶. How D-2-HG enters the cell is not yet clear. In one study, Hagos et al. analyzed different transporters for 2-HG. They identified Organic anion transporter 1 (OAT1, solute carrier family 22 member 6 (SLC22A6)) and Solute carrier family 13 member 3 (SLC13A3) as possible transporters¹³⁷. According to BIOGPS, SLC22A6 is mainly expressed in kidney but also in monocytes, myeloid cells, DCs and all T cells subtypes analyzed. Expression of SLC13A3 in T cells, DCs and monocytes was higher than the expression of SLC22A6. A recently published study in nature medicine showed a positive correlation of SLC13A3 expression and D-2-HG uptake, which was not seen with SLC22A6. In addition, a reduced D-2-HG uptake was shown in SLC13A3 knockdown cells¹³⁶. Already proven is that D-2-HG is able to translocate out of the cell, as it was measured in the sera of AML and glioma patients harboring an IDH mutation^{32,33,138}.

In conclusion there is no need to use ester derivatives of D-2-HG to get D-2-HG into a cell. The derivatization may potentially lead to additional effects which would not be seen with endogenously produced D-2-HG.

4.2.2 D-2-HG inhibits DC differentiation

In electron pictures of D-2-HG treated DCs, a reduced length and number of dendrites was seen before and after activation with LPS (Figure 3.10, 11). Besides morphology, expression of DC marker and IL-12 secretion was reduced (Figure 3.18, 19, 22 and 26). From this we concluded that the differentiation and activation was impaired in D-2-HG treated DCs.

4.2.2.1 T cell stimulation activation in an allogeneic MLR

In allogeneic MLRs with CD4 T cells a reduced proliferation and IFN γ production was measured when co-cultured with D-2-HG treated DCs (Figure 3.37). This could be explained by the reduced IL-12 secretion in these cells. This was in line with allogeneic MLR experiments performed by Böttcher et al., wherein lymphocytes and immature DCs were seeded together with LPS in the presence of 10 mM D-2-HG, resulted in a reduced T cell proliferation. In contrast to our results no change in IFN γ secretion was seen⁷². This can be explained by the lower D-2-HG concentration (10 mM instead of 20 mM) or the different experimental setting as DCs were already differentiated when D-2-HG was added to the MLR culture. We saw no influence on T_{reg} frequencies after co-culture with D-2-HG treated DCs. In contrast Böttcher et al. showed increased T_{reg} frequencies in D-2-HG treated T cells⁷². Xu et al saw a hypermethylation at the FoxP3 locus which led to a reduced FoxP3 expression in TH17 cells with high level of D-2-HG⁷³.

4.2.2.2 Multi-laminar vesicles in DCs

Our hypothesis was that the vascular multi-laminar vesicles seen in DCs were HLA molecule containing vesicles of the antigen presentation pathway. Calafat et al. showed similar structures to carry HLA-DR molecules by gold labeling⁶⁰. In D-2-HG treated DCs these multi-laminar vesicles contained a less dense matrix compared to control DCs (Figure 3.13). Our theory was that the antigen presentation pathway could be impaired in DCs because we saw a reduced HLA class II abundance on the surface. The analysis of intracellular HLA class II levels showed no HLA-DP and -DQ expression, but HLA-DR expression was measurable and decreased in D-2-HG treated DCs (Figure 3.22). Western blot analysis with whole protein lysates revealed a reduced HLA class II expression in D-2-HG treated DCs (Figure 3.24). Taken together, our results suggest that there is no intracellular accumulation of HLA class II molecules; HLA class II molecules were in general less expressed in DCs treated with D-2-HG.

4.2.2.3 Impact of D-2-HG on autophagy

Some studies suggested that increased ROS levels inhibit autophagy^{139,140}. We saw increased ROS levels in D-2-HG treated DC (Figure 3.48) and hypothesized that this may influence autophagy by impairing the levels of LC-3B (a molecule present in autophagosomes). LC-3B is present in three forms pro-LC-3B, LC-3B I and LC-3B II. LC-3B I is formed out of pro-LC-3B which is much bigger than LC3B I/II, ATG7 (essential protein for autophagy) then

conjugates phosphatidylethanolamine (PE) to LC-3B I to form LC3B II ¹⁴¹. We analyzed LC-3B levels by western blot technique (Figure 3.15). D-2-HG treatment led to a reduced abundance of LC-3B II, the active form present in autophagosomes. The reduction of LC-3B II abundance by D-2-HG could be either due to a higher degradation rate or a reduced formation of autophagosomes. To clarify that, DCs were additionally treated with BafA1, an inhibitor of autophagy. BafA1 inhibits the final fusion and degradation of autophagosomes so BafA1 treatment should lead to a higher LC3B II abundance ¹⁴². In western blots performed with lysates of BafA1 treated DCs, the three isoforms (pro-LC-3B, LC-3B I and II) could not be detected. There was only one band at the height of 18kD where the LC-3B I signal was previously detected. After quantification of this signal, results could not be concluded because they were inconsistent and an increased LC-3B signal was only seen in two out of three donors (Figure 3.16). The influence of D-2-HG on autophagy has to be further investigated.

Other reasons to investigate autophagy were the differences seen in vascular structures in the EM pictures and differences in HLA class II expression. HLA molecules are more stable when peptides are bound and autophagy is involved in antigen processing ⁵⁶. We hypothesized that the lower LC-3B abundance could also be an explanation for the reduced HLA class II abundance on the surface. But BafA1 treatment of DCs did not influence the abundance of HLA class II molecules on the surface (Figure 3.22). This was in line with reports from Mintern et al. wherein the authors analyzed the role of autophagy in antigen presentation. They demonstrated that the antigen presentation of HLA class II molecules was not influenced in ATG7 deficient DCs in general, but cross-presentation of soluble factors was decreased ¹⁴³.

4.2.2.4 Intracellular signaling of D-2-HG

Experiments performed in the working group of Prof. Marina Kreutz with a cell permeable substance, which is converted to D-2-HG inside the cell showed different effects than D-2-HG itself (not shown unpublished data). This suggests that D-2-HG also binds to the cell membrane and is involved in signaling. D-2-HG could be a ligand of a G protein-coupled receptor (GPCR). Depending on the G-protein, different signaling pathways would be activated. G_i and G_s coupled receptors are involved in cyclic AMP (cAMP) and protein kinase A signaling. While G_{q/11} coupled receptors activate phospholipase C (PLC) followed by inositol 3 phosphate increase, calcium signaling and protein kinase C (PKC) activation. G_{12/13} and G_{β/γ} coupled receptors activate glykogensynthase-kinase 3 and phosphoinositid-3-kinase

Here we analyzed the translocation of PKC (isoform α , β and γ) to find out if D-2-HG bind to a $G_{q/11}$ coupled receptor. PKC is known to be active when it is located in the cell membrane and inactive when located in the cytosol¹⁴⁵. Cell lysates enriched for cytosolic or membrane-bound and nuclear proteins were generated. In the cytosol as well as the membrane fraction of D-2-HG treated DCs PKC levels were increased compared to the untreated control DCs (Figure 3.31). This could indicate that D-2-HG bind to $G_{q/11}$ coupled receptors. To confirm these findings further upstream calcium measurements were started, but so far no conclusive results were obtained (data not shown).

PKC is also involved in DC differentiation, so a change in translocation caused by D-2-HG could explain its impact on differentiation. PKC α is known to regulate cytokine production in DCs. In PKC $\alpha^{-/-}$ bone marrow derived murine DCs there was a decreased TNF- α and IL-12p40 production¹⁴⁶. Farren et al. showed that inhibition of PKC β II led to an inhibition of DC differentiation¹⁴⁷. This is in line with a report of Cejas et al. showing that PKC β II is important of DC differentiation¹⁴⁸. These reports are inconsistent to our results on D-2-HG causing an inhibition of DC differentiation and an increased PKC level. In contrast to Cejas et al. we did not use an isoform specific antibody, which might explain the different results.

Furthermore, oxidants can interfere with PKC activation. Oxidation of regulatory elements like the zinc finger resulted in a calcium independent PKC activation. If the oxidation takes place at the C-terminal catalytic domain, this leads to an inactivation of PKC. In addition, intracellular distribution of PKC isoforms was influenced by redox status¹¹⁴. Thus, the increased abundance of PKC in the cytosol could be caused by increased ROS level in D-2-HG treated DCs. But the higher overall abundance of PKC could also be partly the cause of the higher ROS levels as Pinton et al. reported that PKC β is also able to produce ROS¹⁴⁹.

In another series of experiments, another GPCR pathway involving activation of G_i and G_s coupled receptors was analyzed by measuring cAMP levels. High levels of cAMP activate protein kinase A, which leads to the activation of cAMP response element-binding protein (CREB). On one hand G_i receptor activation leads to an inhibition of adenylyl cyclase (AC) and results in lower cAMP level. On the other hand G_s coupled receptor activate AC and lead to higher cAMP level¹⁴⁴.

In our results cAMP levels were slightly higher in D-2-HG treated DCs than in untreated DCs (Figure 3.32). The results shown here were measured in DCs after 7 days of culture, where D-2-HG was added in the beginning. For future experiments it would be reasonable to study the short-term impact of D-2-HG in monocytes as cAMP levels might not be stable for several days.

Based on our results on PKC and cAMP it cannot be excluded that D-2-HG binds to a GPCR, but further analyses need to be performed to prove the binding of D-2-HG.

4.2.3 Effect of D-2-HG on metabolism

4.2.3.1 Effect of D-2-HG on glycolytic activity

Higher glycolytic activity of D-2-HG treated DCs was seen to have higher glucose consumption and lactate production (Figure 3.33). It is known that lactate inhibits T cell⁷⁰ and DC function⁷¹. But in our experiments addition of lactate to monocytes did not lead to the same effect on HLA class II expression and other DC markers as seen with D-2-HG treatment (data not shown). In line with the higher lactate concentrations in supernatants of DCs treated with D-2-HG, the pH values dropped first in D-2-HG treated DCs (lactate lowers pH value) (Figure 3.34). This was in line with studies from Malinarich et al., wherein induced tolerogenic DCs showed a higher glycolytic capacity compared to control DCs⁸⁷. In contrast Guak et al. reported an important role of glycolysis for DC migration¹⁵⁰. Thus, the important part might be the balance between glycolysis and OXPHOS activity.

To elucidate which signal molecule is involved in D-2-HG associated increase in glycolysis mTOR phosphorylation was analyzed. No significant effect of D-2-HG on mTOR phosphorylation (activation) was seen in short term or after 7 days of culture (Figure 3.35). But, the problems with isotype staining of one donor made it difficult to conclude the results so far. Based on our data we cannot exclude the possibility that mTOR is involved in D-2-HG signaling, which would explain some results measured in D-2-HG treated DCs. Wei et al. showed that inhibition of mTOR led to a reduced IL-12 secretion in DCs¹⁵¹. Furthermore, as mentioned in the introduction, mTOR is important for differentiation and metabolism of DCs. Results from mice lacking the mTOR signaling complex 1 (mTORC1) gene showed a disruption of DC development¹⁵². The mTORC1 predominantly contains mTOR phosphorylated at serine 2448¹⁵³, the phosphorylation site analyzed here. In another study, short-term (48 h) addition of rapamycin (mTOR inhibitor) caused apoptosis in DCs but not in monocytes¹⁵⁴. Chen et al. incubated immature human DCs with rapamycin for 24h and

observed a dose dependent inhibition of DC-SIGN, as we also saw after D-2-HG incubation¹⁵⁴. But in contrast to them, in our experiments D-2-HG was already added to monocytes at the beginning of the culture. In studies of Ferreira et al. rapamycin was able to rescue HLA-DR expression in vitamin D3 induced tolerogenic DCs¹¹⁶. Thus, rapamycin could be used in further experiments to investigate if this is also possible in D-2-HG treated DCs.

4.2.3.2 Effect of D-2-HG on respiration

Analysis of OXPHOS activity of D-2-HG treated DCs and DCs expressing mutant IDH showed higher ROUTINE (Figure 3.36, 41, 42). In literature the effects of D-2-HG on respiration are inconsistent. In neuronal cell cultures D-2-HG seemed to inhibit ATP synthase (complex V of respiration chain)¹⁵⁵. In line Chen et al. demonstrated an inhibition of complex IV by D-2-HG in the human leukemic monocyte cell line THP-1¹³. In contrast Grassian et al. showed a higher respiration in HT1080 cells expressing mutant IDH1 (R132H or R132C) under hypoxia compared to the parental wild type cells¹⁵⁶. In line with this, experiments done with an IDH1-R132H mutant human oligodendroglioma xenograft model revealed increased mitochondrial activity and mitochondrial content in IDH1 mutant tumor cells compared to IDH1-wild type xenografts¹⁵⁷. D-2-HG added to T cells increased respiration activity⁷². As DCs switch from OXPHOS to glycolysis during maturation it is not unexpected that tolerogenic DCs showed higher oxidative phosphorylation rates^{158,159}. This is in accordance to our findings where D-2-HG caused an increase in oxidative phosphorylation and an impaired T cell stimulation capacity (Figure 3.27).

4.2.4 IDH mutant cells and D-2-HG addition interfere with ROS level

As shown in Figure 3.48 cytosolic ROS levels were increased in D-2-HG treated DCs. These findings are in line with previous work in chick neurons, wherein the addition of 1 mM D-2-HG lead to higher ROS levels¹⁵⁵. In line, studies in U87 cells expressing mutant IDH1 R132H and glioma cells expressing IDH1 R132C showed higher ROS compared to the wild type cells, respectively^{9,160}. The higher ROS level of IDH mutant cells could be explained by the increased consumption of NADPH for D-2-HG production⁴⁵. But in the experiments performed here and in Kölker et al. the addition of D-2-HG also led to an increase in cytosolic ROS. Therefore, D-2-HG itself might increase ROS levels in addition¹⁵⁵.

In Figure 3.48 a reduced cystine uptake of D-2-HG treated cells is shown, this is in line with results published by D'Angelo et al. where an inhibition of the cystine/glutamate

antiporter also inhibits DC differentiation¹⁶¹. A reduced uptake of cystine could also be an explanation for the higher ROS levels seen in D-2-HG treated DCs.

We saw an increased cytosolic ROS level and a reduced differentiation in D-2-HG treated DCs. In contrast, others suggested ROS are important for DC differentiation and activation^{83,84,86}. So we hypothesize that as shown for T cells^{97,162} ROS level have to be carefully balanced also in DCs and that DC function is impaired if ROS level are out of balance.

4.2.5 Rescue of D-2-HG effects with trolox treatment

Trolox is a water soluble derivative of vitamin E¹⁶³. We hypothesized that the anti-oxidative capacity of trolox would lower the increased ROS level (D-2-HG caused) thereby rescuing the effects of D-2-HG on HLA class II, CD1a and DC-SIGN expression as well as IL-12 secretion (Figure 3.50-52).

Results of trolox treatment are difficult to conclude as HLA class II expression was low and D-2-HG treatment did not reduce DC-SIGN expression in these donors. Also the IL-12 secretion was highly variable in these donors. But in median trolox and D-2-HG treated cells had IL-12 levels comparable with control levels. This is in contrast to Xuan et al. who saw an inhibitory effect on IL-12 secretion after addition of vitamin E¹⁶⁴ and reports showing an inhibitory effect of antioxidants and catalase on DC differentiation^{83,86}

4.2.5 Rescue of D-2-HG effects on metabolism with metformin

Surprisingly metformin alone did not reduce respiration (Figure 3.54). The limited effect of metformin could be explained by an insufficient expression of the metformin transporter in the donors tested, but in general metformin transporter were shown to be expressed in DCs^{165,166}. Although respiration was not inhibited by metformin, cytosolic ROS was rescued to control levels by co-treatment of D-2-HG and metformin (Figure 3.54, 57).

In mice Shin et al. showed that metformin inhibits antigen presentation of DCs by suppressing both HLA class I and II expression and expression of co-stimulatory molecules like CD80/CD80 in bone marrow derived DCs. Metformin treatment was performed 2 hours on day 5 of *in vitro* culture¹⁶⁷. In our experiments, HLA-DP expression was slightly decreased and HLA-DR expression slightly increased in metformin treated DCs compared to control DCs. This discrepancy can be explained by the fact that in the experiments of Shin et al. murine bone marrow was used instead of blood of healthy human donors to generate DCs.

4.2.6 Rescue of D-2-HG effects on metabolism with pioglitazone

Peroxisome proliferator-activated receptor γ (PPAR γ) is important for DC metabolism and is activated by pioglitazone. Pioglitazone is used as an anti-diabetic drug, it has the ability to shift the metabolism towards glycolysis¹²⁴. We hypothesized that pioglitazone treatment would lower the increased respiration (caused by D-2-HG) to control levels and thereby also rescuing the D-2-HG effects on DC differentiation. Indeed, pioglitazone treatment rescued the increased respiration and cytosolic ROS levels (Figure 3.54, 57) but had only minor effects on other parameters analyzed (HLA-DP, DC-SIGN and CD1a protein expression and IL-12 secretion). Pioglitazone mono-treatment reduced HLA-DP, DC-SIGN and CD1a expression and IL-12 secretion. This is in line with results of Yan et al. wherein pioglitazone was added to DCs for 24h and a downregulation of DC-SIGN was observed¹⁶⁸. Furthermore, Gosset et al. showed that the addition of pioglitazone significantly reduced IL-12 secretion in DCs¹⁶⁹.

In conclusion, regulation of respiration to control levels and cytosolic ROS was not sufficient to rescue all inhibitory effects seen by D-2-HG. This means that not all effects caused by D-2-HG in DCs were connected to the same pathway and that D-2-HG might interfere with several pathways.

4.2.7 Effect of D-2-HG on DNA methylation and vitamin C treatment

As D-2-HG is an epigenetics modulator and expression of HLA class II molecules is known to be also regulated by epigenetics¹⁷⁰, analysis of DNA methylation was performed. D-2-HG treatment was combined with vitamin C, as vitamin C is a co-factor of the demethylase TET2. Addition of vitamin C to TET2 deficient mice increased demethylation and suppressed human leukemic colony formation¹²⁶. Thus, it was hypothesized that a vitamin C treatment of IDH mutant blasts producing D-2-HG could be beneficial. This was done in a murine leukemic model expressing IDH1 R132H. Mingay et al. showed that vitamin C treatment led to demethylation at enhancer sequences involved in myeloid differentiation¹²². Other studies showed that vitamin C enhances TET2 activity¹²⁵. In a murine model vitamin C was mainly found in hematopoietic stem cells (HSC) and less if cells were more differentiated. Agathocleous et al. concluded that vitamin C accumulated in HSCs to promote TET2 activity, to limit HSC frequency and suppressed leukemogenesis¹⁷¹.

In our experiments, addition of vitamin C once at the beginning of the monocyte culture led to a faster demethylation of loci which should get demethylated during DC differentiation (Figure 3.59). D-2-HG treatment decreased demethylation velocity. These

results were expected and in accordance with published literature^{125,170}. An increased level of methylation correlated with impaired murine hematopoietic differentiation⁴¹. This is in line with the results shown with D-2-HG treatment of DCs resulting in an impaired differentiation and hypermethylation compared to untreated control. But in presence of D-2-HG, vitamin C had only a minor effect on some loci analyzed. The effect of vitamin C was not strong enough to counteract the effect of D-2-HG. Using a lower D-2-HG or higher vitamin C concentration might be beneficial. With these results we cannot finally answer the question if the positive effects of vitamin C seen on HLA class II and DC-SIGN expression were regulated epigenetically or not.

In addition, an involvement of ROS in epigenetics regulation was reported. Studies showed that DNA damage caused by ROS resulted in a reduced methylation status due to the impaired binding of methylases (like DNMTs) to the damaged DNA¹⁷². In contrast, a study showed that ROS can induce DNA methylation of promoters like the catalase promotor to further increase ROS¹⁷³.

The results of the experiments with vitamin C treated cells cannot be finally concluded. We saw a slight improvement in the HLA class II molecule expression (Figure 58) and a minor effect on demethylation by vitamin C treatment in the presence of D-2-HG. To get a final answer how the differentiation is inhibited by D-2-HG further experiments need to be planned regarding the mechanisms. For example, with TET2 knockout cells one needs to check if the effect of D-2-HG is due the inhibition of TET2 or there is an additional cellular target.

4.2.8 Expression of mutant IDH protein versus exogenous D-2-HG

We saw higher respiration rates in DCs treated with D-2-HG (Figure 3.37) and in DCs expressing mutant IDH after electroporation with *in vitro* transcribed mRNA (Figure 3.41, 42). This was in line with the lower expression of HLA class II molecules in DCs treated with D-2-HG as well as AML blasts expressing mutant IDH (Figure 3.18, 19, 22, 61 and 62).

However, there are obvious differences in cells expressing mutant IDH and cells where D-2-HG was added. Chaturvedi et al. showed gene set enrichment data of D-2-HG treated cells and cells expressing mutant IDH each compared to untreated wild type cells. Gene sets enriched in D-2-HG treated and IDH mutant cells did only overlap for 16% of gene sets. Results from methylation analyses also separated samples of IDH mutant expressing from D-2-HG treated cells in different clusters¹⁷⁴. Oizel et al. looked at the metabolism of

IDH mutant and D-2-HG treated cells and concluded that D-2-HG does not mimic all effects of mutant IDH¹⁷⁵. For sure, in cells expressing mutant IDH and endogenous converting D-2-HG from α -ketoglutarate, the NADPH balance is more affected. Wild type IDH produce NADPH during the conversion of α -ketoglutarate to isocitrate, mutant IDH consumes NADPH by the production of D-2-HG⁴⁵.

As shown in Figure 3.61, mRNA levels of HLA-DP were significantly reduced in AML patients expressing mutant IDH1, but not in IDH2 mutant blasts. This could be due to the different locations inside the cell. IDH1 is present in the cytosol, whereas IDH2 is expressed in mitochondria. If D-2-HG produced by mutant IDH2 can translocate into the cytosol is not yet clarified. But as IDH2 and IDH1 mutant cells have epigenetic alterations, it is likely that D-2-HG is able to translocate in different compartments including the nucleus⁴¹.

Analysis of surface expression of HLA class II molecules showed a reduced expression in primary AML blasts expressing mutant IDH compared to wild type blasts. The downregulation of HLA molecules on solid tumors as well as AML blasts is a well-known immune-escape mechanism¹⁷⁶. The data shown here with IDH mutant AML blasts and D-2-HG treated DC clearly show an impact of D-2-HG on immune cells. This is in line with two studies on D-2-HG impairing T cell function^{72,73} and another recently published paper where D-2-HG was shown to inhibit T cell function and abundance in glioma patients¹⁷⁷. In addition Kohanbash et al. showed improved T cell infiltration in a mutant IDH1 expressing glioma model¹⁷⁸.

Taken together our results D-2-HG seemed to inhibit the differentiation of monocytes to DCs and thereby also reduced the immunological anti-tumor activity. D-2-HG promoted immune escape on both sites; it reduced the stimulatory capacity of DCs and decreased the immunogenicity of the AML blast by reduced HLA-class II expression.

The effect of D-2-HG could partially be rescued by pioglitazone and the antioxidants trolox and vitamin C. But during the work of this thesis it was not possible to find a drug which fully rescues all effects of D-2-HG on surface marker and metabolism. In future experiments drugs like diclofenac or rapamycin could be used in rescue experiments. Diclofenac was found to lower glucose uptake and lactate secretion⁹⁸, in addition also oxidative phosphorylation was found to be inhibited¹⁷⁹. Thus, diclofenac could be used to normalize the metabolic reprogramming of DCs caused by D-2-HG treatment. The normalization of the metabolism may also have a positive effect on DC differentiation and

fully rescue the D-2-HG effects on differentiation. This could also be combined with agent interfering with DNA methylation, as this might also play a role for the altered phenotype. In a long perspective, the substance which rescued the D-2-HG effects on DCs and AML blasts could be used to prevent immune escape of IDH mutant tumors or other diseases with elevated D-2-HG or L-2-HG concentration.

5 Summary

5.1 Generation of IDH2 R140Q specific T cells

In the last decades, immunotherapy has become an important part of cancer treatment. For a cancer-specific immunotherapy, it is essential to find a target structure which is restricted to cancer cells but is not expressed on other cells. This is possible with “tumor-specific” antigens. In the first part of the project the goal was to create a T cell population expressing a T cell receptor specifically recognizing the mutated IDH2 R140Q enzyme. T cells were either stimulated with antigen presenting cells (APCs) loaded with a IDH2 R140Q protein specific peptide or with APCs transfected with the IDH2 R140Q protein. Suitable peptides were estimated by online tools (BIMAS, SYFPETHI and NET MHC Pan). The most promising binding properties were found for the HLA-B*15:01 restricted 9mer IQNILGGTV (IQN9) having the mutated amino acid at the second position (anchor position). Although we successfully generated IQN9-peptide specific T cells, it was not possible to find a T cell population specifically recognizing APCs expressing the IDH2 R140Q protein upon transfection. This could be explained by the fact that the mutated amino acid was on an anchor position and not in the T cell receptor binding region. T cells stimulated with IQN9-peptide loaded APCs recognized a neuramidase protein (expressed by influenza A viruses) derived peptide which showed a similar amino acid sequence, in addition to the IQN9-peptide. Apparently, neuramidase-specific T cells were re-stimulated by the IDH2 R140Q derived peptide, a phenomenon known as molecular mimicry.

5.2 Effect of D-2-HG on metabolism and differentiation of monocyte-derived dendritic cells

In the second part of the project the impact of the onco-metabolite D-2-Hydroxyglutarate (D-2-HG), produced by the mutated IDH, on myeloid cells was analyzed. D-2-HG is known to be released by different tumor entities as leukemia or glioma harbouring IDH mutations. The impact of D-2-HG on the differentiation of monocytes into DCs and on DC metabolism was examined. Monocytes are able to take up D-2-HG. Besides increased cell sizes, D-2-HG treated DCs had less and shorter dendrites than control cells after 7 days of culture. Cell yield and viability remained unaffected by D-2-HG treatment. CD1a, a differentiation marker was not expressed in D-2-HG treated DCs. DC-SIGN, HLA-DR and –DP, required for T cell priming and activation, were also significantly less expressed on D-2-HG treated DCs. Furthermore, D-2-HG treatment changed the cytokine profile of mature DCs. The pro-

inflammatory cytokine IL-12 was significantly less secreted in the presence of D-2-HG. To analyze the functional consequences of the D-2-HG induced DC phenotype on T cell stimulation, we performed allogenic mixed lymphocyte reactions with CD4 T cells. D-2-HG treated DCs were characterized by a reduced stimulatory capacity, indicated by a reduced IFN γ production and diminished proliferation of CD4 T cells.

In a next step, the metabolic profile of DCs was analyzed in the presence of D-2-HG. Respiration analyses revealed higher oxygen consumptions in D-2-HG treated DCs as well as in DCs expressing mutated IDH1 or IDH2 enzyme. Moreover, glycolytic activity analyzed by glucose consumption and lactate secretion was increased, in line with the earlier pH drop measured by the PreSens technology. The higher respiratory and glycolytic activity resulted in increased ATP levels. Furthermore, cytosolic reactive oxygen species (ROS) levels were significantly increased in the presence of D-2-HG. Since respiration displays an important source of ROS, we hypothesized that, antioxidants like vitamin C might reduce the increased ROS levels and thereby also the inhibitory effect of D-2-HG on DC differentiation. Vitamin C had a positive effect on HLA-DP expression, but only a minor effect on HLA-DR expression. DC-SIGN expression reached control levels in vitamin C and D-2-HG treated DCs.

In another series of experiments, anti-diabetic drugs modulating the metabolism were applied with the aim to rescue inhibitory D-2-HG effects on DC differentiation, as metformin (an inhibitor of complex I of the electron transport chain) and pioglitazone (a ligand for peroxisome proliferator-activated receptor γ). In contrast to metformin, pioglitazone treatment partially neutralized the effects induced by D-2-HG.

As D-2-HG is a known modulator of DNA methylation, DCs were analyzed by MassARRAY in the presence of D-2-HG and vitamin C. Vitamin C acts as a co-factor for TET2, an important demethylase in DC differentiation. We hypothesized that vitamin C could rescue marker expression on an epigenetic level. As expected, D-2-HG delayed the demethylation of sites, which are known to be important for DC differentiation. A single treatment with vitamin C did speed up the demethylation process. Vitamin C was able to partly compensate for the inhibitory effect of D-2-HG on demethylation in some regions, but levels of untreated DCs were not reached.

Finally, primary AML blasts with IDH mutations were analyzed, regarding their HLA class expression. In line with the results obtained for D-2-HG treated monocyte-derived DCs, HLA class II expression was also decreased in primary IDH mutated AML blasts.

Taken together, our results indicate that D-2-HG inhibits the differentiation of monocyte to DCs, which can have in turn an impact on T cell stimulation. Thereby D-2-HG is indirectly able to reduce the immunological anti-tumor response. D-2-HG can promote immune escape by reducing HLA class II expression in an autocrine and paracrine way. Moreover, D-2-HG diminishes the stimulatory capacity of DCs and decreases the immunogenicity of AML blasts.

6 Zusammenfassung

6.1 Generierung von IDH2 R140Q spezifischer T Zellen

In den letzten Jahrzehnten ist die Immuntherapie ein wichtiger Bestandteil in der Behandlung von Krebsleiden geworden. Für eine Krebs-spezifische Immuntherapie ist es essentiell, eine geeignete zelluläre Zielstruktur zu finden, die ausschließlich von Tumorzellen, jedoch nicht von anderen Zellen exprimiert wird. Dies ist mit tumor-spezifischen Antigenen möglich. Ein Ziel im ersten Teil dieses Projekts war die Generation von T Lymphozyten, die spezifisch die mutierte Isozitat Dehydrogenase (IDH) 2 (R140Q) erkennen. T Zellen wurden mit Antigen präsentierenden Zellen (APCs) stimuliert, die entweder mit dem IDH2 R140Q Peptid beladenen wurden oder mit dem IDH2 R140Q mRNA transfiziert wurden. Geeignete Peptide wurden mittels Online-Vorhersageprogrammen (BIMAS, SYFPETHI und NET MHC Pan) ermittelt. Die erfolgversprechendsten HLA-Molekül-Bindungseigenschaften hatte das HLA-B*15:01 restringierte 9mer IQNILGGTV (IQN9), bei dem die Aminosäure an der zweiten Stelle mutiert ist (Ankerposition). Obwohl wir erfolgreich IDH2 R140Q Peptid spezifische T Zellen generierten, war es nicht realisierbar eine T Zell Population zu generieren, die das IDH2 R140Q Protein auf transfizierten APCs erkennt. Grund hierfür war vermutlich, dass die mutierte Aminosäure an eine Ankerposition und nicht in der Region in der der T Zellrezeptor bindet lag. T Zellen, die mit IQN9-Peptid beladenen APCs stimuliert wurden, erkannten zusätzlich zum IQN9-Peptid ein Neuramidase Protein (exprimiert von Influenza A Viren). Scheinbar wurden Neuramidase spezifische T Zellen durch das von der IDH2 R140Q abstammende Peptid re-stimuliert, ein Phänomen, das als molekulares Mimikry bekannt ist.

6.2 Effekt von D-2-HG auf den Metabolismus und die Differenzierung von aus Monozyten gereiften dendritischen Zellen

Im zweiten Teil des Projekts wurde der Effekt des Onko-Metabolits D-2-Hydroxyglutarat (D-2-HG), das von der mutierten IDH produziert wird, auf myeloide Zellen untersucht. D-2-HG wird von verschiedenen Tumoren, wie Leukämien oder Gliomen, die eine mutierte IDH aufweisen, abgegeben. Der Effekt von D-2-HG auf die Differenzierung von Monozyten zu dendritischen Zellen (DZs) und auf den Metabolismus von DZs wurde untersucht. Monozyten sind in der Lage D-2-HG aufzunehmen. Nach 7 Tagen wiesen D-2-HG behandelte DZs sowohl einen signifikant größeren Zelldurchmesser als auch weniger und kürzere Dendriten als unbehandelte Kontrollzellen auf. Die Zellausbeute und die Viabilität blieben durch die Behandlung mit D-2-HG unverändert. CD1a, ein Differenzierungsmarker, wurde in mit D-2-

HG behandelten DZs nicht mehr exprimiert. Die Expression der Marker DC-SIGN, HLA-DR und –DP, welche wichtig für das T Zell Priming und die Aktivierung sind, war in D-2-HG behandelten DZs signifikant niedriger. Des Weiteren veränderte die Behandlung mit D-2-HG das Zytokin-Profil der ausgereiften DZs. Das pro-inflammatorische Zytokin IL-12 wurde in Gegenwart von D-2-HG signifikant weniger ausgeschüttet. Um die funktionellen Konsequenzen des durch die D-2-HG Behandlung induziert Phänotyps zu analysieren, wurde eine allogene Gemischte-Lymphozyten-Reaktion mit CD4 T Zellen durchgeführt. Mit D-2-HG behandelte DZs waren durch eine verminderte Stimulationsfähigkeit gekennzeichnet, wobei die IFN γ Produktion und die Proliferation von CD4 Zellen erniedrigt war.

In einem weiteren Schritt wurde das metabolische Profil von DZs in der Gegenwart von D-2-HG analysiert. Die Analyse der Respiration zeigte einen erhöhten Sauerstoffverbrauch sowohl in D-2-HG behandelten DZs, als auch in IDH1 und IDH2 mutierten DZs. Außerdem war die glykolytische Aktivität, gemessen durch Glukoseabnahme und Laktatsekretion, erhöht, was mit dem verfrühten Abfall des pH-Wertes einherging, welcher mit Hilfe der PreSens Technologie bestimmt wurde. Die erhöhte glykolytische und respiratorische Aktivität führte zu höheren ATP Spiegeln. Zudem waren zytosolische reaktive Sauerstoff Spezies (ROS) Level in Anwesenheit von D-2-HG signifikant erhöht. Da eine erhöhte Atmungsaktivität eine wichtige Quelle für ROS darstellen kann, stellten wir die Hypothese auf, das Antioxidationsmittel wie Vitamin C erhöhte ROS Level verringern und hierdurch auch der inhibitorische Effekt von D-2-HG auf die Differenzierung von DZs reduziert werden könnte. Vitamin C erhöhte die HLA-DP Expression, hatte jedoch nur einen geringen Effekt auf die HLA-DR Expression. Die DC-SIGN Expression auf Vitamin C und D-2-HG behandelten DZs erreichte ein Level das mit dem der Kontrolle vergleichbare war.

In weiteren Experimenten, wurden anti-diabetische Substanzen verwendet, die den Metabolismus modifizieren, wie Metformin (ein Inhibitor des Komplex I der Atmungskette) und Pioglitazon (ein Ligand für den Peroxisom Proliferator-aktivierten Rezeptor γ), um den inhibitorischen D-2-HG Effekt auf die DZ Differenzierung auszugleichen. Im Gegensatz zu Metformin, war die Pioglitazon Behandlung in der Lage sowohl die Atmung als auch die HLA-DR Expression von D-2-HG behandelten DZs auf den Level unbehandelten DZs auszugleichen.

Da D-2-HG einen bekannten Modulator der DNA Methylierung darstellt, wurden DZs, die mit D-2-HG und Vitamin C behandelt wurden, mit Hilfe von MassARRAY analysiert. Vitamin C ist ein Ko-Faktor für TET2, einer wichtigen Demethylase während der DZ

Differenzierung. Deshalb vermuteten wir, dass Vitamin C die Expression bestimmter Marker auf epigenetischer Ebene wiederherstellen kann. Wie zu erwarten, verzögerte D-2-HG die Demethylierung von Gen Bereichen, die bekannter Weise wichtig für die DZ Differenzierung sind. Eine Behandlung mit Vitamin C allein führte zu einer Beschleunigung des Demethylierungsprozesses. In Anwesenheit von D-2-HG, führte Vitamin C nur in geringem Maße zu höheren Demethylierungsanteil, wobei vergleichbare Level zu unbehandelten DZs nicht erreicht werden konnten.

Zuletzt wurde die HLA Klasse II Expression in primären AML Blasten, die eine IDH Mutation aufweisen, untersucht. Vergleichbar zu den Ergebnissen, die mit D-2-HG behandelten DZs gewonnen wurden, war die HLA Klasse II Expression in primären, IDH mutierten AML Blasten ebenfalls erniedrigt.

Zusammenfassend, zeigen unsere Daten, dass D-2-HG die Differenzierung von DZs aus Monozyten hemmte. Durch die vermindert HLA Klasse II Expression verringert D-2-HG die stimulatorische Kapazität von DZs und Immunogenität von AML Blasten. So kann D-2-HG indirekt die immunologische anti-tumorale Antwort auf autokrinem und parakrinem Weise vermindern und so zur Immunevasion führen.

References

1. Murphy, K. M., Travers, P. & Walport, M. *Janeway's immuno biology*. (Garland Science, 2008).
2. Juliusson, G. *et al.* Age and acute myeloid leukemia : real world data on decision to treat and outcomes from the Swedish Acute Leukemia Registry. *Blood* **113**, 4179–4187 (2014).
3. Döhner, H. *et al.* Diagnosis and management of acute myeloid leukemia in adults: recommendations from an international expert panel, on behalf of the European LeukemiaNet. *Blood* **115**, 453–474 (2010).
4. DiNardo, C. D. *et al.* Durable Remissions with Ivosidenib in IDH1-Mutated Relapsed or Refractory AML. *N. Engl. J. Med.* NEJMoa1716984 (2018). doi:10.1056/NEJMoa1716984
5. Perl, A. E. The role of targeted therapy in the management of patients with AML. *Blood Adv.* **1**, 2281–2294 (2017).
6. Shen, Y. *et al.* Gene mutation patterns and their prognostic impact in a cohort of 1185 patients with acute myeloid leukemia. *Blood* **118**, 5593–5603 (2012).
7. Naoe, T. & Kiyoi, H. Gene mutations of acute myeloid leukemia in the genome era. *Int. J. Hematol.* **97**, 165–174 (2013).
8. Dohner, H. *et al.* Diagnosis and management of AML in adults: 2017 ELN recommendations from an international expert panel. *Blood* **129**, 424–448 (2017).
9. Chaturvedi, A. *et al.* Mutant IDH1 promotes leukemogenesis in vivo and can be specifically targeted in human AML. *Blood* **122**, 2877–2887 (2013).
10. Döhner, H. & Gaidzik, V. I. Impact of genetic features on treatment decisions in AML. *Hematology Am. Soc. Hematol. Educ. Program* **2011**, 36–42 (2011).
11. Levis, M. FLT3 mutations in acute myeloid leukemia: what is the best approach in 2013? *ASH Educ. Progr. B.* **2013**, 220–226 (2013).
12. Patel, J. P. *et al.* Prognostic Relevance of Integrated Genetic Profiling in Acute Myeloid Leukemia. *N. Engl. J. Med.* **366**, 1079–1089 (2012).
13. Chan, S. M. *et al.* Isocitrate dehydrogenase 1 and 2 mutations induce BCL-2 dependence in acute myeloid leukemia. *Nat. Med.* **21**, 178–184 (2015).
14. Martelli, M. P., Sportoletti, P., Tiacci, E., Martelli, M. F. & Falini, B. Mutational landscape of AML with normal cytogenetics: Biological and clinical implications. *Blood Rev.* **27**, 13–22 (2013).
15. Colombo, E., Marine, J. C., Danovi, D., Falini, B. & Pelicci, P. G. Nucleophosmin regulates the stability and transcriptional activity of p53. *Nat. Cell Biol.* **4**, 529–533 (2002).
16. Marcucci, G., Haferlach, T. & Döhner, H. Molecular genetics of adult acute myeloid leukemia: Prognostic and therapeutic implications. *J. Clin. Oncol.* **29**, 475–486 (2011).

17. Renneville, A. *et al.* Prognostic significance of DNA methyltransferase 3A mutations in cytogenetically normal acute myeloid leukemia: a study by the Acute Leukemia French Association. *Leukemia* **26**, 1247–1254 (2012).
18. Im, A. P. *et al.* DNMT3A and IDH mutations in acute myeloid leukemia and other myeloid malignancies: associations with prognosis and potential treatment strategies. *Leukemia* **28**, 1774–1783 (2014).
19. Salamanca-Cardona, L. *et al.* In Vivo Imaging of Glutamine Metabolism to the Oncometabolite 2-Hydroxyglutarate in IDH1/2 Mutant Tumors. *Cell Metab.* **26**, 830–841.e3 (2017).
20. Gross, S. *et al.* Cancer-associated metabolite 2-hydroxyglutarate accumulates in acute myelogenous leukemia with isocitrate dehydrogenase 1 and 2 mutations. *J. Exp. Med.* **207**, 339–344 (2010).
21. Dang, L. *et al.* Cancer-associated IDH1 mutations produce 2-hydroxyglutarate. *Nature* **462**, 739–44 (2009).
22. Patel, K. P. *et al.* Acute Myeloid Leukemia with IDH1 or IDH2 Mutations: Frequency and Clinicopathologic Features. *Am. J. Clin. Pathol.* **135**, 35–45 (2011).
23. Reitman, Z. J. & Yan, H. Isocitrate dehydrogenase 1 and 2 mutations in cancer: Alterations at a crossroads of cellular metabolism. *J. Natl. Cancer Inst.* **102**, 932–941 (2010).
24. Parsons, D. W. *et al.* An integrated genomic analysis of human glioblastoma multiforme. *Science (80-.)*. **321**, 1807–12 (2008).
25. Weller, M. *et al.* Molecular predictors of progression-free and overall survival in patients with newly diagnosed glioblastoma: A prospective translational study of the German Glioma Network. *J. Clin. Oncol.* **27**, 5743–5750 (2009).
26. Yan, H. & Parsons, D. W. IDH1 and IDH2 Mutations in Gliomas. *N Engl J Med* **360**, 765–773 (2010).
27. Wang, J.-H. *et al.* Prognostic significance of 2-hydroxyglutarate levels in acute myeloid leukemia in China. *Proc. Natl. Acad. Sci. U. S. A.* **110**, 17017–22 (2013).
28. Balss, J. *et al.* Pretreatment D-2-hydroxyglutarate serum levels negatively impact on outcome in IDH1-mutated acute myeloid leukemia. *Leukemia* 782–788 (2015). doi:10.1038/leu.2015.317
29. Feng, J.-H. *et al.* Prognostic significance of IDH1 mutations in acute myeloid leukemia: a meta-analysis. *Am J Blood Res* **2**, 254–264 (2012).
30. Dinardo, C. D. *et al.* Characteristics, clinical outcome, and prognostic significance of IDH mutations in AML. *Am. J. Hematol.* **90**, 732–736 (2015).
31. Yang, H., Ye, D., Guan, K. L. & Xiong, Y. IDH1 and IDH2 mutations in tumorigenesis: Mechanistic insights and clinical perspectives. *Clin. Cancer Res.* **18**, 5562–5571 (2012).
32. Janin, M. *et al.* Serum 2-hydroxyglutarate production in IDH1- And IDH2-mutated de novo acute myeloid leukemia: A study by the acute leukemia french association group. *J. Clin. Oncol.* **32**, 297–305 (2014).
33. Dinardo, C. D. *et al.* Serum 2-hydroxyglutarate levels predict isocitrate dehydrogenase

- mutations and clinical outcome in acute myeloid leukemia. **121**, 4917–4924 (2013).
34. Terunuma, A. *et al.* MYC-driven accumulation of 2-hydroxyglutarate is associated with breast cancer prognosis. *J. Clin. Invest.* **124**, 398–412 (2014).
 35. Intlekofer, A. M. *et al.* Hypoxia Induces Production of L-2-Hydroxyglutarate. *Cell Metab.* **22**, 304–311 (2015).
 36. Shim, E. H. *et al.* L-2-hydroxyglutarate: An epigenetic modifier and putative oncometabolite in renal cancer. *Cancer Discov.* **4**, 1290–1298 (2014).
 37. Achouri, Y. *et al.* Identification of a dehydrogenase acting on D-2-hydroxyglutarate. *Biochem. J.* **381**, 35–42 (2004).
 38. Gelman, S. J. *et al.* Consumption of NADPH for 2-HG Synthesis Increases Pentose Phosphate Pathway Flux and Sensitizes Cells to Oxidative Stress. *Cell Rep.* **22**, 512–522 (2018).
 39. Parker, S. J. & Metallo, C. M. Metabolic consequences of oncogenic IDH mutations. *Pharmacol. Ther.* **152**, 54–62 (2015).
 40. Sasaki, M. *et al.* D-2-hydroxyglutarate produced by mutant Idh1 perturbs collagen maturation and basement membrane function. *Genes Dev.* **26**, 2038–2049 (2012).
 41. Figueroa, M. E. *et al.* Leukemic IDH1 and IDH2 Mutations Result in a Hypermethylation Phenotype, Disrupt TET2 Function, and Impair Hematopoietic Differentiation. *Cancer Cell* **18**, 553–567 (2010).
 42. Xu, W. *et al.* Oncometabolite 2-Hydroxyglutarate Is a Competitive Inhibitor of α -Ketoglutarate-Dependent Dioxygenases. **86**, 3279–3288 (2008).
 43. Chowdhury, R. *et al.* The oncometabolite 2-hydroxyglutarate inhibits histone lysine demethylases. *EMBO Rep.* **12**, 463–469 (2011).
 44. Yang, M., Soga, T. & Pollard, P. J. Oncometabolites: Linking altered metabolism with cancer. *J. Clin. Invest.* **123**, 3652–3658 (2013).
 45. Clark, O., Yen, K. & Mellinghoff, I. K. Molecular pathways: Isocitrate dehydrogenase mutations in cancer. *Clin. Cancer Res.* **22**, 1837–1842 (2016).
 46. Virani, S., Virani, S., Colacino, J. A., Kim, J. H. & Rozek, L. S. Cancer epigenetics: a brief review. *ILAR J.* **53**, 359–69 (2012).
 47. Guillaumet-Adkins, A. *et al.* Epigenetics and Oxidative Stress in Aging. *Oxid. Med. Cell. Longev.* **2017**, (2017).
 48. Jin, B., Li, Y. & Robertson, K. D. DNA methylation: Superior or subordinate in the epigenetic hierarchy? *Genes and Cancer* **2**, 607–617 (2011).
 49. Bonetta, L. Epigenomics: The new tool in studying complex diseases. *Nat. Educ.* **1**, 178 (2008).
 50. Vento-Tormo, R. *et al.* IL-4 orchestrates STAT6-mediated DNA demethylation leading to dendritic cell differentiation. *Genome Biol.* **17**, 1–18 (2016).
 51. Pålsson-McDermott, E. M. & O’Neill, L. A. J. Signal transduction by the lipopolysaccharide receptor, Toll-like receptor-4. *Immunology* **113**, 153–162 (2004).
 52. Choi, N. M., Majumder, P. & Boss, J. M. Regulation of major histocompatibility

- complex class II genes. *Curr. Opin. Immunol.* **23**, 81–87 (2011).
53. Landmann, S. *et al.* Maturation of dendritic cells is accompanied by rapid transcriptional silencing of class II transactivator (CIITA) expression. *J. Exp. Med.* **194**, 379–391 (2001).
 54. Roche, P. a & Furuta, K. The ins and outs of MHC class II-mediated antigen processing and presentation. *Nat. Rev. Immunol.* **15**, 203–216 (2015).
 55. Sanderson, F. *et al.* Accumulation of HLA-DM, a regulator of antigen presentation, in MHC class II compartments. *Science* **266**, 1566–9 (1994).
 56. Walseng, E., Bakke, O. & Roche, P. A. Major histocompatibility complex class II-peptide complexes internalize using a clathrin- and dynamin-independent endocytosis pathway. *J. Biol. Chem.* **283**, 14717–14727 (2008).
 57. Kleijmeer, M. *et al.* Reorganization of multivesicular bodies regulates MHC class II 11 antigen presentation by dendritic cells. *J. Cell Biol.* **155**, 53–63 (2001).
 58. Stern, L. J., Potoличchio, I. & Santambrogio, L. MHC class II compartment subtypes: Structure and function. *Curr. Opin. Immunol.* **18**, 64–69 (2006).
 59. Potoличchio, I. *et al.* Conformational variation of surface class II MHC proteins during myeloid dendritic cell differentiation accompanies structural changes in lysosomal MIIC. *J. Immunol.* **175**, 4935–4947 (2005).
 60. Calafat, J. *et al.* Major histocompatibility complex class II molecules induce the formation of endocytic MIIC-like structures. *J. Cell Biol.* **126**, 967–977 (1994).
 61. Pagès, F. *et al.* Immune infiltration in human tumors: A prognostic factor that should not be ignored. *Oncogene* **29**, 1093–1102 (2010).
 62. Gao, Q. *et al.* Intratumoral balance of regulatory and cytotoxic T cells is associated with prognosis of hepatocellular carcinoma after resection. *J. Clin. Oncol.* **25**, 2586–2593 (2007).
 63. Bates, G. J. *et al.* Quantification of regulatory T cells enables the identification of high-risk breast cancer patients and those at risk of late relapse. *J. Clin. Oncol.* **24**, 5373–5380 (2006).
 64. Finn, O. J. Human Tumor Antigens Yesterday, Today, and Tomorrow. *Cancer Immunol. Res.* **5**, 347–354 (2017).
 65. Jäger, D., Jäger, E. & Knuth, a. Immune responses to tumour antigens: implications for antigen specific immunotherapy of cancer. *J. Clin. Pathol.* **54**, 669–674 (2001).
 66. Krackhardt, A. M. Identification and Characterization of Neoantigens As Well As Respective Immune Responses in Cancer Patients. **8**, 1–8 (2017).
 67. Disis, M. L., Bernhard, H. & Jaff, E. M. Use of tumour-responsive T cells as cancer treatment. 673–683 (2009). doi:10.1016/S0140-6736(09)60404-9
 68. Kaufman, H. L. & Disis, M. L. Immune system versus tumor: Shifting the balance in favor of DCs and effective immunity. *J. Clin. Invest.* **113**, 664–667 (2004).
 69. Sciacovelli, M. & Frezza, C. Oncometabolites: Unconventional triggers of oncogenic signalling cascades. *Free Radic. Biol. Med.* **100**, 175–181 (2016).

70. Brand, A. *et al.* LDHA-Associated Lactic Acid Production Blunts Tumor Immunosurveillance by T and NK Cells. *Cell Metab.* **24**, 657–671 (2016).
71. Gottfried, E. *et al.* Tumor-derived lactic acid modulates dendritic cell activation and antigen expression. *Differentiation* **107**, 2013–2021 (2013).
72. Böttcher, M. *et al.* D-2-hydroxyglutarate interferes with HIF-1 α stability skewing T-cell metabolism towards oxidative phosphorylation and impairing Th17 polarization. *Oncoimmunology* 1–26 (2018). doi:10.1080/2162402X.2018.1445454
73. Xu, T. *et al.* Metabolic control of TH17 and induced Tregcell balance by an epigenetic mechanism. *Nature* **548**, 228–233 (2017).
74. Campbell, N. A. & Reece, J. B. *Biologie*. (Spektrum Akademischer Verlag, 2003).
75. Mailloux, R. J., McBride, S. L. & Harper, M. E. Unearthing the secrets of mitochondrial ROS and glutathione in bioenergetics. *Trends Biochem. Sci.* **38**, 592–602 (2013).
76. Le Naour, F. *et al.* Profiling Changes in Gene Expression during Differentiation and Maturation of Monocyte-derived Dendritic Cells Using Both Oligonucleotide Microarrays and Proteomics. *J. Biol. Chem.* **276**, 17920–17931 (2001).
77. Ishikawa, F. *et al.* The developmental program of human dendritic cells is operated independently of conventional myeloid and lymphoid pathways The developmental program of human dendritic cells is operated independently of conventional myeloid and lymphoid pathways. **110**, 3591–3601 (2009).
78. Zaccagnino, P. *et al.* An active mitochondrial biogenesis occurs during dendritic cell differentiation. *Int. J. Biochem. Cell Biol.* **44**, 1962–1969 (2012).
79. Rehman, A. *et al.* Role of Fatty-Acid Synthesis in Dendritic Cell Generation and Function. *J. Immunol.* **190**, 4640–4649 (2013).
80. Pearce, E. J. & Everts, B. Dendritic cell metabolism. *Nat. Rev. Immunol.* **15**, 18–29 (2014).
81. Krawczyk, C. M. *et al.* Toll-like receptor–induced changes in glycolytic metabolism regulate dendritic cell activation. *Blood* **115**, 4742–4749 (2010).
82. Deneke, S. M. & Fanburg, B. L. Regulation of cellular glutathione. *Am. J. Physiol.* **257**, L163–L173 (1989).
83. Harari, O. & Liao, J. K. Inhibition of MHC II gene transcription by nitric oxide and antioxidants. *Curr. Pharm. Des.* **10**, 893–8 (2004).
84. Yamada, H. *et al.* LPS-induced ROS generation and changes in glutathione level and their relation to the maturation of human monocyte-derived dendritic cells. *Life Sci.* **78**, 926–933 (2006).
85. Rutault, K., Alderman, C., Chain, B. M. & Katz, D. R. Reactive oxygen species activate human peripheral blood dendritic cells. *Free Radic Biol Med* **26**, 232–238 (1999).
86. Del Prete, A. *et al.* Role of mitochondria and reactive oxygen species in dendritic cell differentiation and functions. *Free Radic. Biol. Med.* **44**, 1443–1451 (2008).
87. Malinarich, F. *et al.* High Mitochondrial Respiration and Glycolytic Capacity

- Represent a Metabolic Phenotype of Human Tolerogenic Dendritic Cells. *J. Immunol.* **194**, 5174–5186 (2015).
88. Rammensee, H., Bachmann, J., Emmerich, N. P., Bachor, O. A. & Stevanović, S. SYFPEITHI: database for MHC ligands and peptide motifs. *Immunogenetics* **50**, 213–9 (1999).
89. Parker, K. C., Bednarek, M. A. & Coligan, J. E. Scheme for ranking potential HLA-A2 binding peptides based on independent binding of individual peptide side-chains. *J. Immunol.* **152**, 163 LP-175 (1994).
90. Hoof, I. *et al.* NetMHCpan, a method for MHC class I binding prediction beyond humans. *Immunogenetics* **61**, 1–13 (2009).
91. Schaft, N. *et al.* Generation of an Optimized Polyvalent Monocyte-Derived Dendritic Cell Vaccine by Transfecting Defined RNAs after Rather Than before Maturation. *J. Immunol.* **174**, 3087–3097 (2005).
92. Birnboim, H. C. & Doly, J. A rapid alkaline extraction procedure for screening recombinant plasmid DNA. *Nucleic Acids Res.* **7**, 1513–23 (1979).
93. Felzmann, T. *et al.* Monocyte enrichment from leukapheresis products for the generation of DCs by plastic adherence, or by positive or negative selection. *Cytotherapy* **5**, 391–398 (2003).
94. Dauer, M. *et al.* Mature Dendritic Cells Derived from Human Monocytes Within 48 Hours: A Novel Strategy for Dendritic Cell Differentiation from Blood Precursors. *J. Immunol.* **170**, 4069–4076 (2003).
95. Thomas, S. *et al.* Human CD8⁺ memory and EBV-specific T cells show low alloreactivity invitro and in CD34⁺ stem cell-engrafted NOD/SCID/IL-2R γ null mice. *Exp. Hematol.* **42**, 28–38 (2014).
96. Wehler, T. C. *et al.* Targeting the activation-induced antigen CD137 can selectively deplete alloreactive T cells from antileukemic and antitumor donor T-cell lines. *Blood* **109**, 365–373 (2007).
97. Siska, P. J. *et al.* Fluorescence-based measurement of cystine uptake through xCT shows requirement for ROS detoxification in activated lymphocytes. *J. Immunol. Methods* **438**, 51–58 (2016).
98. Gottfried, E. *et al.* New Aspects of an Old Drug - Diclofenac Targets MYC and Glucose Metabolism in Tumor Cells. *PLoS One* **8**, (2013).
99. Kuznetsov, A. V. *et al.* Analysis of mitochondrial function in situ in permeabilized muscle fibers, tissues and cells. *Nat. Protoc.* **3**, 965–976 (2008).
100. Klug, M. *et al.* Active DNA demethylation in human postmitotic cells correlates with activating histone modifications, but not transcription levels. *Genome Biol.* **11**, (2010).
101. Klug, M., Schmidhofer, S., Gebhard, C., Andreesen, R. & Rehli, M. 5-Hydroxymethylcytosine is an essential intermediate of active DNA demethylation processes in primary human monocytes. *Genome Biol.* **14**, R46 (2013).
102. Lowry, O. H., Rosebrough, N. J., Farr, A. L. & Randall, R. J. Protein measurement with the Folin phenol reagent. *J. Biol. Chem.* **193**, 265–75 (1951).
103. Zhang, G. L. *et al.* Machine learning competition in immunology - Prediction of HLA

- class I binding peptides. *J. Immunol. Methods* **374**, 1–4 (2011).
104. Gonzalez-Galarza, F. F., Christmas, S., Middleton, D. & Jones, A. R. Allele frequency net: A database and online repository for immune gene frequencies in worldwide populations. *Nucleic Acids Res.* **39**, 913–919 (2011).
105. Bonini, C., Lee, S. P., Riddell, S. R. & Greenberg, P. D. Targeting antigen in mature dendritic cells for simultaneous stimulation of CD4⁺ and CD8⁺ T cells. *J. Immunol.* **166**, 5250–7 (2001).
106. Lin, K. Y. *et al.* Treatment of established tumors with a novel vaccine that enhances major histocompatibility class II presentation of tumor antigen. *Cancer Res.* **56**, 21–26 (1996).
107. Bonehill, A. *et al.* Messenger RNA-electroporated dendritic cells presenting MAGE-A3 simultaneously in HLA class I and class II molecules. *J. Immunol.* **172**, 6649–6657 (2004).
108. Cusick, M. F., Libbey, J. E. & Fujinami, R. S. Molecular mimicry as a mechanism of autoimmune disease. *Clin. Rev. Allergy Immunol.* **42**, 102–111 (2012).
109. Ziegler-Heitbrock, H. W. L. & Ulevitch, R. J. CD14: Cell surface receptor and differentiation marker. *Immunol. Today* **14**, 121–125 (1993).
110. Cao, X. *et al.* CD1 Molecules Efficiently Present Antigen in Immature Dendritic Cells and Traffic Independently of MHC Class II During Dendritic Cell Maturation. *J. Immunol.* **169**, 4770–4777 (2002).
111. Garcia-Vallejo, J. J. & van Kooyk, Y. The physiological role of DC-SIGN: A tale of mice and men. *Trends Immunol.* **34**, 482–486 (2013).
112. Geijtenbeek, T. B. H., Engering, A. & Van Kooyk, Y. DC-SIGN, a C-type lectin on dendritic cells that unveils many aspects of dendritic cell biology. *J. Leukoc. Biol.* **71**, 921–931 (2002).
113. Gemmell, E. & Seymour, G. J. Cytokines and T cell switching. *Crit. Rev. Oral Biol. Med.* **5**, 249–79 (1994).
114. Cosentino-Gomes, D., Rocco-Machado, N. & Meyer-Fernandes, J. R. Cell signaling through protein kinase C oxidation and activation. *Int. J. Mol. Sci.* **13**, 10697–10721 (2012).
115. Bustos, G., Cruz, P., Lovy, A. & Cárdenas, C. Endoplasmic Reticulum–Mitochondria Calcium Communication and the Regulation of Mitochondrial Metabolism in Cancer: A Novel Potential Target. *Front. Oncol.* **7**, 1–8 (2017).
116. Ferreira, G. B. *et al.* Vitamin D3 induces tolerance in human dendritic cells by activation of intracellular metabolic pathways. *Cell Rep.* **10**, 711–725 (2015).
117. Brand, M. D. & Nicholls, D. G. Assessing mitochondrial dysfunction in cells. *Biochem. J.* **435**, 297–312 (2011).
118. Wheaton, W. W. *et al.* Metformin inhibits mitochondrial complex I of cancer cells to reduce tumorigenesis. *Elife* **2014**, 1–18 (2014).
119. Balaban, R. S., Nemoto, S. & Finkel, T. Mitochondria, oxidants, and aging. *Cell* **120**, 483–495 (2005).

120. Wu, D. & Yotnda, P. Production and Detection of Reactive Oxygen Species (ROS) in Cancers. *J. Vis. Exp.* 2–5 (2011). doi:10.3791/3357
121. Shelly C. Lu, M. D. Glutathione Synthesis. *Biochim Biophys Acta* **1830**, 3143–3153 (2014).
122. Mingay, M. *et al.* Vitamin C-induced epigenomic remodelling in IDH1 mutant acute myeloid leukaemia. *Leukemia* 11–20 (2017). doi:10.1038/leu.2017.171
123. Fu, X. *et al.* 2-Hydroxyglutarate Inhibits ATP Synthase and mTOR Signaling. *Cell Metab.* **22**, 508–515 (2016).
124. Madhu, S. Use Of Oral Anti-Diabetic Agents In Diabetes With Chronic Kidney Disease. *Med. Updat.* 156–159 (2011).
125. Blaschke, K. *et al.* Vitamin C induces Tet-dependent DNA demethylation and a blastocyst-like state in ES cells. *Nature* **500**, 222–226 (2013).
126. Cimmino, L. *et al.* Restoration of TET2 Function Blocks Aberrant Self-Renewal and Leukemia Progression. *Cell* **170**, 1079–1095.e20 (2017).
127. Charlton, J., John, M. & Bird, A. P. Spl sites in the mouse. *Genes Dev.* 2282–2292 (1994).
128. Bassani-Sternberg, M. *et al.* Direct identification of clinically relevant neoepitopes presented on native human melanoma tissue by mass spectrometry. *Nat. Commun.* **7**, (2016).
129. Leisegang, M., Kammertoens, T., Uckert, W. & Blankenstein, T. Targeting human melanoma neoantigens by T cell receptor gene therapy. *J clin invest* **2**, 1–5 (2016).
130. Leisegang, M. *et al.* Eradication of large solid tumors by gene therapy with a T-cell receptor targeting a single cancer-specific point mutation. *Clin. Cancer Res.* **22**, 2734–2743 (2016).
131. Calis, J. J. A., de Boer, R. J. & Keşmir, C. Degenerate T-cell recognition of peptides on MHC molecules creates large holes in the T-cell repertoire. *PLoS Comput. Biol.* **8**, (2012).
132. Yin, Y., Li, Y. & Mariuzza, R. A. Structural basis for self-recognition by autoimmune T-cell receptors. *Immunol. Rev.* **250**, 32–48 (2012).
133. Wucherpfennig, K. W. Structural basis of molecular mimicry. *J. Autoimmun.* **16**, 293–302 (2001).
134. Arstila, T. P. *et al.* A direct estimate of the human alpha beta T cell receptor diversity. *Science* **286**, 958–961 (1999).
135. Grassian, A. R. *et al.* IDH1 mutations alter citric acid cycle metabolism and increase dependence on oxidative mitochondrial metabolism. *Cancer Res.* **74**, 3317–3331 (2014).
136. Bunse, L. *et al.* Suppression of antitumor T cell immunity by the oncometabolite (R)-2-hydroxyglutarate. *Nat. Med.* 1–12 (2018). doi:10.1038/s41591-018-0095-6
137. Hagos, Y. *et al.* Organic anion transporters OAT1 and OAT4 mediate the high affinity transport of glutarate derivatives accumulating in patients with glutaric acidurias. *Pflugers Arch. Eur. J. Physiol.* **457**, 223–231 (2008).

138. Capper, D. *et al.* 2-Hydroxyglutarate concentration in serum from patients with gliomas does not correlate with IDH1/2 mutation status or tumor size. *Int. J. Cancer* **131**, 766–768 (2012).
139. Ci, Y. *et al.* ROS inhibit autophagy by downregulating ULK1 mediated by the phosphorylation of p53 in selenite-treated NB4 cells. *Cell Death Dis.* **5**, 1–10 (2014).
140. Frudd, K., Burgoyne, T. & Burgoyne, J. R. Oxidation of Atg3 and Atg7 mediates inhibition of autophagy. *Nat. Commun.* **9**, 1–15 (2018).
141. Tanida, I., Ueno, T. & Kominami, E. in 77–88 (2008). doi:10.1007/978-1-59745-157-4_4
142. Barth, S., Glick, D. & Macleod, K. F. Autophagy: Assays and artifacts. *J. Pathol.* **221**, 117–124 (2010).
143. Mintern, J. D. *et al.* Differential use of autophagy by primary dendritic cells specialised in cross-presentation. *Autophagy* **11**, 906–17 (2015).
144. Zhao, J., Deng, Y., Jiang, Z. & Qing, H. G protein-coupled receptors (GPCRs) in Alzheimer's disease: A focus on BACE1 related GPCRs. *Front. Aging Neurosci.* **8**, 1–15 (2016).
145. Ganguly, U., Ghosh Chaudhury, A., Basu, A. & Sen, P. C. STa-induced translocation of protein kinase C from cytosol to membrane in rat enterocytes. *FEMS Microbiol. Lett.* **204**, 65–69 (2001).
146. Langlet, C. *et al.* PKC- α controls MYD88-dependent TLR/IL-1R signaling and cytokine production in mouse and human dendritic cells. *Eur. J. Immunol.* **40**, 505–515 (2010).
147. Farren, M. R., Carlson, L. M. & Lee, K. P. Tumor-mediated inhibition of dendritic cell differentiation is mediated by down regulation of protein kinase C beta II expression. *Immunol. Res.* **46**, 165–176 (2010).
148. Cejas, P. J. *et al.* Protein kinase C β II plays an essential role in dendritic cell differentiation and autoregulates its own expression. *J. Biol. Chem.* **280**, 28412–28423 (2005).
149. Pinton, P. *et al.* Protein Kinase C beta and Prolyl Isomerase 1 Regulate Mitochondrial Effects of the Life-Span Determinant p66Shc. *Science (80-.)*. **315**, 659–663 (2007).
150. Guak, H. *et al.* Glycolytic metabolism is essential for CCR7 oligomerization and dendritic cell migration. *Nat. Commun.* **9**, 2463 (2018).
151. Wei, W.-C. *et al.* Mammalian target of rapamycin complex 2 (mTORC2) regulates LPS-induced expression of IL-12 and IL-23 in human dendritic cells. *J. Leukoc. Biol.* **97**, 1071–1080 (2015).
152. Lee, P. Y. *et al.* The metabolic regulator mTORC1 controls terminal myeloid differentiation. *Sci. Immunol* **2**, (2017).
153. Copp, J., Manning, G. & Hunter, T. TORC-specific phosphorylation of mTOR: phospho-Ser2481 is a marker for intact mTORC2. *Cancer Res.* **69**, 1821–1827 (2010).
154. Woltman, A. M. *et al.* Rapamycin specifically interferes with GM-CSF signaling in human dendritic cells, leading to apoptosis via increased p27KIP1 expression. *Blood* **101**, 1439–1445 (2003).

155. Kölker, S. *et al.* NMDA receptor activation and respiratory chain complex V inhibition contribute to neurodegeneration in D-2-hydroxyglutaric aciduria. *Eur. J. Neurosci.* **16**, 21–28 (2002).
156. Grassian, A. R. *et al.* Dependence on Oxidative Mitochondrial Metabolism IDH1 Mutations Alter Citric Acid Cycle Metabolism and Increase IDH1 Mutations Alter Citric Acid Cycle Metabolism and Increase Dependence on Oxidative Mitochondrial Metabolism. *Publ. OnlineFirst April Cancer Res* **74**, 3317–3331 (2014).
157. Navis, A. C. *et al.* Increased mitochondrial activity in a novel IDH1-R132H mutant human oligodendroglioma xenograft model: in situ detection of 2-HG and α -KG. *Acta Neuropathol. Commun.* **1**, 18 (2013).
158. Bakdash, G., Sittig, S. P., van Dijk, T., Figdor, C. G. & de Vries, I. J. M. The nature of activatory and tolerogenic dendritic cell-derived signal II. *Front. Immunol.* **4**, 1–18 (2013).
159. Sim, W. J. *et al.* Metabolism Is Central to Tolerogenic Dendritic Cell Function. *Mediators Inflamm.* **2016**, 1–10 (2016).
160. Shi, J. *et al.* An IDH1 mutation inhibits growth of glioma cells via GSH depletion and ROS generation. *Neurol. Sci.* **35**, 839–845 (2014).
161. D'Angelo, J. A. *et al.* The cystine/glutamate antiporter regulates dendritic cell differentiation and antigen presentation. *J. Immunol.* **185**, 3217–26 (2010).
162. Belikov, A. V., Schraven, B. & Simeoni, L. T cells and reactive oxygen species. *J. Biomed. Sci.* **22**, 1–11 (2015).
163. Scott, J. W., Cort, W. M., Harley, H., Parrish, D. R. & Saucy, G. 6-Hydroxychroman-2-carboxylic acids: Novel antioxidants. *J. Am. Oil Chem. Soc.* **51**, 200–203 (1974).
164. Xuan, N. T. *et al.* Klotho sensitive regulation of dendritic cell functions by vitamin E. *Biol. Res.* **49**, 45 (2016).
165. Minuesa, G. *et al.* Expression and functionality of anti-human immunodeficiency virus and anticancer drug uptake transporters in immune cells. *J. Pharmacol. Exp. Ther.* **324**, 558–567 (2008).
166. Zhou Mingyan, Xia LI, W. J. Metformin Transport by a Newly Cloned Proton-Stimulated Organic Cation Transporter (Plasma Membrane Monoamine Transporter) Expressed in Human Intestine. *Drug Metab. Desposition* **49**, 1841–1850 (2009).
167. Shin, S. *et al.* Metformin suppresses MHC-restricted antigen presentation by inhibiting co-stimulatory factors and MHC molecules in APCs. *Biomol. Ther.* **21**, 35–41 (2013).
168. Yan, H. *et al.* [Pioglitazone inhibits dendritic cell adhesion and transmigration through down-regulation of dendritic cell-specific intercellular adhesion molecule-3 grabbing nonintegrin]. *Zhonghua Yi Xue Za Zhi* **88**, 835–9 (2008).
169. Gosset, P. *et al.* Peroxisome proliferator-activated receptor gamma activators affect the maturation of human monocyte-derived dendritic cells. *Eur. J. Immunol.* **31**, 2857–65 (2001).
170. Wright, K. L. & Ting, J. P. Epigenetic regulation of MHC-II and CIITA genes. **27**, (2006).
171. Agathocleous, M. *et al.* Ascorbate regulates haematopoietic stem cell function and

- leukaemogenesis. *Nature* **549**, 476–481 (2017).
172. Franco, R., Schoneveld, O., Georgakilas, A. G. & Panayiotidis, M. I. Oxidative stress, DNA methylation and carcinogenesis. *Cancer Lett.* **266**, 6–11 (2008).
173. Afanas'ev, I. Mechanisms of Superoxide Signaling in Epigenetic Processes: Relation to Aging and Cancer. *Aging Dis.* **6**, 216 (2015).
174. Chaturvedi, a *et al.* Enantiomer-specific and paracrine leukemogenicity of mutant IDH metabolite 2-hydroxyglutarate. *Leukemia* 1–8 (2016). doi:10.1038/leu.2016.71
175. Oizel, K. *et al.* D-2-Hydroxyglutarate does not mimic all the IDH mutation effects, in particular the reduced etoposide-triggered apoptosis mediated by an alteration in mitochondrial NADH. *Cell Death Dis.* **6**, e1704 (2015).
176. Masuda, K. *et al.* Loss or down-regulation of HLA class I expression at the allelic level in freshly isolated leukemic blasts. *Cancer Sci.* **98**, 102–108 (2007).
177. Williams, B. & Williams, B. Mutant IDH1 regulates the tumor- associated immune system in gliomas. *Genes Dev.* 1–13 (2017). doi:10.1101/gad.294991.116.
178. Kohanbash, G. *et al.* Isocitrate dehydrogenase mutations suppress STAT1 and CD8+ T cell accumulation in gliomas. *J. Clin. Invest.* **127**, 1425–1437 (2017).
179. Syed, M., Skonberg, C. & Hansen, S. H. Mitochondrial toxicity of diclofenac and its metabolites via inhibition of oxidative phosphorylation (ATP synthesis) in rat liver mitochondria: Possible role in drug induced liver injury (DILI). *Toxicol. Vitr.* **31**, 93–102 (2016).

Danksagung

Es gibt viele Menschen, die zum Gelingen dieser Doktorarbeit in den letzten vier Jahren beigetragen haben, und bei denen ich mich an dieser Stelle bedanken möchte.

Das erste Dankeschön gilt meinen Doktorvater Prof. Dr. Wolfgang Herr und meinen zwei Mentoren Prof. Dr. Marina Kreutz und Prof. Dr. Bodo Plachter, vielen Dank für die hilfreichen Diskussionen während der jährlichen Treffen und die Betreuung meiner Doktorarbeit. Zusätzlich möchte ich mich bei Prof. Dr. Barbara Schmidt, Prof. Dr. Jonathan Jantsch und Prof. Dr. Wolfram Gronwald bedanken, die mir zusammen mit Prof. Dr. Wolfgang Herr und Prof. Marina Kreutz beim letzten Schritt, der mündlichen Prüfung, zur Seite stehen werden.

Nochmal danken möchte ich Prof. Dr. Marina Kreutz, die mich nach dem ersten Jahr zu einem Teil ihrer Arbeitsgruppe hat werden lassen. Vielen Dank für die Unterstützung im alltäglichen Laboralltag. Neben Prof. Dr. Marina Kreutz, möchte ich auch meinen zwei anderen „scientific mothers“ PD. Dr. Simone Thomas und PD. Dr. Kathrin Renner-Sattler herzlich danken, die Diskussion der Ergebnisse im HG-Klubs ergab immer neue Ideen, die das Projekt vorangebracht haben. Auch für die Unterstützung beim Verfassen des Manuskriptes meiner Erstautorenschaft möchte ich euch herzlich danken.

PD. Dr. Simone Thomas möchte ich zusätzlich für die Möglichkeit danken, dieses spannende aber auch herausfordernde Projekt in ihrer Forschungsgruppe durchführen zu dürfen. Außerdem geht mein Dank für die schnelle und hilfreiche Korrektur meiner Doktorarbeit an PD. Dr. Simone Thomas, PD. Dr. Kathrin Renner-Sattler, Dr. Sakhila Ghimire und M.Sc. Christina Bruß.

Bei PD. Dr. Kathrin Renner-Sattler, Stephanie Färber, M.Sc. Christina Bruß, M.Sc. Mareile Siebörger, Johanna Raithel und M.Sc. Karina Mendes möchte ich mich für die Unterstützung bei der Durchführung von Respirometrie Experimenten, ATP, Laktat und Glukose Bestimmungen, ELISpot und Methylierungsanalysen bedanken. Vielen Dank für eure Zeit.

Außerdem möchte ich mich beim Institut für Pathologie (Uniklinikum Regensburg) vor allem bei Heiko Siegfried und Prof. Dr. Christoph Brochhausen-Delius für die eindrucksvollen elektronmikroskopischen Aufnahmen meiner dendritischen Zellen bedanken. Des Weiteren, möchte ich mich bei dem Institut für Funktionelle Genomik (Universität Regensburg), vor allem bei Raffaella Berger für die 2-HG Bestimmungen danken.

Aber ich wurde nicht nur mit der Durchführung von Experimenten und Korrekturen unterstützt, für die seelische und moralische Unterstützung möchte ich mich bei allen Arbeitsgruppen im H1, besonders bei allen Mitgliedern der AG Thomas, AG Rehli und AG

Kreutz, herzlich bedanken. Während der nicht immer leichten vier Jahre hattet ihr immer ein offenes Ohr und habt mich immer wieder dazu motiviert nicht aufzugeben. Thanks for your help and support!

Zuletzt möchte ich bei meinen Freunden, meinem Freund und meiner Familie für die Geduld und Unterstützung an weniger guten Tagen bedanken. Ihr habt immer Verständnis gezeigt, auch wenn der ein oder andere Event ohne mich stattfinden musste. Dafür von ganzem Herzen DANKE.